REVIEW

ORIGINAL RESEARCH

EDITOR'S OFFICE

SCRIPTA MEDICA
Editor-in-Chief
M. Korcová
Faculty of Medicine
Masaryk University
Kamenice 5
CZ–625 00 Brno, Czech Republic
Tel.: +420 549 493 998
E-mail: scriptme@med.muni.cz
mkorcova@med.muni.cz

Publisher: Faculty of Medicine,
Masaryk University, Brno

Periodicity: 4 issues per volume
The journal Scripta Medica is printed
in 500 copies.

Printed by Tiskárna Helbich, a.s., Brno

Art studio: Metoda, s.r.o., Brno

Advertising is accepted in the journal.
Further information including rates, specification,
etc. is available on request.

ISSN 1211–3395

MK ČR E 4996

Scripta Medica is available free online at
http:/www.med.muni.cz/biomedjournal/

Cena: 230,- CZK vč. DPH za 1 číslo; 920,- CZK vč. DPH za 4 čísla celého ročníku (zahrnuje poštovné a balné)

Price in EUR - I: EUR 10.00 incl. VAT/1 issue (postage and packing included); EUR 40.00 incl. VAT/4 issues of whole volume

Price in EUR - II: EUR 09.00 without VAT/1 issue (postage and packing included); EUR 36.00 without VAT/4 issues of whole volume

SCRIPTA MEDICA is indexed in

EMBASE/Excerpta Medica

DIALOG DataStar

MEDLINE

EBSCO

ProQuest

Scopus

PubMed

Bibliographia Medica Čechoslovaca

Online Computer Library Center, Inc.

Deutsches Institut für Medizinische Dokumentation
und Information

SUBSCRIPTION TO THE JOURNAL SCRIPTA MEDICA – INTERNATIONAL ORDERING FORM

http:/www.med.muni.cz/biomedjournal/

Publisher:
Masaryk University
Faculty of Medicine
Komenského nám. 2
CZ-662 43 Brno
Identification No.: 00216224; VAT registration No.: CZ00216224
Masaryk University is a public higher-learning institution pursuant to Act No. 111/1998 of the Coll. of Laws in valid wording, not entered in the register of companies.

Address of Editorial Board:
Faculty of Medicine
Masaryk University
Kamenice 5
CZ–625 00 Brno, Czech Republic
Tel.: +420 549 493 998
E-mail: scriptme@med.muni.cz
mkorcova@med.muni.cz

PŘEDPLATNÉ ČASOPISU SCRIPTA MEDICA – OBJEDNÁVKOVÝ KUPÓN

http:/www.med.muni.cz/biomedjournal/

Vydavatel:
Masarykova univerzita
Lékařská fakulta
Komenského nám. 2
662 43 Brno
IČ: 00216224, DIČ: CZ00216224
Masarykova univerzita je veřejnou vysokou školou dle zák. 111/1998 Sb. v platném znění nezapsaná v obchodním rejstříku

Adresa redakce:
Lékařská fakulta
Masarykova Univerzita
Kamenice 5
CZ–625 00 Brno, Czech Republic
Tel.: +420 549 493 998
E-mail: scriptme@med.muni.cz
mkorcova@med.muni.cz

CENTRAL AND PERIPHERAL CIRCADIAN CLOCK GENES, THEIR STATISTICAL ANALYSIS FOR RHYTHMS, AND RELATIONSHIP TO HEALTH AND DISEASE

Sothern R. B.*[1,3], Yamamoto T.[2], Cornélissen G.[3], Takumi T.[4], Halberg F.[3]

[1]The Rhythmometry Lab, Dept of Plant Biology, College of Biological Sciences, University of Minnesota, St. Paul, USA
[2]Life Science Laboratory, Advanced Material Laboratories, Sony Corporation, Shinagawa, Tokyo, Japan
[3]Halberg Chronobiology Center, Dept of Lab Medicine and Pathology, University of Minnesota, Minneapolis, USA
[4]Laboratory of Integrative Bioscience, Graduate School of Biomedical Sciences, Hiroshima University, Hiroshima, Japan

Received after revision April 2009

KEY WORDS

Circadian
Clock gene
Cosinor
Peripheral organs
Rhythm

CORRESPONDING AUTHOR

Robert B. Sothern, Ph.D.,
The Rhythmometry Laboratory, Dept of Plant Biology, College of Biological Sciences, 250 Biological Sciences Center, University of Minnesota, 1445 Gortner Ave, St. Paul, MN, 55108, USA

ABSTRACT

Molecular clocks present in organs and individual cells throughout the body are central for the temporal coordination of rhythms in internal biological processes among themselves and with external environmental cycles; altered function of specific clock gene (CG) components can have significant impact relevant to health and disease. We herein review current knowledge pertaining to the presence and robustness of circadian rhythms in CGs in the suprachiasmatic nucleus and peripheral organs, and the importance of CGs to general health and the diagnosis and treatment of human disorders and disease. Also discussed are developmental aspects of rhythms in some CGs and tissues, time of day vs. circadian stage, using synchronized vs. constant conditions to monitor a rhythm, and subjective vs. objective interpretations of rhythms. To emphasize the latter, chronobiological statistics (ANOVA, single cosinor) are applied to published circadian CG mRNA expression data (which had been described subjectively) as an example of objectively determining rhythm probability and obtaining estimates for circadian amplitudes and acrophases. The data base consisted of 14 CGs (*mPer1,2,3*, *mCry1,2*, *mBmal1*, *mCK1*δ,ε, *mClock*, *mDbp*, *mNpas2, mRev-erb*α,β, *mTim*) in each of 7 mouse organs harvested every 4h for 24h from male Balb/c mice on day 3 in continuous darkness. Excluding the usually non–24h-rhythmic testis and CG *mTim*, rhythms significant at $p \leq 0.05$ were found in 81% (63/78) of CGs and when including borderline significant at $p \leq 0.10$, in 97% (76/78) of CGs. A statistically-determined circadian amplitude and acrophase for each CG in each tissue can be useful in making objective comparisons of rhythm parameters in CGs between various peripheral organs, species, and/or studies of different conditions (e.g., photoperiods, feeding schedules, aging, disease). Use of

these parameters adds new endpoints for diagnoses and approaches for therapeutic interventions in conditions where disturbance of circadian CG expression is an important cause of morbidity associated with chronic illnesses and diseases with a strong circadian component, including cardiovascular disease, epilepsy, cancer, metabolic syndrome, and sleep-related disorders, among others, also reviewed herein.

INTRODUCTION TO THE BIOLOGICAL CLOCK

The rhythmic nature of life influences the very existence of organisms, from bacteria [1] to mammals [2], and as such is an integral part of health and survival; any rhythm alteration may be a harbinger of disorder or disease. Circadian rhythms are important regulatory processes, which almost universally are used by organisms to harmonize physiology and behavior with the environmental 24h geophysical cycles of light and temperature. Circadian biological timekeeping clocks with common elements have emerged ubiquitously over several billion years, having been conserved phylogenetically from bacteria to fish to plants to insects to birds to mammals, with some evolutionary divergence (i.e., convergent evolution) of different gene products (homologs) of the core oscillator components, because endogenous daily timekeeping provides fitness and survival advantage, and as such are a core property of life on Earth [2–9]. Internal molecular circadian clocks are not only central for the temporal coordination with external environmental cycles, but also among internal biological metabolic processes themselves.

The molecular basis of circadian rhythms in mammals

The molecular clock machinery in mammals consists of a number of clock genes (CGs) and their resultant proteins that form multiple interlocking auto-regulatory transcription-translation feedback loops within cells [10] consisting of positive and negative elements that drive self-sustaining clock oscillations of approximately 24 hours. CGs are located in cells of the brain's central circadian pacemaker, the suprachiasmatic nucleus (SCN) [2], and in most, if not all, peripheral organs studied to date. Under normal conditions, these transcriptional loops operate to generate and maintain 24h CG mRNA and protein oscillations and consequential biological and physiological rhythms [3]. Some elements of the molecular clock have been shown to be partially functional in rat fetal SCN [11–13], and fully functional in the SCN within days of birth, as well as in peripheral tissues, such as the rat heart [14] or liver [15]. Persistent and robust circadian rhythms in CG expression have also been demonstrated in isolated mammalian fibroblast cells [16,17], as well as in cyanobacteria [18], indicating endogenicity and cell autonomy across diverse organisms.

Many features of the intracellular molecular clock machinery in mammals have been elucidated [2]. Major positive components in the CG feedback-feedsideward loop are a pair of transcription factors in the nucleus, BMAL1 and CLOCK, which can form heterodimers to drive the rhythmic expression of three *Period* genes (*Per1*, *Per2*, *Per3*) and two *Cryptochrome* genes (*Cry1, Cry2*) in the cytoplasm. The resultant PER:CRY protein dimers act as negative components and translocate back from the cytoplasm into the nucleus and inhibit CLOCK:BMAL1 activity, thereby completing the negative limb of the feedback loop. Posttranslational processes and some other secondary feedback or feedsideward loops involving clock-controlled genes (CCGs) also contribute to the precision of the cell clockwork machinery by playing important roles in fine-tuning, stabilization, and/or resetting the clock [19,20]. This cell clockwork machinery may conceptually be likened to a highly-sophisticated, finely-tuned, self-winding mechanical Swiss watch, but consisting of molecular nano-gears (CGs, CCGs) and mechanisms (feedback loops).

While synchronized by environmental cues such as photoperiod and feeding schedules, robust circadian CG oscillations can persist in constant darkness (DD) in the absence of external photoperiodic time cues, thereby authenticating their endogenous rhythmicity, rather than mere responses to a rhythmic environment. To this end, circadian oscillations in CG mRNA have been shown for up to 32 days in *Per1*-luciferase(Luc) expression in rat SCN [20], up to 25 days in *Per2*-Luc expression in mouse retinas in which photoreceptors had degenerated [22], up to 20 or more cycles in *Per2*-Luc expression in mouse SCN, liver and lung explants [23], and during 3 to 12 cycles in *Per1*-Luc expression in rat cardiovascular tissues [24].

Clock genes in peripheral tissues

In addition to CGs in the central circadian pacemaker located in the suprachiasmatic nucleus (SCN) in the ventral part of the hypothalamus, self-sustaining rhythmic expressions of mammalian CGs have also been found in peripheral tissues, confirming the existence of both central and peripheral oscillators [19,25]. To date, circadian oscillations in CGs have been documented in nearly every peripheral tissue studied, including heart, lung, liver, kidney, stomach, spleen, pancreas, gut, thymus, oviduct, bone marrow, skin, oral mucosa, cornea, retina, submandibular (salivary) glands, blood, hypothalamus, pineal, striatum, skeletal muscle, and extratesticular accessory tissues (epididymis, vas deferens, prostate, seminal vesicles) in mammals such as mice [21–23, 26–40], rats [41–49], hamsters [50–54] and humans [55–62].

The lack of reproducible data to show that peripheral tissues in mammals receive direct photic input suggests a hi-

erarchical model where the SCN provides an essential link as a primary coordinator or synchronizer between the outside world and internal autonomous circadian time-keeping mechanisms throughout the body [4]. Another potential influence on synchronizing CG circadian expression is timed or restricted feeding that can cause periodic availability of circulating macronutrients and signaling pathways, which may then influence the timing of molecular clocks in a tissue-specific manner in both the SCN and peripheral tissues [63–68].

Clock genes and physiology

CG output is thought to indirectly (via a transcriptional cascade) coordinate the rhythmic expression of downstream genes within the same cell that are involved with the regulation of physiology and behavior [4,69–72]. It has been estimated that ≥8–10% of all genes in mouse heart and up to 50% in liver exhibit high-amplitude circadian coordination, and perhaps a considerably greater prevalence of genes show circadian "regulation" with lower amplitudes, all with probable impact on diverse physiological processes [29,73,74].

In mammals, functional CGs have been shown to influence nearly all aspects of behavior and physiology, including cardiovascular activity, endocrinology, hepatic metabolism, gastro-intestinal tract functions, cell cycle regulation, body temperature, and sleep-wake cycles, among others [19,75]. For example, intracellular circadian clock mechanisms in vascular smooth muscle cells and cardiomyocytes have been identified that appear to coordinate myocardial metabolism both directly and indirectly [76], thereby giving rise to the potential role of the circadian clock as a modulator of physiological and pathophysiological cardiovascular events [77–81]. To illustrate, a disruption of the circadian clock within the cardiomyocyte can influence disruption in the 24h heart rate rhythm, responsiveness of the heart to workload changes, myocardial metabolism, and changes in myocardial genes known to influence transport, transcription, signal transduction, protein turnover and metabolism [82].

CHRONOBIOLOGICAL ANALYSIS OF CLOCK GENE RHYTHMS

Systematic analyses of the expression of CGs in peripheral tissues are underway in order to address how peripheral oscillators share similarly-timed molecular machinery and how changes in rhythm characteristics may be involved in or be a result of biological consequences, such as impaired CG function and/or disease. While the expression profiles of principal CGs have been characterized extensively in mammals and other species, time-effects and any rhythm features (i.e., period, amplitude, acrophase) in CGs are often described macroscopically (i.e., by eye) or by statistical comparisons of paired values (e.g., peak value vs. values at other times) and not quantitatively by chronobiological statistical analysis involving curve-fitting procedures. Consequently, subjective observation can lead to less accuracy in both recognition of a rhythm, description of the amplitude or acrophase, and comparisons of rhythm characteristics among CGs in peripheral tissues [83], across species and studies, and by extension, to pathophysiologic conditions. Indeed, it has been pointed out that the statistical analysis of circadian rhythms is important for a complete understanding of both physiology and pathology in mammalian and other species [84].

As an example of objectively describing the molecular clock in peripheral tissues, we sought to apply chronobiological inferential statistical procedures (i.e., ANOVA, single cosinor) to CG data for 14 clock and clock-controlled genes in 7 peripheral organs in the mouse which were previously described subjectively via graphs of timepoint means ±SEs by two of us (TY, TT) [29]. Our aim was to statistically establish rhythm probability levels, as well as compute numerical estimates for amplitudes and acrophases for use in comparisons between CGs and/or tissues. This approach has previously been applied to the same database using CG data from the heart only [85]. The importance of CGs to health, as well as the general treatment and prognosis of human disease and the use of rhythm characteristics, are reviewed after this section.

Database used for rhythm analysis

Full study details, including CG molecular assays, for the CG data base analyzed herein are reported elsewhere [29]. Briefly, 5-week-old male Balb/c mice were exposed to 2 weeks of 12h light/12h dark (LD) cycles, then kept in complete darkness (DD) in 3 separate studies. In each study, 7 organs (lung, heart, liver, stomach, spleen, kidney, testis) were harvested from a single mouse every 4h for 24h (6/study; 18 total) beginning at the onset of the 3rd DD cycle (i.e., at circadian time [CT] = 00h, which corresponded to the previous onset of light during LD) and examined for CG mRNA expression. Results for 14 CGs[1] obtained by quantitative real-time reverse transcription-polymerase chain reaction (RT-PCR) (performed in

1 *Per* = period, *Cry* = cryptochrome, *Bmal1* = brain and muscle ARNT-like protein 1, *Rev-erb* = reverse strand of TR alpha(α) or beta (β), *Tim* = timeless, *Clock* = circadian locomotor output cycles kaput), *Dbp* = D-element (or D-box) binding protein, *CK1* = casein kinase 1 epsilon (ε) or delta (δ); *Npas2* = neuronal PAS domain protein 2, a redox-sensitive C*lock* homologue. For reference, organisms are identified by prefix: *m* = mouse, *r* = rat, *ha* = hamster, *h* = human.

triplicate) included: three isoforms of *Period* (*mPer1*, *mPer2*, *mPer3*), two isoforms of *Cryptochrome* (*mCry1*, *mCry2*), *mBmal1*, *mCK1*δ, *mCK1*ε, *mClock*, *mDbp*, *mNpas2, mRev-erb*α, *mRev-erb*β, and *mTim*. The relative levels of each mRNA were normalized to the corresponding G3-PDH RNA values used as control.

ANOVA and Cosinor analyses for time effect and rhythm characteristics

Relative levels of all mRNAs were standardized by re-expressing each value as percent of the highest value (max = 100%) for each CG in each organ in each study and combined for graphing and statistical analyses. Each time-series was analyzed for time-effect across the 6 timepoints by one-way analysis of variance (ANOVA) and for circadian rhythm characteristics by the single cosinor procedure involving the fit of a 24h cosine to the data by least-squares linear regression [86], using the ChronoLab statistical package [87]. A 24h&12h composite cosine was also fit to each time series to test for ultradian periodicity and/or a better approximation of the circadian waveform. An R^2 value (= % reduction of total variability by fitted cosine, which is similar to the R^2 obtained when fitting a straight line by linear regression when testing for a trend) and a p-value from a zero-amplitude test were determined for the cosine model, with rhythm detection considered statistically significant if $p \leq 0.05$ and borderline significant if $p \leq 0.10 > 0.05$. Rhythm characteristics and their dispersion indices determined from the best-fitting 24h cosine include: the "mesor" (**m**idline-**e**stimating **s**tatistic **o**f **r**hythm = the middle of the cosine representing an adjusted 24h average if unequidistant sampling); the "amplitude" (the distance from the mesor to the peak or trough of the fitted curve, with the double amplitude indicating a predictable range of change defined by the cosine); and the "acrophase" (the peak of the cosine in hours from an external reference event, such as local midnight or time of light onset, indicating the estimated time of highest values).

Rhythm detection and characteristics for 14 CGs in 7 organs

Figures 1–14 show chronograms, in alphabetical order, of each CG in the 3 individual studies (left panels) and overall timepoint means±SE along with the best-fitting 24h cosine (right panels) for each of the 7 organs. In general, 24h patterns were highly reproducible across the 3 studies in terms of amplitudes and the timing of peaks and troughs for a particular CG in 6 of the 7 organs (see discussion of testis below) (left panels). Although circadian variation is suggested in *mTim* in patterns from individual studies, peaks were widely dispersed across the 3 studies and various tissues, resulting in suppressed overall average circadian patterns that were not significant, except for spleen (Figure 14).

Results of analyses of each CG are listed alphabetically for time-effect by ANOVA and rhythm detection by single cosinor in Tables 1 and 2. Apart from testis, which has been reported to be clock independent without circadian rhythmicity due to being a rapidly differentiating immature tissue (see Methodological considerations), a significant circadian time-effect by ANOVA and/or circadian rhythm by single cosinor was detected at $p \leq 0.05$ in each of the remaining 6 peripheral tissues for seven CGs (*mBmal1*, *mDbp*, *mNpas2*, *mPer1,2,3, mRev-erb*α), in 5 tissues for two CGs (*mCry1*, *mRev-erb*β), in 4 tissues for *mClock*, in 3 tissues for *mCry2*, in 2 tissues for *mCKI*δ and in 1 tissue for *mCKI*ε and *mTim* (Tables 1 & 2). Of note, significant circadian time-effects were found in testis for *mBmal1* and *mDbp* (Table 1, Figures 1 & 7). In addition, a 12h rhythm was found in testis at $p = 0.043$ for *mPer3* and $p = 0.045$ for *mPer1*, while a 12h rhythm was borderline significant at $p = 0.062$ for *mPer2*. While the addition of a 12h component to a 24h&12h cosine slightly improved waveform characterization for several CGs in some tissues, no other CG showed a significant 12h rhythm in any tissue if the 24h rhythm was not significant, as was the case for *mPer1,2,3* in testis.

Acrophases identify integrated location of peaks

The acrophase does not always exactly coincide with the time of the highest value measured and can therefore be especially useful in estimating an integrated peak time between high values obtained in sampling schedules that are either equidistant or unequidistant. In our cosinor analysis of CG data obtained every 4h, there was good agreement between the original approximate estimates of maxima by eyeballing and with the point and interval estimates (i.e., ±95% limits) of the acrophase for each CG. Calculated acrophases of CG mRNA expression in each tissue, arranged in approximate temporal order of rhythm peaks from previous light-onset (CT = 00h) for each CG, are shown in an acrophase chart in Figure 15. Apart from *mTim*, peaks (acrophases) for distinct CGs were generally synchronous among the 7 tissues, especially when the 24h cosine fit was significant, indicating a congruence in timing for a specific CG among the peripheral organs studied.

Using clusters of acrophases as reference, five CGs (*mRev-erb*α*, mDbp, mRev-erb*β*, mPer3, mPer1*) reached their maxima in the second half of the previous light span in LD (i.e., late in the presumed resting span), 5 CGs (*mPer2, mCry2, mCry1, mCK1*δ*, mCK1*ε) reached their peak in the first half of the previous dark span in LD (i.e., early to middle of the presumed activity span), while 3 CGs (*mClock, mBmal1, mNpas2*) reached their peaks near the end of the previous dark span

in LD (i.e., late in the presumed activity span). As mentioned above, two peaks in testis, one late in the previous light span and one late in the previous dark span (shown as open symbols in Figure 15), were detected in *mPer1* and *mPer3* (a borderline significant 12h cosine fit to *mPer2* also showed two similarly-timed peaks).

Circadian amplitude: does magnitude = importance?

With regard to amplitude, the original report of a circadian rhythm was based upon a subjective determination of a "robust" peak to trough variation in mRNA expression over 24 hours in only 8 of the 14 CGs. However, the perception that a high-amplitude rhythm should be considered as more biologically important, and thus more consequential, overlooks the possibility that a low-amplitude protein rhythm upstream might drive a high-amplitude physiological rhythm if the protein participates in a specific downstream supportive process [26,71]. Analysis of the data found a statistically significant circadian rhythm in each of the 14 CGs, including *mTim*, *mCK1δ,* and *mCK1ε*, in at least one tissue by objective chronobiological inferential procedures even though 6 CGs (*mCry1, mCry2, mCK1δ, mCK1ε, mClock, mTim*) had comparatively small amplitudes (Tables 1, 2).

METHODOLOGICAL CONSIDERATIONS

Time of day vs. stage of rhythm

The circadian time structure of most species, including human beings and laboratory rodents, is driven by the central pacemaker (SCN) as well as a series of peripheral clocks (34) that are entrained to the ambient light-dark schedule [88]. Thus, environmental cues, such as a regular LD cycle, plus associated social cues, allow the biological clock to fine-tune the staging of circadian rhythms of body functions to meet the predictable-in-time demands of the environment specific to the various times of the day-night cycle [89]. This entrainment allows for generalizations as to the characteristics of circadian rhythms across groups of humans and other animals.

When considering the phasing of rhythms in rodents, results derived from studies involving laboratory animals generally can be extrapolated to humans with the caveat being that the findings must be adjusted for the about 12 h differences in the phasing during the 24 h activity-rest span of the respective species: mice and rats are nocturnally active, while human beings are diurnally active. Thus, circadian "stage", such as hours after awakening or light-onset, and not external clock time, allows for representative comparisons of the internal timing and the translation of findings between species and/or different lighting schedules [90]. When using mice and rats, reference to peaks and troughs observed during studies in LD can be referenced in relation to "hours after awakening" or "hours after light onset" (HALO) when working in LD, and as "circadian time" (CT) for studies in DD indicating the number of hours from the clock hour of L-onset in the previous LD synchronizing schedule (i.e., 06:00 = 00h, 12:00 = 06h, 18:00 = 12h, etc.).

Studying circadian rhythms in constant conditions

By way of some background, it should be noted that circadian rhythms are almost always characterized by a stable 24h period under natural synchronized conditions; measuring an organism under constant conditions can indicate the built-in, endogenous nature of 24h oscillations in the absence of daily light-dark alterations. When isolated from external cycles, the endogenous daily period in an organism will usually differ slightly from precisely 24h and become about (*circa*) 24h. Thus, after several days in constant conditions (CC), such as continuous light (LL) or darkness (DD), the period will drift from 24h and usually become established somewhere within the circadian range of roughly 20h and 28h. This period is known as the endogenous or "free-running" circadian period and usually, after the first couple of days with some unstable cycles (i.e., transients) between the period established under synchronizing LD conditions and the free-running period in CC, remains comparatively stable with regard to length [91]. When studying CGs on the 3rd day in constant conditions as far as DD is concerned, it could therefore be expected that the underlying circadian period might have started to slowly drift either longer or shorter from precisely 24h in the mice under study, resulting in a movement of the acrophase away from its previous location during 24h synchronized LD conditions and a possible dampening of the amplitude.

Examples of similar circadian characteristics in LD vs. the first few days in DD

An earlier report by Takekida et al. [41] of *rPer1* and *rPer2* in rat pineal studied for 24h in LD and on the 2nd day in DD observed nearly identical circadian patterns in both lighting conditions for each CG, indicating the endogenous nature of the rhythmic expression in CGs that persists under CC, but does not change very much during at least the first few days in DD. When cosinor analysis was applied to these data, we could confirm statistically that the amplitudes did not differ significantly between LD and DD (27±11% vs. 35±10% for *rPer1* and 41±5% vs. 36±9% for *rPer2*), and the acrophases (referenced to time of L-onset in LD = CT 00) differed by <1h during LD & day 2 in DD (17:52h vs. 17:11h for *rPer1* and 18:54h vs. 18:30h for *rPer2*).

In the current data set, CGs in mice were not measured during synchronized LD conditions, so no data were available in order to test for any change in rhythm characteristics during

CC. However, using cosinor analysis we made comparisons between circadian patterns for CGs in mice in DD in this study with 24h patterns found in the literature in some of the same CGs studied in LD for mice or rats. We found that amplitudes and acrophases in the current study were virtually identical for 7 CGs in liver, spleen, and kidney for mice sampled in LD by Liu et al. [37], e.g., acrophases differed by an hour or less between CGs in LD vs. day 3 in DD, while for 8 CGs in rat heart studied in LD by Young et al. [43], amplitudes were comparable and acrophases were slightly, but not significantly, advanced by 1–2 hours in LD vs. day 3 in DD in the current study. These findings suggest that the rhythms observed on day 3 in DD in CG mRNA expression were still comparable to patterns found during LD and thus allow for analysis and discussion of circadian characteristics for CGs in the current data set using a precise 24h cosine to describe the oscillations observed during DD in relation to the previous synchronizing light-dark/rest-activity cycle.

Developmental aspect of circadian profiles for some CGs and tissues

The lack of a significant time-effect for *mTim* in 6 out of 7 tissues is not surprising, since mammalian *Tim (Timeless)* has been reported to be a developmental gene without substantial circadian function [2]. Most reports failed to detect a significant time-of-day change or only a weak circadian oscillation for *Tim* in the SCN and its functional role in peripheral mammalian clocks, such as its interaction with CRY proteins in DNA repair pathways, is still open to question [90]. Similarly, it was demonstrated that clock genes could be expressed in a more or less constant or erratic, rather than rhythmic, manner in organs composed primarily of differentiating cells, like testis [93] and thymus [30]. Based on these findings, it was hypothesized that clock gene expression is developmentally regulated, and that the circadian clock does not operate in immature cells that are undergoing differentiation. This concept was extended to the non–24h rhythmic expression in most of the key CGs (*mPer1, mRev-erbα, mBmal, mCry1, mClock*, but not *mPer2*) in mouse bone marrow primitive stem cells [35] and for some CGs (*hCry1, hBmal1, hRev-erbα, hClock*, but not *hPer1,2, hCry1*) in human bone marrow stem/progenitor cells [58], indicating weaker circadian profiles in these primitive cells as compared to those reported in other mature tissues. These findings corroborate the lack of a fully-developed circadian system in rapidly proliferating tissues, similar to the testis and thymus.

Subjective vs. objective interpretations of rhythms

In the original publication of the data used as the basis for the current review, subjective visual inspection was used to interpret the temporal expression of 14 clock and clock-related genes in 7 peripheral tissues in the mouse [29][2]. With a focus on objective interpretation of the same data, we herein reanalyzed all the CG data using ANOVA and the single cosinor technique in order to make a comparison of macroscopic (i.e., subjective, by eye) vs. microscopic (i.e., objective, inferential statistical) interpretation of the presence and characteristics of circadian variations in CGs.

With regard to rhythm detection, the original publication [29] reported that mRNA expression of 8 genes (*mPer1,2,3, mBmal1, mRev-erbα,β, mNpas2 and mDbp*) "showed a robust circadian rhythm" in all peripheral tissues and speculated that these 8 genes "likely constitute the core molecules of a molecular circadian clock." It was also noted that the rhythm of mRNA expression for *mCry1* "was obviously circadian…, but the peak-trough amplitude was relatively smaller than that of the above genes." In addition, it was mentioned that *mCry2* and *mClock* were "rather weak and not clearly circadian", and that "no circadian rhythms were observed in … *mCK1δ, mCK1ε,* and *mTim*." When these same data were subjected to ANOVA and cosinor statistics, however, each clock gene was shown to be circadian rhythmic in at least one tissue: a significant or borderline-significant circadian rhythm was found in all 7 tissues for *mBmal1* and *mDbp*, 6 tissues for *mPer1,2,3*, *mRev-erbα,β*, *mCry1*, *mClock* and *Npas2*, 3 tissues for *mCry2* and *mCKIδ*, and one tissue for *mCKIε* and *mTim*.

Objective comparisons using amplitudes and acrophases

With the cosinor technique we demonstrate that statistical determination of rhythm parameters for CGs allows for a quantitative description of a circadian amplitude and acrophase for each CG in each tissue. Accordingly, we propose that both values can be beneficial in making objective comparisons of CG circadian characteristics between various peripheral organs, species, and/or studies utilizing a variety of experimental conditions, such as different photoperiods and/or phase shifts [29,47,53,94,95], feeding schedules [63,64,68,94,96], during development and aging [12,13,15,40,41,49,63,97,98], as well as between health and disease or induced disorders, such as gene mutations. For such comparisons, parameter tests have been developed to objectively compare rhythm parameters between single series or groups [87,99].

In addition, the statistical determination of the acrophase by itself can also be of importance, since a phase shift can

2 It should be noted that in the original publication by Yamamoto et al., 2004 [29], the first two columns of chronograms in Figure 1 were inadvertently labeled 'heart' and 'lung' and should have been labeled 'lung' and 'heart'.

be equivalent to a down-regulation at a defined timepoint, indicating that gene interaction needs to be interpreted in the context of the phase of a circadian oscillation [73]. Along these lines with regard to the effect of meal timing on CG acrophase relationships, access to food restricted to 4h early in the daily L-span (CT 02–05h) shifted CG expression at the RNA and protein level in mouse gastrointestinal tract, but did not shift CG expression in the SCN, indicating altered acrophase relationships between the central clock and the periphery [68].

In a search of the literature, we found that time-series analysis to obtain rhythm detection probability and characteristics has been applied using one form of cosinor or curve-fitting technique or another [100] to CG data in studies of **fish** retina, liver and gut [7], **mouse** SCN [2,83], skeletal muscle, kidney and thymus [32], liver and mammary tumor [101], bone marrow [35], adipose, cardiac and liver tissues [93], liver, kidney, spleen, testis, thymus, and blood [37], calvarial (skull) bone [38], gastrointestinal tract [36,68], as well as in blood pressure and heart rate of *Clock*-mutant mice [102]; in **rat** SCN and pineal [103]; and in **human** skin and oral mucosa [55], bone marrow [58], and peripheral blood leukocytes [57,59,60].

RHYTHMS IN HEALTH AND DISEASE – THE CLOCK GENE ASSOCIATION

Under synchronized conditions nearly every body function studied displays a circadian time-structure in health, with known times of highest and lowest values – the "hands of the clock" in the current vernacular – in relation to an individual's sleep-wake schedule. Circadian mechanisms influence nearly all aspects of physiology, psychology and behavior, which includes sleep-wake cycles and nearly all functions involving cardiovascular, respiratory, digestive, integumentary, nervous, endocrine, immune/lymphatic, excretory (urine), reproductive, muscular, skeletal, behavioral and whole body systems; circadian characteristics have been established in health for 100's of these variables [104,105].

There is now a growing appreciation that the feeling of well-being and susceptibility to a variety of medical disorders depend on the proper expression and synchrony of circadian clocks throughout the body, including the SCN and peripheral tissues [23]. Numerous reports of humans or mice with mutations or targeted knock-out disruptions of core CGs have shown that the molecular clock influences different biochemical pathways involved in pathophysiology. Consequently, studies have linked altered function (i.e., overexpression, downregulation, mutations, gene absence, etc.) of specific CG components of the circadian clock with numerous metabolic and psychopathological disorders, including aging-related pathologies, bipolar disorders, cancer development and regulation, cardiovascular control and disease, diabetes, obesity and metabolic syndrome, hepatotoxicity, reproductive performance, seasonal affective disorder, sleep apnea, and sleep-phase syndromes (Table 3), among others (c.f., Table 2 in Ko & Takahashi, 2006 [19]; Table 3 in Borgs et al., 2009 [9]). There has also been speculation that deregulation of clock-associated biological processes, such as clock-regulated androgen expressions, could be involved with the high prevalence of prostate cancer, with circadian genes proposed as novel risk factors and prognostic biomarkers [39,107,144].

Future perspectives – CGs from bench to bedside and beyond

Molecular models are growing in complexity and with it comes a better understanding of how biological clocks and timing systems function. Appreciating relationships between circadian clocks and normal vs. abnormal organ physiology can have an important impact relevant to more effective treatments and prognoses of human disease processes [127]. Accumulating information on the molecular clock in a tissue-specific manner presents new avenues for therapeutic intervention, including chronotherapy [145] in conditions where disturbance of circadian CG expression is an important cause of morbidity in chronic illnesses and diseases with a strong circadian component, including coronary vascular disease [146], epilepsy [147], cancer [101,145] asthma [148,149], and possibly Parkinson's Disease [150]. For example, targeted regulation of CG expression of a mammalian clock gene (*mPer2)* was effective as a novel therapy for the treatment of malignant tumors in mice [151]. It could also lead to new strategies for pharmacological manipulation of the human time structure to improve the treatment of various circadian system-related sleep and psychiatric disorders, jet lag and other human disorders and diseases [152].

Since genetic molecular mechanisms of about 24h rhythms may be related to more than just one spectral component, the molecular basis of how infradian rhythms (e.g., weekly, monthly, yearly, etc.) enter CG time structures (genomes) directly, as seems likely, or via circadians, and how they depend on circadians is another area awaiting investigation [153].

ACKNOWLEDGEMENT

The lead author (RBS) dedicates this review to Franz Halberg on the occasion of his 90th birthday on July 5, 2009. Halberg, who may well be the last remaining original pioneer in the field of biological rhythms [154, 155], coined the term 'circadian' in 1959 [156] and many other terms commonly used in

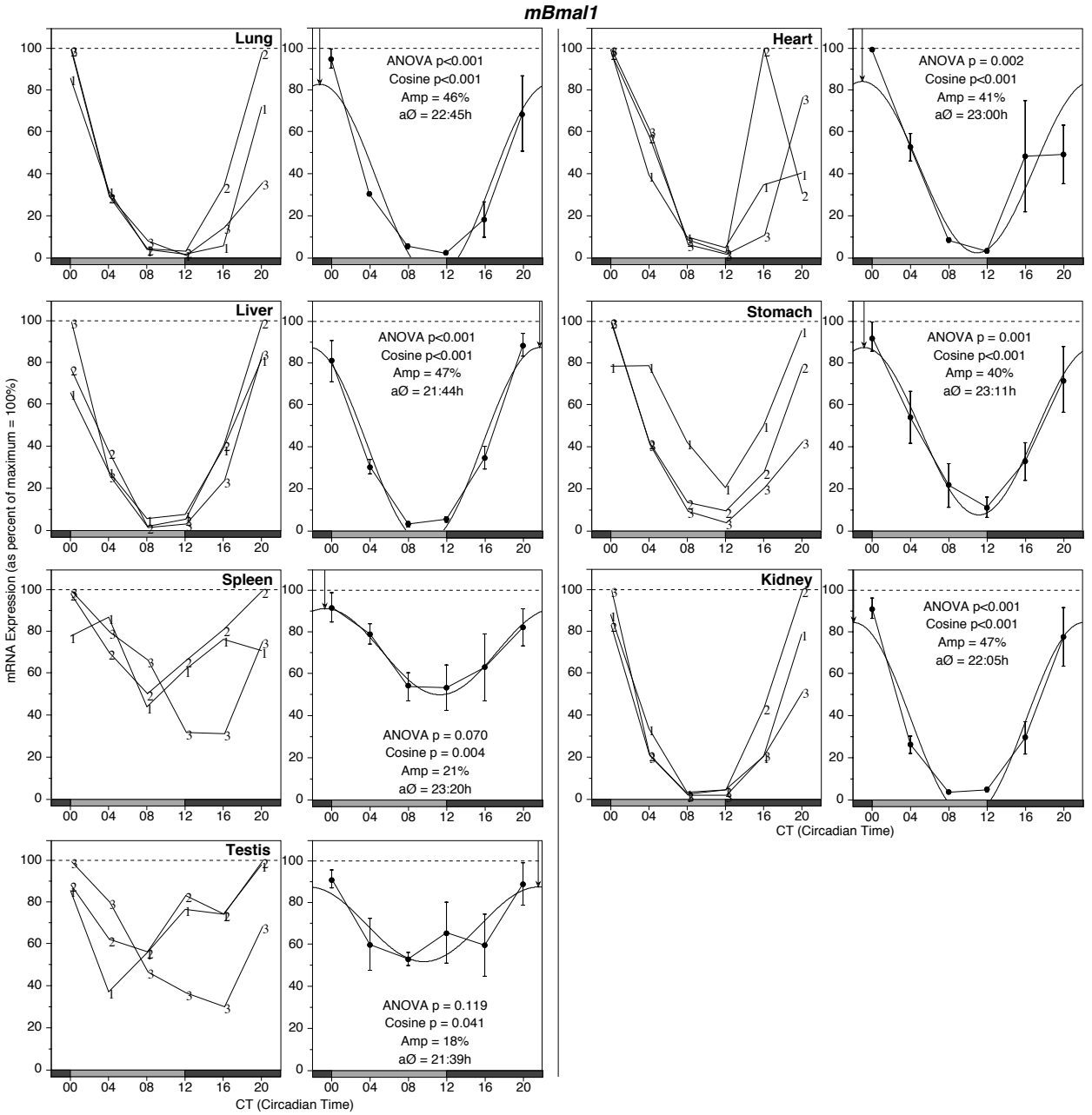

Figure 1

Circadian chronograms for clock gene *mBmal1* mRNA expression in 7 mouse peripheral organs. Male Balb/c mice exposed to LD12:12 for two weeks followed by complete darkness (DD), then examined every 4h for 24h on the 3rd day in DD beginning at previous light onset in LD (= 00h Circadian Time [CT]). Relative CG mRNA levels normalized to the corresponding G3-PDH RNA levels and each sample expressed as % of maximum value (= 100%) in each time series. Y-axis = mRNA amounts; x-axis = CT, gray and black bars along x-axis indicate the duration of prior light and dark spans in LD, respectively. Left panels for each organ: 3 single studies showing extent of reproducibility of 24h patterns. Right panels: overall timepoint means±SE with best-fitting 24h cosine. For time-effect, p-values from ANOVA and 24h cosine, and amplitude & acrophase (aØ, arrow) are listed.

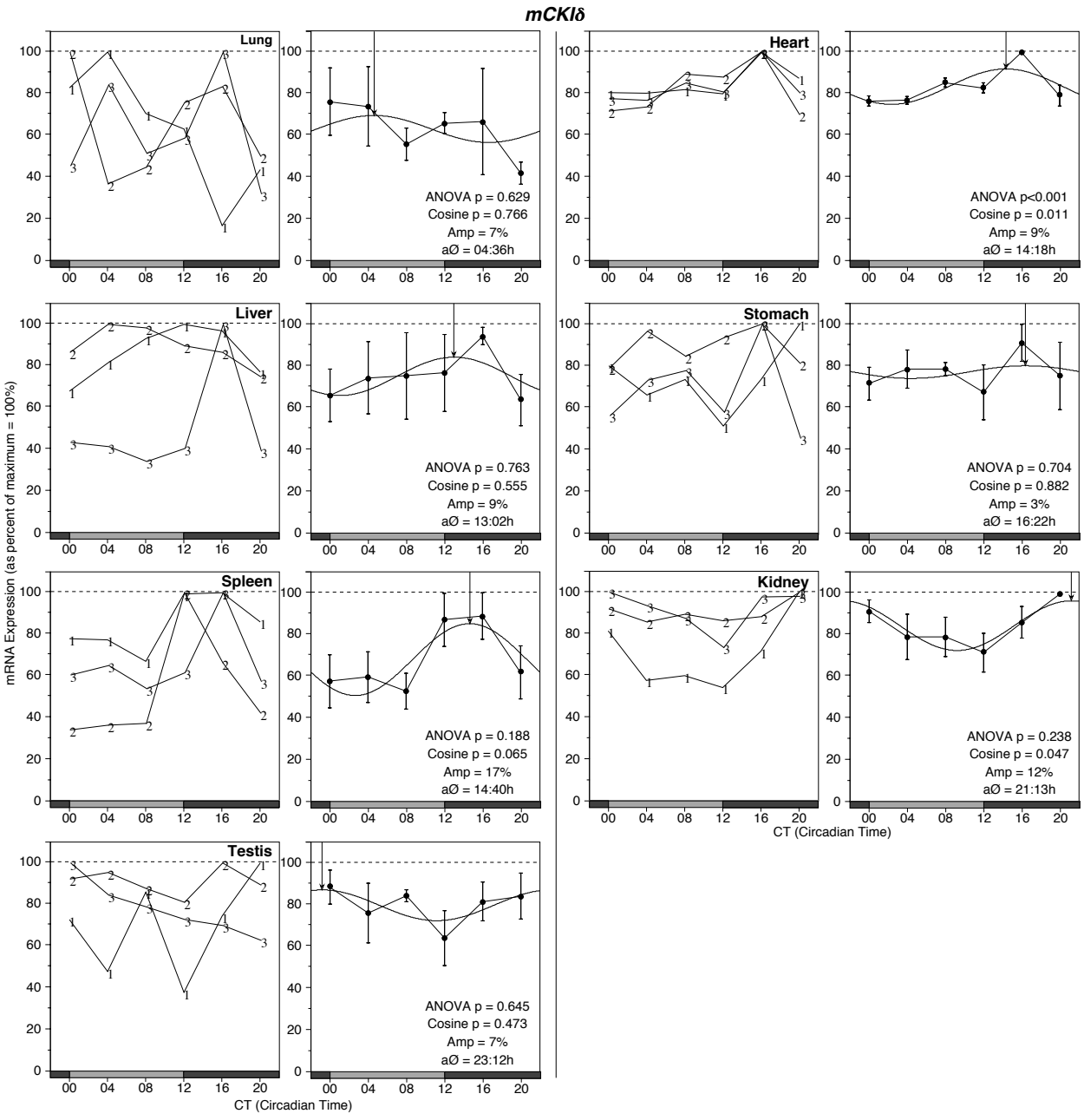

Figure 2
Circadian chronograms for clock gene *mCKI*δ mRNA expression in 7 mouse peripheral organs. See legend to Figure 1 for details.

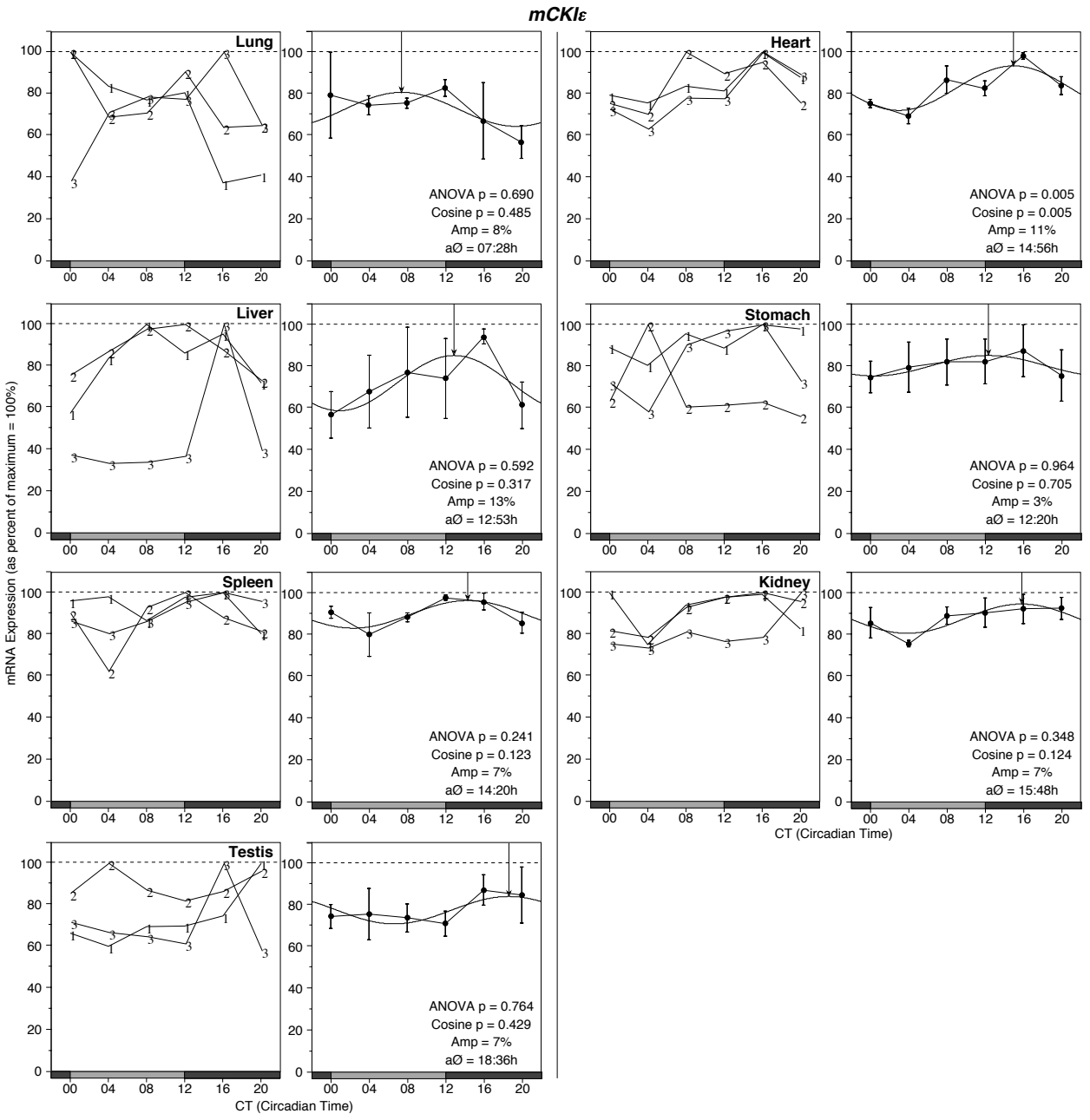

Figure 3
Circadian chronograms for clock gene *mCKIε* mRNA expression in 7 mouse peripheral organs. See legend to Figure 1 for details.

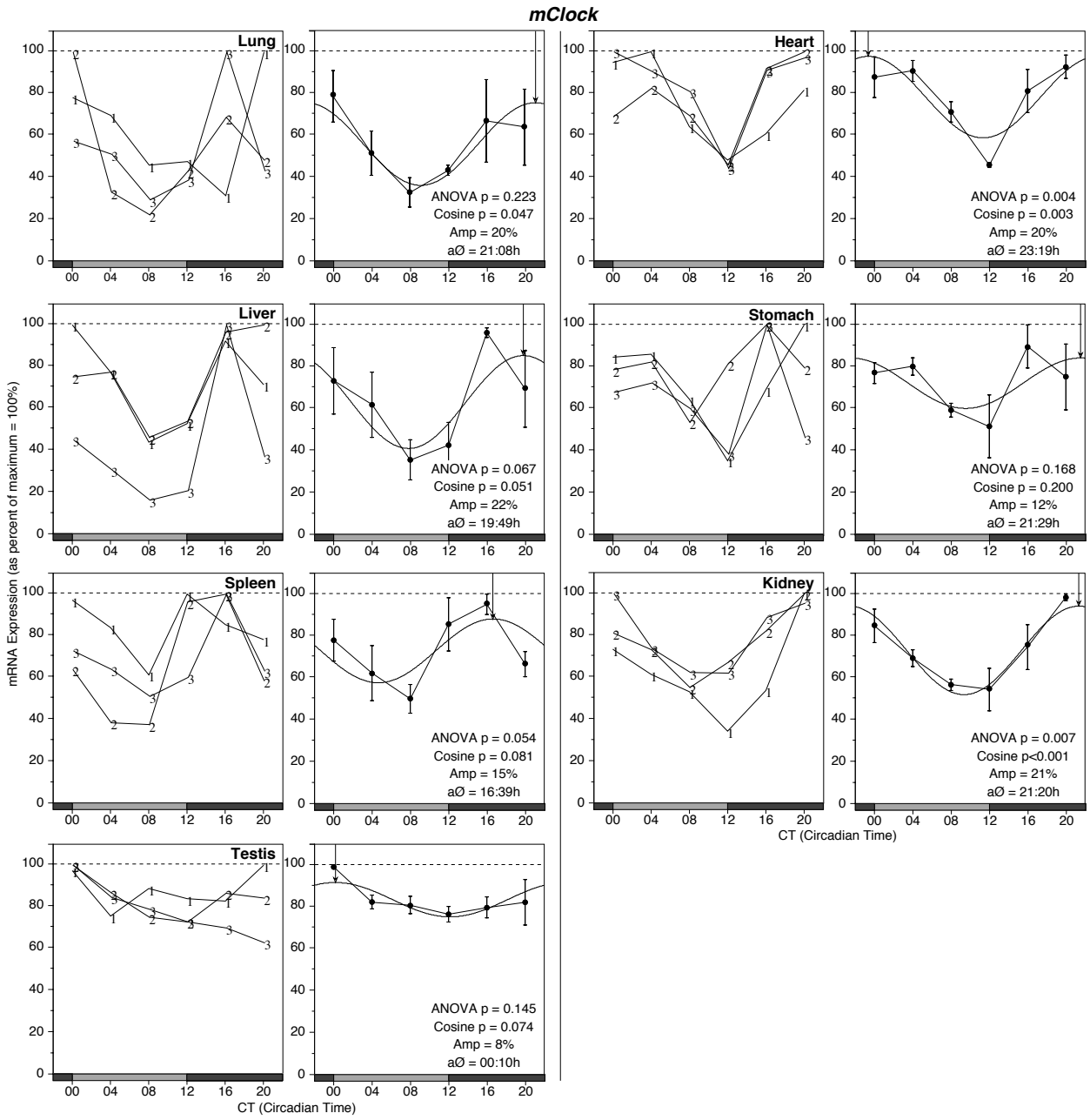

Figure 4
Circadian chronograms for clock gene *mClock* mRNA expression in 7 mouse peripheral organs. See legend to Figure 11 for details.

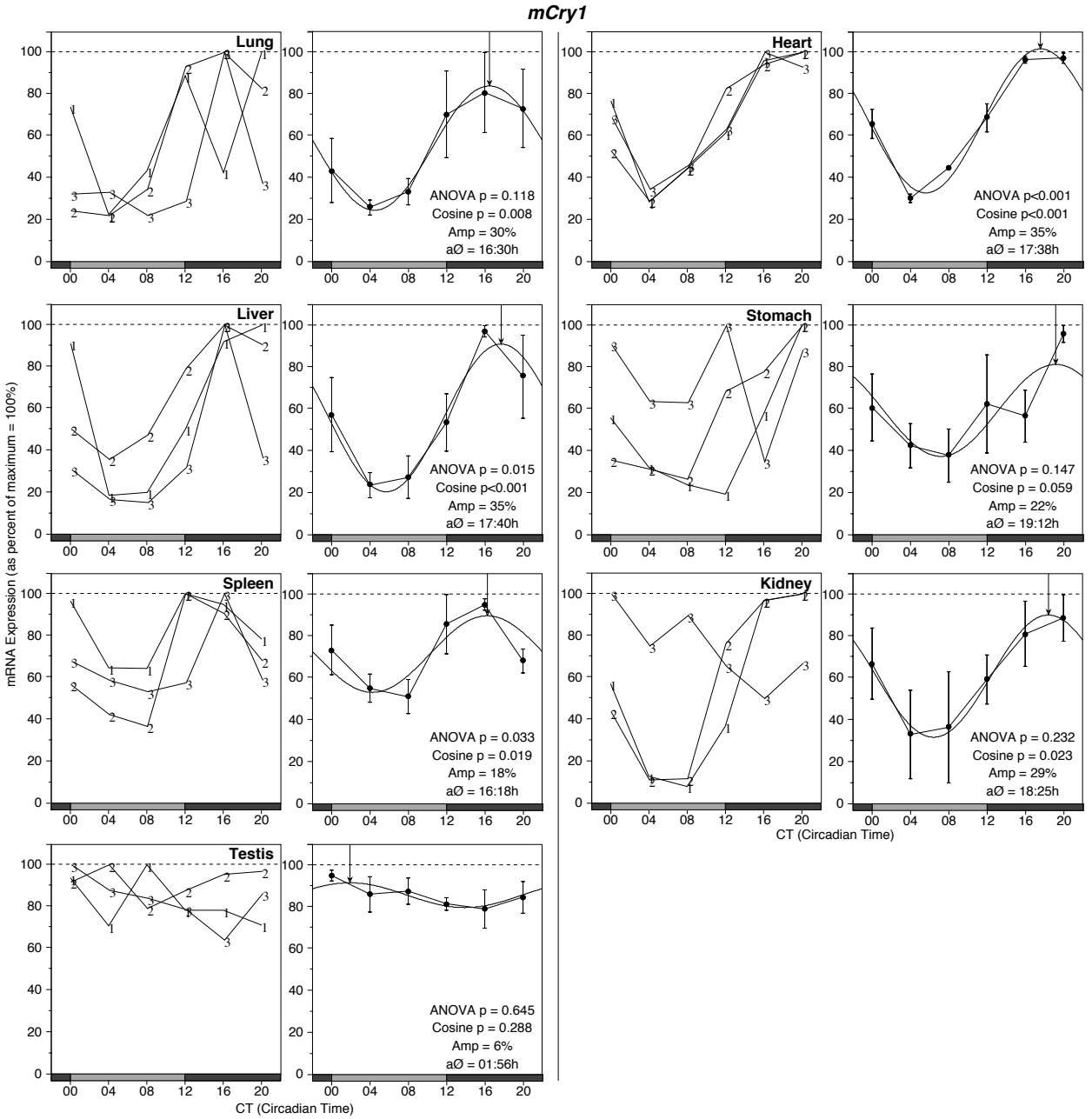

Figure 5
Circadian chronograms for clock gene *mCry1* mRNA expression in 7 mouse peripheral organs. See legend to Figure 1 for details.

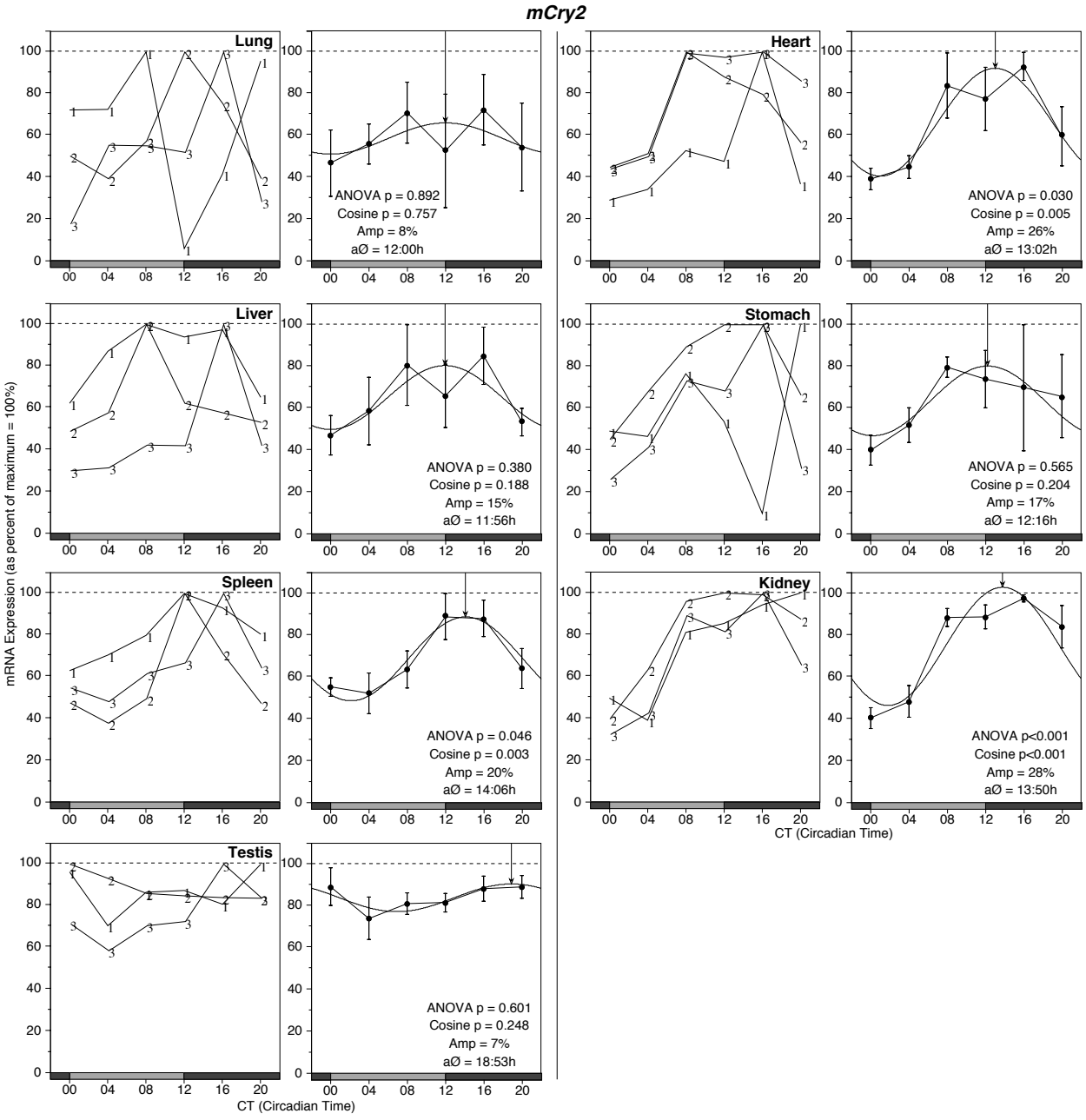

Figure 6
Circadian chronograms for clock gene *mCry2* mRNA expression in 7 mouse peripheral organs. See legend to Figure 1 for details.

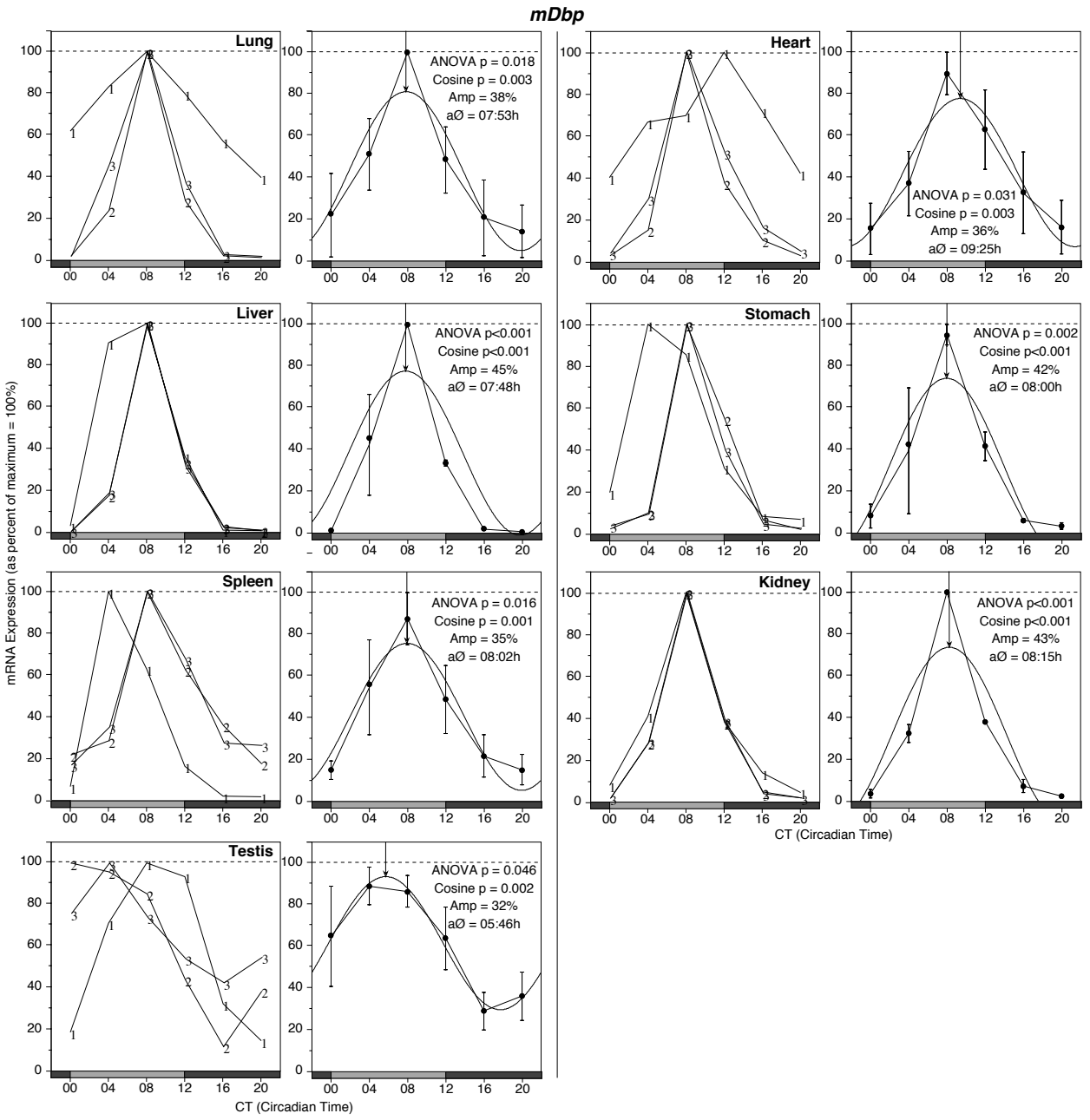

Figure 7
Circadian chronograms for clock gene *mDbp* mRNA expression in 7 mouse peripheral organs. See legend to Figure 1 for details

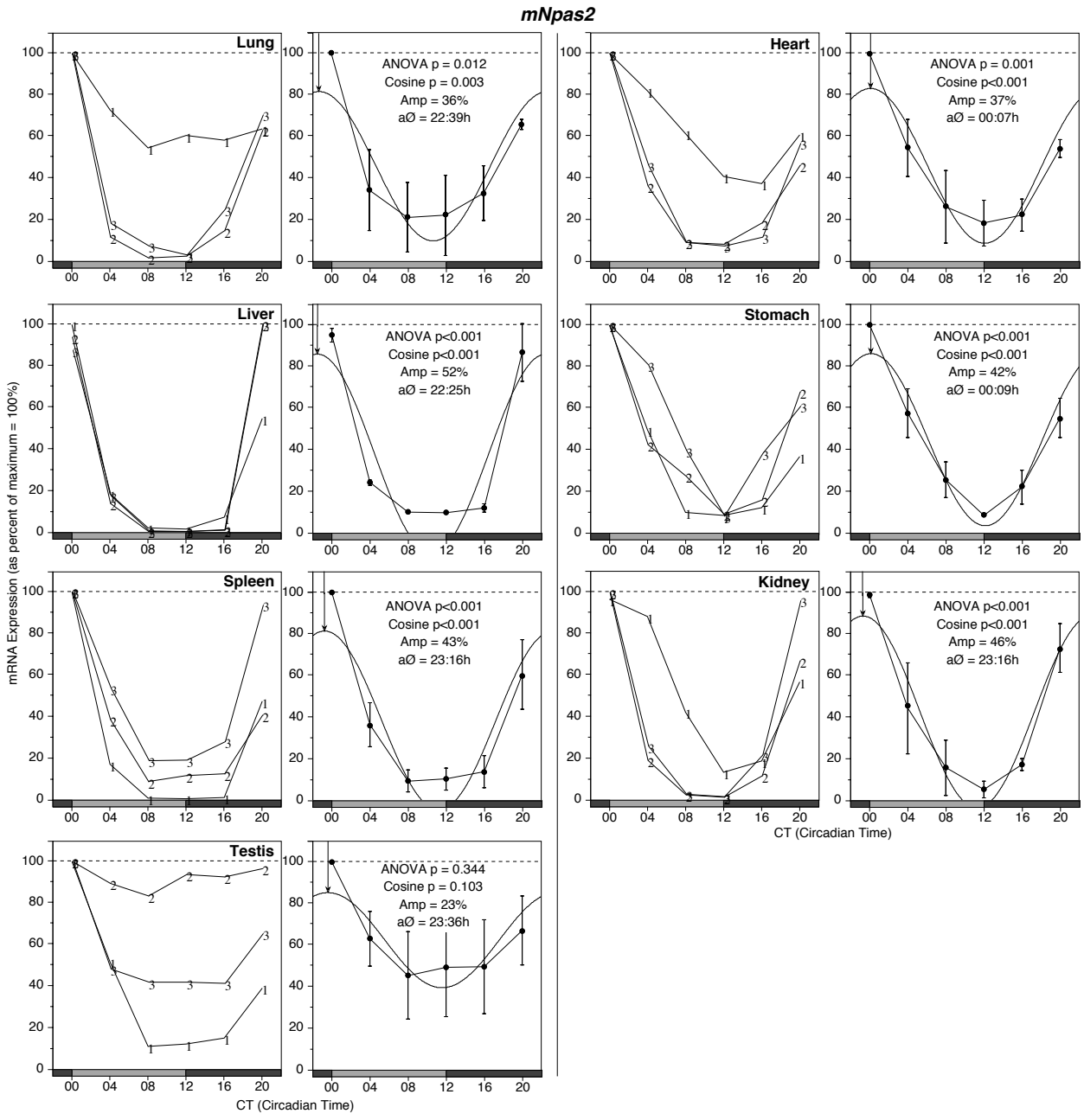

Figure 8
Circadian chronograms for clock gene *mNpas2* mRNA expression in 7 mouse peripheral organs. See legend to Figure 1 for details.

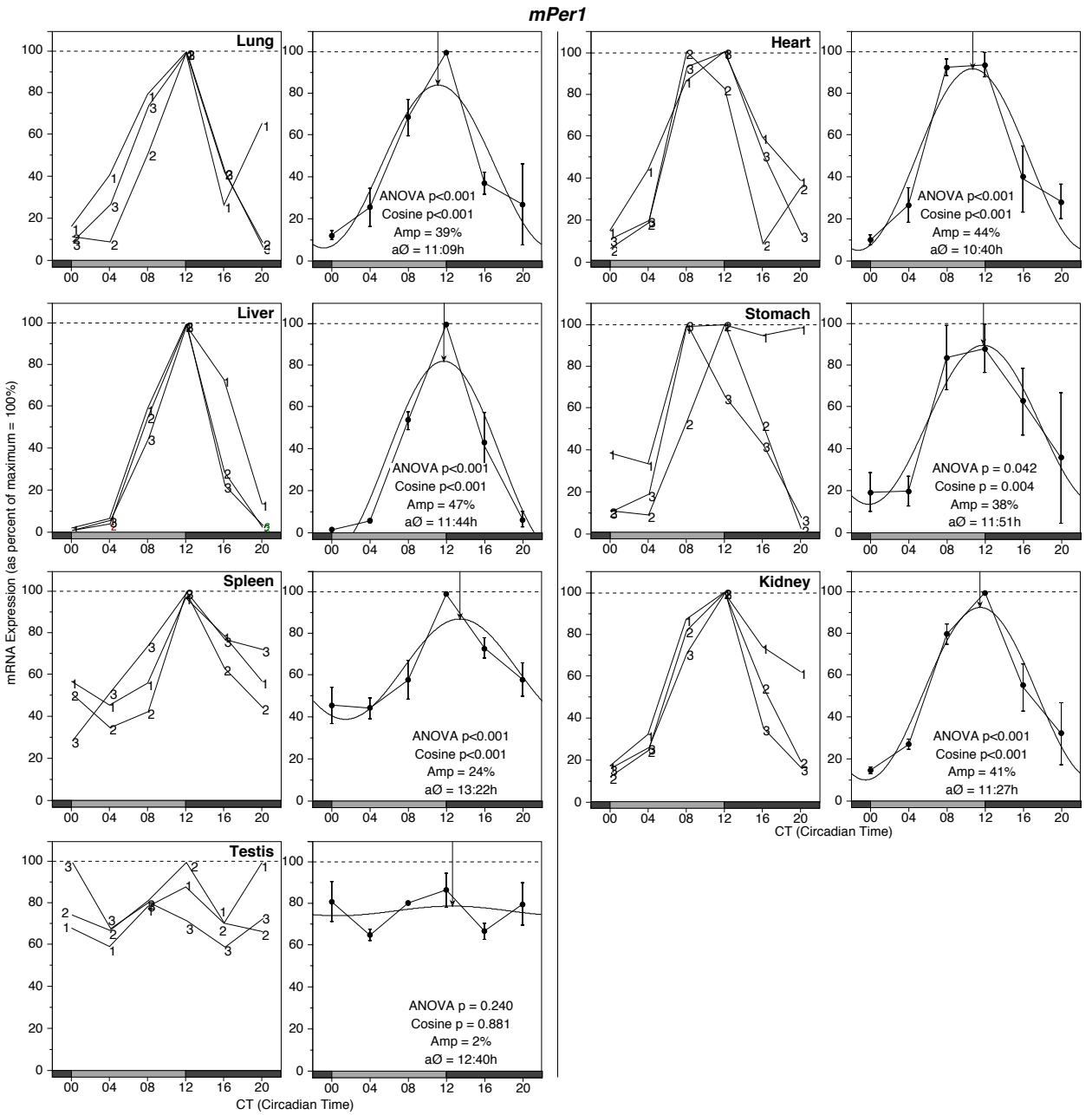

Figure 9
Circadian chronograms for clock gene *mPer1* mRNA expression in 7 mouse peripheral organs. See legend to Figure 1 for details.

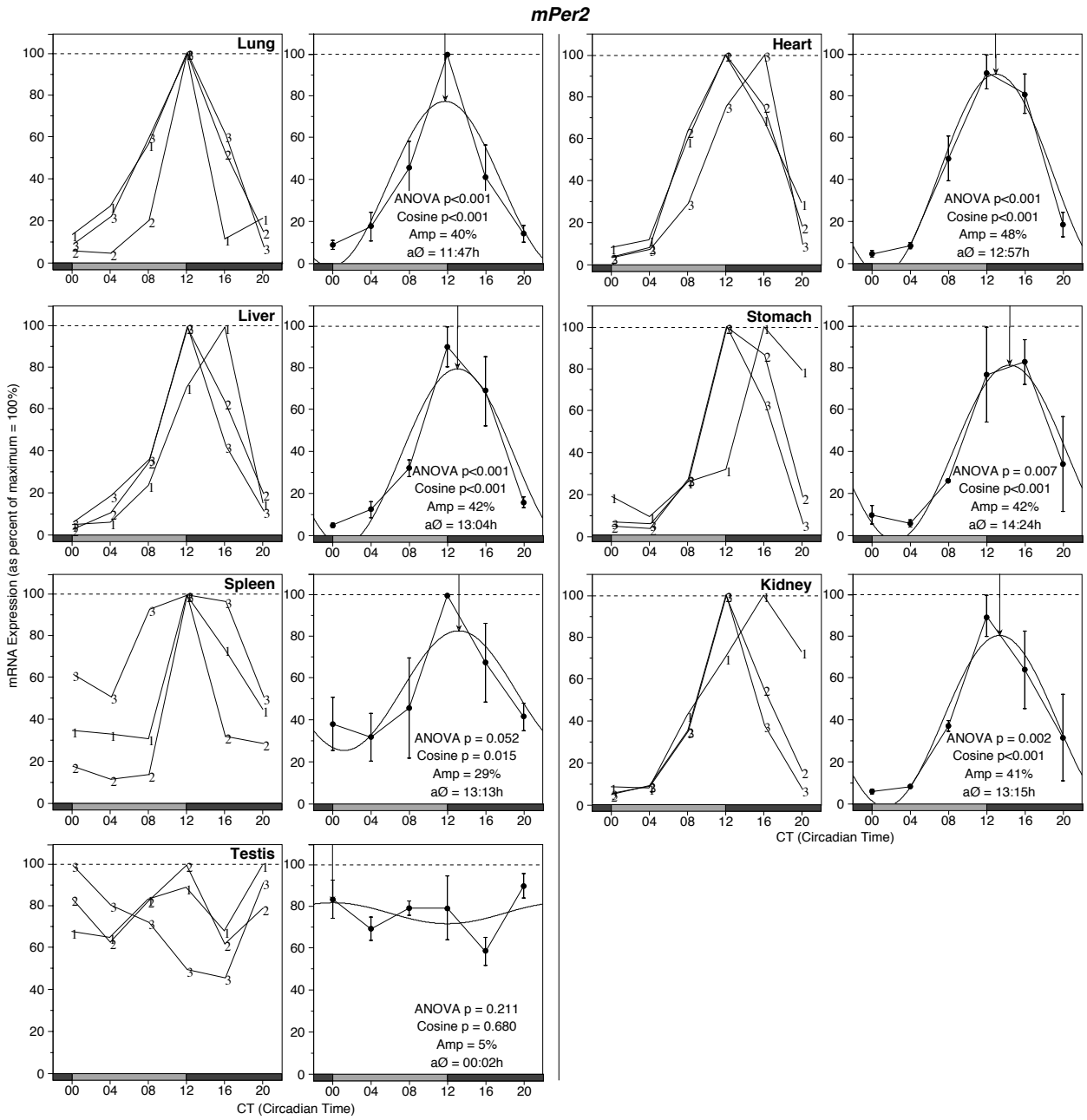

Figure 10
Circadian chronograms for clock gene *mPer2* mRNA expression in 7 mouse peripheral organs. See legend to Figure 1 for details

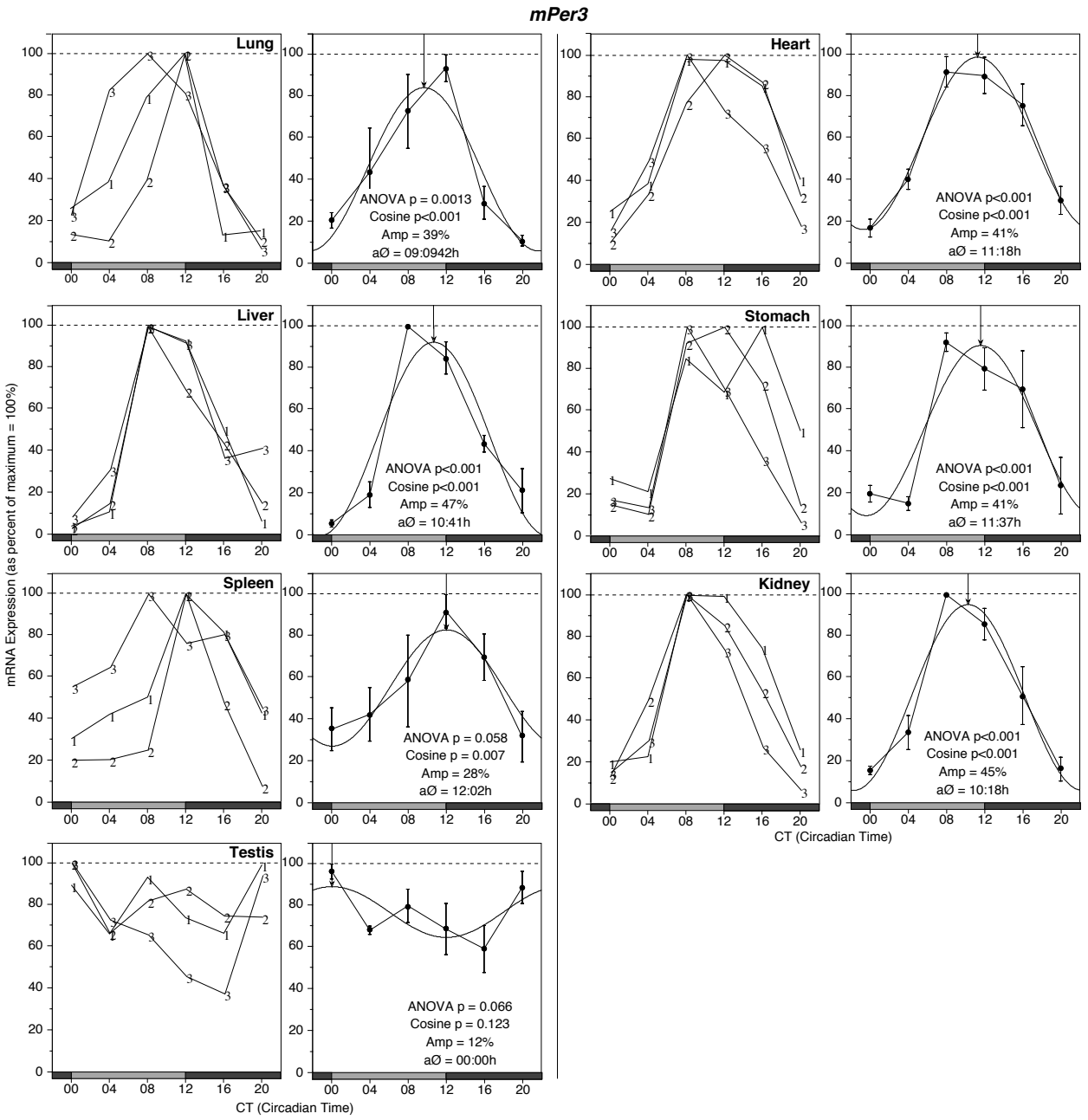

Figure 11
Circadian chronograms for clock gene *mPer3* mRNA expression in 7 mouse peripheral organs. See legend to Figure 1 for details.

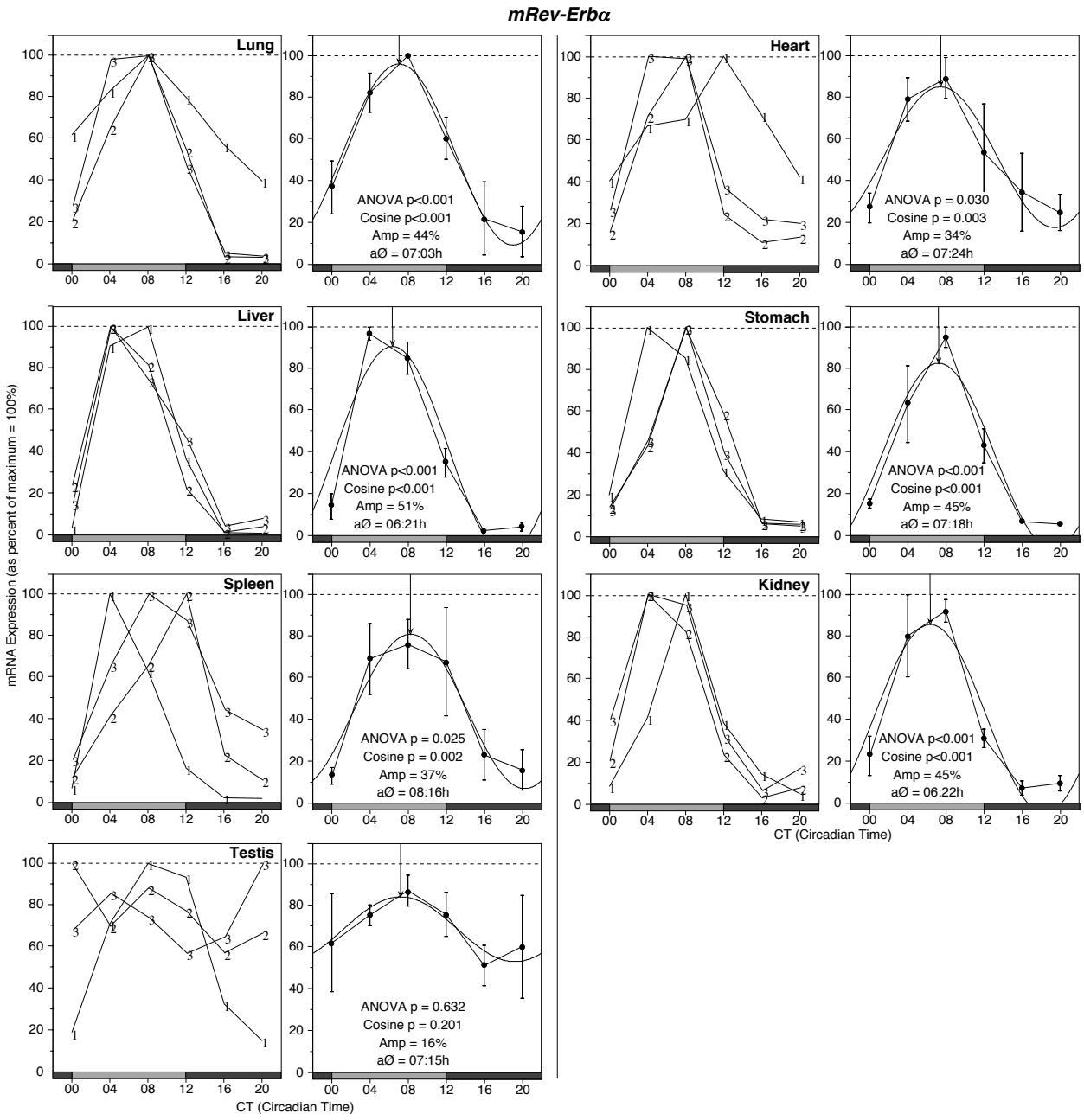

Figure 12
Circadian chronograms for clock gene *mRev-erbα* mRNA expression in 7 mouse peripheral organs. See legend to Figure 1 for details.

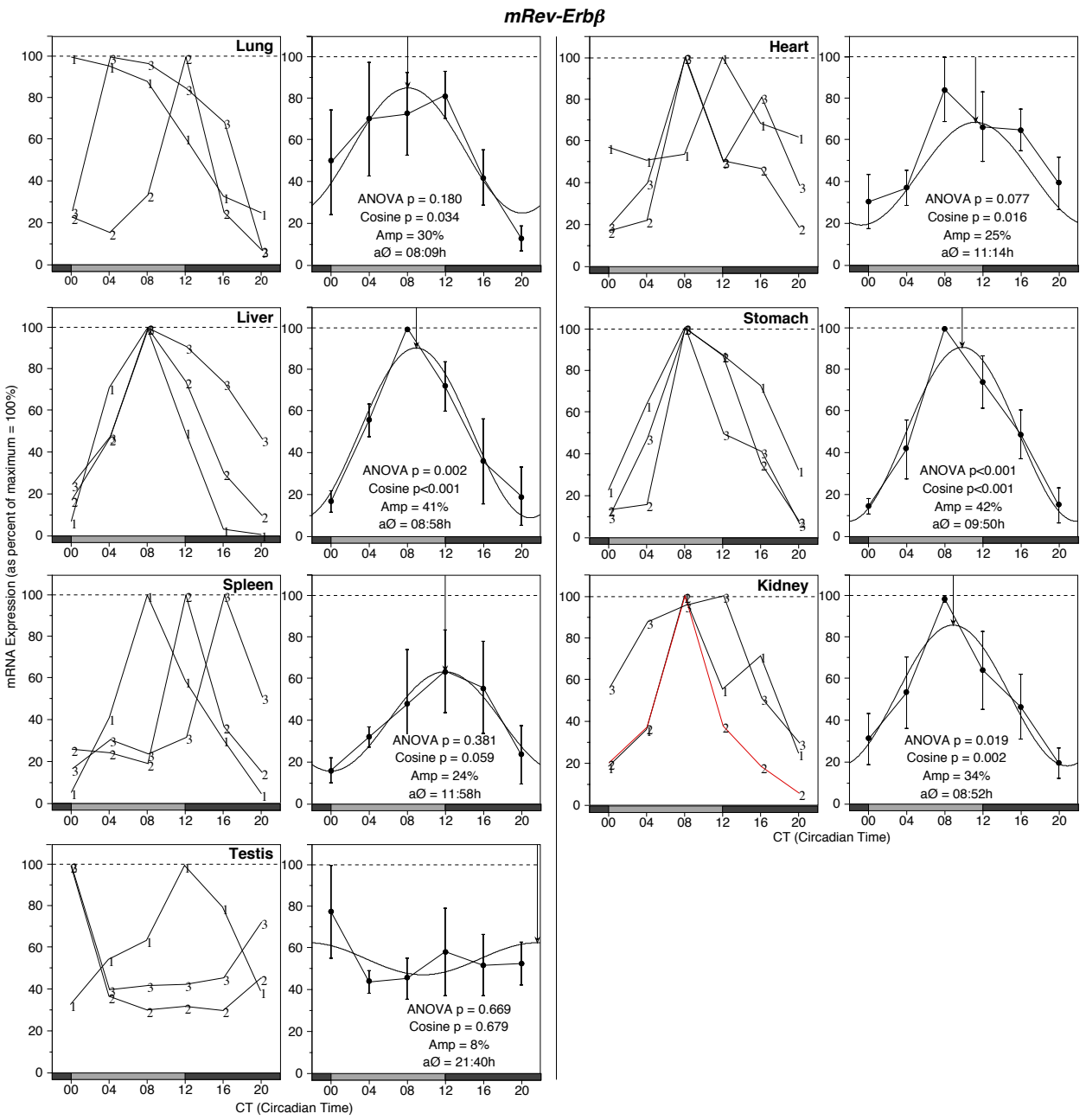

Figure 13
Circadian chronograms for clock gene *mRev-erb*β mRNA expression in 7 mouse peripheral organs. See legend to Figure 1 for details.

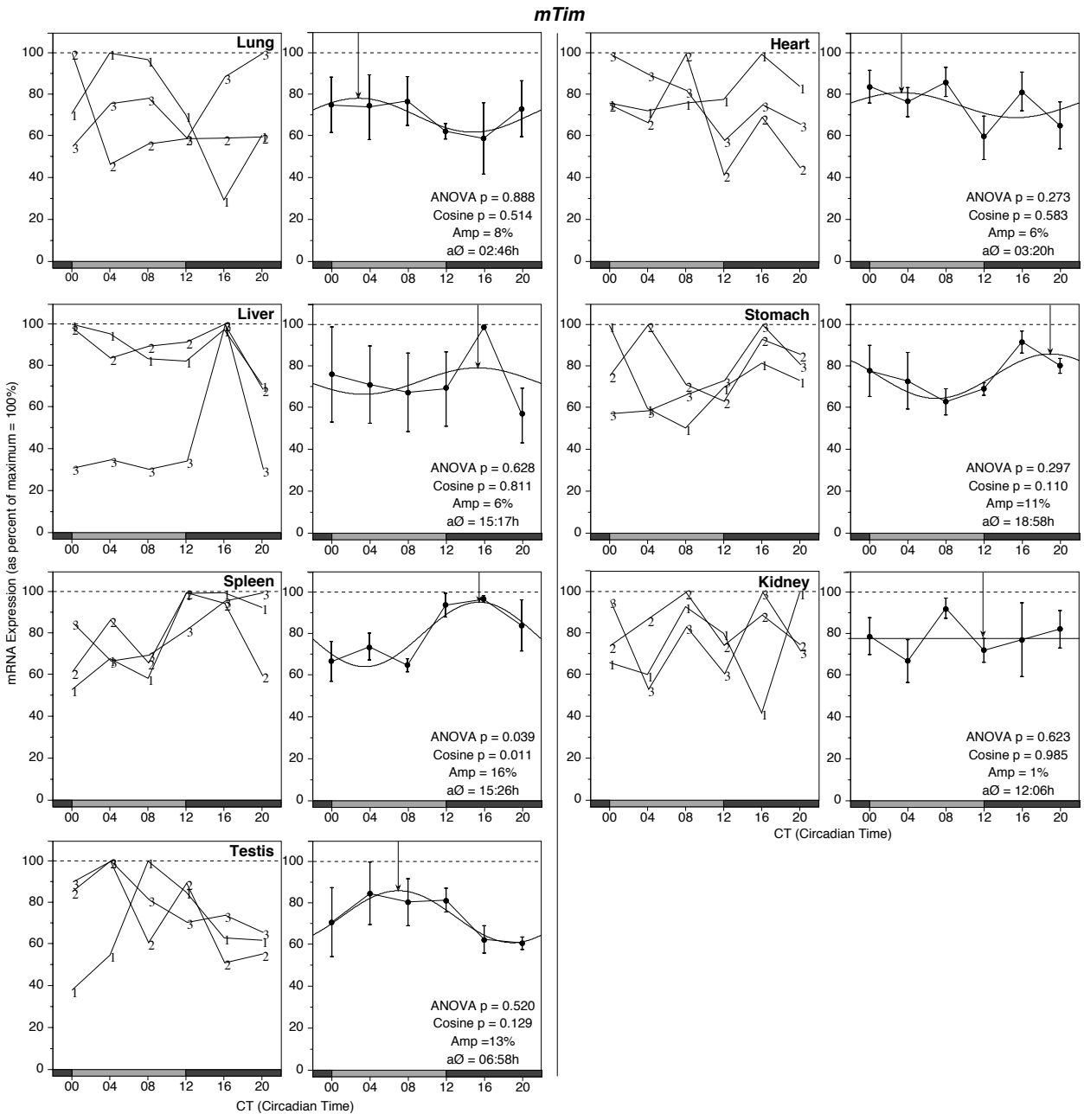

Figure 14
Circadian chronograms for clock gene *mTim* mRNA expression in 7 mouse peripheral organs. See legend to Figure 1 for details.

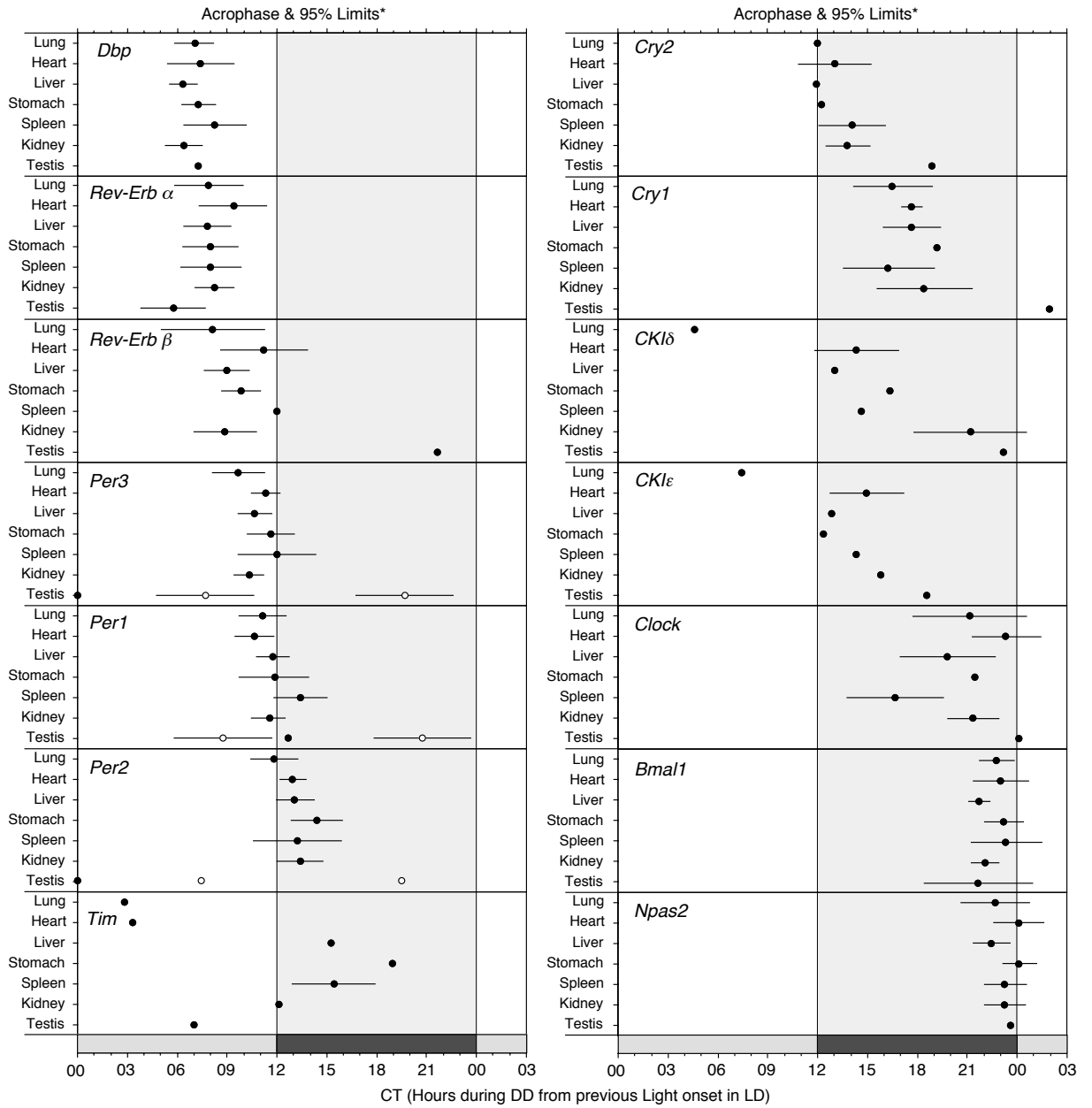

Figure 15

Acrophase chart indicating timing of peak expression of mRNA for 14 key clock genes in each of 7 peripheral organs of mice (arranged in approximate chronologic order from mid-L; see Figure 1 legend for details). Acrophase (Ø) = peak of fitted 24h cosine using all data from 3 studies (n = 18); 95% confidence limits added to Ø if p≤0.05 from non-zero amplitude test. Lighter and darker gray bars along x-axis indicate the duration of light (L) and dark (D) spans, respectively, during LD schedule prior to DD (continuous darkness); CT = circadian time.

Table 1: Circadian Parameters for mRNA Expression of 7 Key Clock Genes in 7 Peripheral Tissues in Mice on Day 3 of DD*

Results for Time-Effect by Analysis of Variance (ANOVA) and Single Cosinor**

		ANOVA		24h cosine					
Gene	Tissue	F	p	%R	p	Mesor ±SE	Amp ±SE	aØ	(95% Conf Limits)
Bmal1	lung	19.9	<0.001	81	<0.001	36.8 ±4.1	46.2 ±5.8	22:45h	(21:44, 23:48h)
″	heart	7.7	0.002	63	<0.001	43.6 ±5.8	41.1 ±8.2	23:00h	(21:20, 00:40h)
″	liver	46.7	<0.001	92	<0.001	40.8 ±2.4	46.9 ±3.5	21:44h	(21:08, 22:20h)
″	stomach	8.9	0.001	77	<0.001	47.6 ±4.0	40.1 ±5.6	23:11h	(22:00, 00:20h)
″	spleen	2.8	0.070	52	0.004	70.8 ±3.6	20.6 ±5.1	23:20h	(21:12, 01:28h)
″	kidney	28.2	<0.001	86	<0.001	37.8 ±3.4	46.7 ±4.9	22:05h	(21:12, 22:56h)
″	testis	2.2	0.119	35	0.041	70.0 ±4.5	17.9 ±6.3	21:39h	(18:24, 00:56h)
*Ckl*δ	lung	0.7	0.629	4	0.766	63.2 ±6.2	6.5 ±8.8	04:36h	- -
″	heart	9.9	<0.001	45	0.011	83.5 ±1.7	8.5 ±2.4	14:18h	(11:48, 16:48h)
″	liver	0.5	0.763	8	0.555	75.0 ±5.9	9.2 ±8.3	13:02h	- -
″	stomach	0.6	0.704	2	0.882	77.0 ±7.3	3.0 ±6.0	16:22h	- -
″	spleen	1.8	0.188	31	0.065	67.9 ±4.8	17.2 ±6.7	14:40h	- -
″	kidney	1.6	0.238	34	0.047	84.2 ±3.1	11.9 ±4.3	21:13h	(17:48, 00:36h)
″	testis	0.7	0.645	10	0.473	79.6 ±4.2	7.4 ±5.9	23:12h	- -
*CKI*ε	lung	0.6	0.690	9	0.485	72.7 ±4.7	8.2 ±6.6	07:28h	- -
″	heart	6.2	0.005	51	0.005	83.0 ±1.9	10.7 ±2.7	14:56h	(12:44, 17:08h)
″	liver	0.8	0.592	14	0.317	72.0 ±5.9	13.3 ±8.4	12:53h	- -
″	stomach	0.2	0.964	5	0.705	80.3 ±4.1	2.9 ±5.8	12:20h	- -
″	spleen	1.6	0.241	24	0.123	89.8 ±2.1	6.6 ±3.0	14:20h	- -
″	kidney	1.2	0.348	24	0.124	87.7 ±2.3	7.0 ±3.2	15:48h	- -
″	testis	0.6	0.764	11	0.429	77.8 ±3.5	6.6 ±1.9	18:36h	- -
Clock	lung	1.6	0.223	33	0.047	56.0 ±5.1	19.8 ±7.2	21:08h	(17:44, 00:32h)
″	heart	6.6	0.004	53	0.003	78.4 ±3.3	19.5 ±4.7	23:19h	(21:16, 01:24h)
″	liver	2.8	0.067	33	0.051	63.1 ±5.8	22.2 ±8.2	19:49h	(17:04, 22:36h)
″	stomach	1.9	0.168	19	0.200	72.1 ±4.5	12.1 ±6.4	21:29h	- -
″	spleen	3.0	0.054	29	0.081	72.8 ±4.4	15.3 ±6.2	16:39h	- -
″	kidney	5.5	0.007	66	<0.001	73.1 ±2.8	21.2 ±3.9	21:20h	(19:48, 22:52h)
″	testis	2.0	0.145	29	0.074	83.5 ±2.3	8.2 ±3.3	00:10h	- -
Cry1	lung	2.2	0.118	48	0.008	54.4 ±5.7	29.8 ±8.1	16:30h	(14:08, 18:52h)
″	heart	40.7	<0.001	92	<0.001	67.5 ±1.8	34.5 ±2.6	17:38h	(17:04, 18:16h)
″	liver	4.6	0.015	62	<0.001	55.7 ±5.1	35.4 ±7.2	17:40h	(15:56, 19:24h)
″	stomach	2.0	0.147	31	0.059	59.3 ±6.0	22.0 ±8.4	19:12h	- -
″	spleen	3.6	0.033	41	0.019	71.5 ±4.0	18.3 ±5.7	16:18h	(13:32, 19:04h)
″	kidney	1.6	0.232	39	0.023	60.9 ±6.6	29.3 ±9.4	18:25h	(15:32, 21:16h)
″	testis	0.7	0.645	15	0.288	85.7 ±2.6	5.9 ±3.6	01:56h	- -
Cry2	lung	0.3	0.892	4	0.757	58.7 ±7.0	7.5 ±9.9	12:00h	- -
″	heart	3.7	0.030	51	0.005	66.5 ±4.7	25.9 ±6.6	13:02h	(10:48, 15:12h)
″	liver	1.2	0.380	20	0.188	65.1 ±5.6	15.3 ±7.9	11:56h	- -
″	stomach	0.8	0.565	19	0.204	63.5 ±6.3	16.7 ±8.9	12:16h	- -
″	spleen	3.2	0.046	54	0.003	68.7 ±3.4	20.1 ±4.8	14:06h	(12:04, 16:08h)
″	kidney	14.5	<0.001	71	<0.001	74.7 ±3.3	28.3 ±4.7	13:50h	(12:28, 15:12h)
″	testis	0.8	0.601	17	0.248	83.9 ±2.7	6.6 ±3.8	18:53h	- -
Dbp	lung	4.3	0.018	55	0.003	42.6 ±6.4	38.2 ±9.0	07:53h	(05:52, 09:56h)
″	heart	3.6	0.031	54	0.003	42.2 ±6.0	35.6 ±8.5	09:25h	(07:20, 11:24h)
″	liver	15.4	<0.001	71	<0.001	29.9 ±5.3	45.4 ±7.5	07:48h	(06:24, 09:12h)
″	stomach	7.3	0.002	63	<0.001	32.2 ±5.8	41.8 ±8.2	08:00h	(06:20, 09:40h)
″	spleen	4.4	0.016	59	0.001	40.4 ±5.4	35.3 ±7.7	08:02h	(06:12, 09:52h)
″	kidney	255.0	<0.001	78	<0.001	30.5 ±4.2	42.7 ±5.9	08:15h	(07:04, 09:24h)
″	testis	3.2	0.046	56	0.002	61.4 ±5.1	31.9 ±7.3	05:46h	(03:48, 07:41h)

* Mice synchronized to LD12:12 for 2 weeks and released into constant darkness (DD) by a continuation of D in 3 studies. Mice (6/study, 18 total) sampled every 4h for 24h beginning on day 3 in DD at previous L-onset in LD . Units = values normalized to corresponding control gene G3-PDH RNA level and expressed as % of maximum value, with highest value = 100%.

** Single cosinor analysis = fit of a 24h cosine to all data by least-squares linear regression. Cosine parameters = %R (percent rhythm) = % reduction by cosine of overall varaibility; p from zero-amplitude test; Mesor = 24h mean; Amp (amplitude) = distance from Mesor to peak or trough of cosine; Acrophase (aØ) = peak of best-fitting 24h cosine; 95% limits added if p≤0.05. Phase time units (hh:mm) in Circadian Time (CT), where L-onset = 00:00h.

Table 2: Circadian Parameters for mRNA Expression of 7 Key Clock Genes in 7 Peripheral Tissues in Mice on Day 3 of DD*

Results for Time-Effect by Analysis of Variance (ANOVA) and Single Cosinor**

		ANOVA		24h cosine					
Gene	Tissue	F	p	%R	p	Mesor ±SE	Amp ±SE	aØ	(95% Conf Limits)
Npas2	lung	4.8	0.012	54	0.003	45.9 ±6.1	36.0 ±8.7	22:39h	(20:36, 00:44h)
"	heart	8.2	0.001	68	<0.001	46.1 ±4.7	37.3 ±6.7	00:07h	(22:36, 01:36h)
"	liver	46.8	<0.001	79	<0.001	33.3 ±4.9	51.5 ±7.0	22:25h	(21:20, 23:32h)
"	stomach	17.9	<0.001	82	<0.001	44.8 ±3.5	41.5 ±5.0	00:09h	(23:08, 01:08h)
"	spleen	15.5	<0.001	74	<0.001	38.3 ±4.7	43.1 ±6.7	23:16h	(22:00, 00:32h)
"	kidney	10.0	<0.001	75	<0.001	42.4 ±4.9	46.2 ±6.9	23:16h	(22:00, 00:32h)
"	testis	1.3	0.344	26	0.103	62.4 ±7.0	22.9 ±9.9	23:36h	- -
Per1	lung	11.4	<0.001	70	<0.001	45.1 ±4.7	39.1 ±6.6	11:09h	(09:44, 12:32h)
"	heart	17.6	<0.001	77	<0.001	48.5 ±4.4	43.6 ±6.2	10:40h	(09:28, 11:48h)
"	liver	31.1	<0.001	82	<0.001	34.9 ±4.0	46.8 ±5.6	11:44h	(10:44, 12:44h)
"	stomach	3.3	0.042	53	0.004	51.6 ±6.6	38.2 ±9.4	11:51h	(09:44, 13:56h)
"	spleen	9.1	<0.001	66	<0.001	63.1 ±3.2	24.1 ±4.5	13:22h	(11:48, 14:56h)
"	kidney	17.3	<0.001	82	<0.001	51.3 ±3.5	41.4 ±5.0	11:27h	(10:28, 12:28h)
"	testis	1.6	0.240	2	0.881	76.7 ±3.2	2.3 ±4.6	12:40h	- -
Per2	lung	14.6	<0.001	71	<0.001	37.8 ±4.7	39.7 ±6.6	11:47h	(10:24, 13:12h)
"	heart	27.6	<0.001	89	<0.001	42.4 ±3.1	48.1 ±4.4	12:57h	(12:12, 13:44h)
"	liver	17.7	<0.001	79	<0.001	37.4 ±4.0	42.3 ±5.7	13:04h	(11:56, 14:12h)
"	stomach	5.7	0.007	67	<0.001	39.4 ±5.4	42.0 ±7.6	14:24h	(12:52, 15:56h)
"	spleen	3.1	0.052	43	0.015	54.2 ±6.1	28.7 ±8.6	13:13h	(10:36, 15:52h)
"	kidney	7.3	0.002	71	<0.001	39.5 ±4.8	41.1 ±6.8	13:22h	(12:00, 14:44h)
"	testis	1.7	0.211	5	0.680	77.1 ±4.0	5.0 ±5.7	00:02h	- -
Per3	lung	7.1	0.003	66	<0.001	44.9 ±5.1	39.3 ±7.2	09:42h	(08:08, 11:16h)
"	heart	20.1	<0.001	87	<0.001	57.4 ±3.0	41.4 ±4.2	11:18h	(10:28, 12:08h)
"	liver	39.0	<0.001	82	<0.001	45.6 ±4.0	46.6 ±5.6	10:41h	(09:40, 11:40h)
"	stomach	10.6	<0.001	69	<0.001	49.9 ±5.0	40.9 ±7.1	11:37h	(10:12, 13:04h)
"	spleen	3.0	0.058	48	0.007	54.9 ±5.3	28.0 ±7.5	12:02h	(09:40, 14:20h)
"	kidney	21.8	<0.001	85	<0.001	50.4 ±3.5	44.7 ±5.0	10:18h	(09:24, 11:12h)
"	testis	2.8	0.066	24	0.123	76.9 ±3.9	12.2 ±5.6	00:00h	- -
Rev-erbα	lung	8.5	<0.001	77	<0.001	52.6 ±4.4	43.6 ±6.2	07:03h	(05:52, 08:12h)
"	heart	3.7	0.030	55	0.003	51.4 ±5.7	33.9 ±8.0	07:24h	(05:24, 09:24h)
"	liver	66.2	<0.001	86	<0.001	39.5 ±3.7	51.1 ±5.2	06:21h	(05:32, 07:12h)
"	stomach	17.7	<0.001	82	<0.001	37.9 ±3.9	44.8 ±5.5	07:18h	(06:16, 08:20h)
"	spleen	3.9	0.025	57	0.002	43.9 ±5.8	37.2 ±8.3	08:16h	(06:24, 10:08h)
"	kidney	14.7	<0.001	78	<0.001	40.3 ±4.4	45.4 ±6.2	06:22h	(05:16, 07:32h)
"	testis	0.7	0.632	19	0.201	68.8 ±5.8	15.6 ±8.2	07:15h	- -
Rev-erbβ	lung	1.8	0.180	36	0.034	55.0 ±7.3	30.1 ±10.3	08:09h	(05:04, 11:16h)
"	heart	2.7	0.077	43	0.016	53.8 ±5.3	24.7 ±7.4	11:14h	(08:36, 13:52h)
"	liver	7.5	0.002	72	<0.001	49.7 ±4.7	40.9 ±6.7	08:58h	(07:36, 10:20h)
"	stomach	11.7	<0.001	77	<0.001	49.0 ±4.2	41.9 ±5.9	09:50h	(08:40, 11:00h)
"	spleen	1.2	0.381	31	0.059	39.6 ±6.5	23.9 ±9.1	11:58h	- -
"	kidney	4.2	0.019	57	0.002	52.1 ±5.4	33.9 ±7.6	08:52h	(07:00, 10:44h)
"	testis	0.6	0.669	5	0.679	55.0 ±6.1	7.7 ±8.6	21:40h	- -
Tim	lung	0.3	0.888	9	0.514	70.2 ±4.9	8.2 ±6.9	02:46h	- -
"	heart	1.5	0.273	7	0.583	75.6 ±4.0	6.0 ±5.7	03:20h	- -
"	liver	0.7	0.628	3	0.811	73.3 ±6.9	6.4 ±9.8	15:17h	- -
"	stomach	1.4	0.297	26	0.110	75.6 ±3.3	10.7 ±4.7	18:58h	- -
"	spleen	3.4	0.039	45	0.011	80.2 ±3.1	15.5 ±4.4	15:26h	(12:56, 17:56h)
"	kidney	0.7	0.623	0.2	0.985	78.1 ±4.3	1.1 ±6.1	12:06h	- -
"	testis	0.9	0.520	24	0.129	73.6 ±4.1	12.5 ±5.8	06:58h	- -

* Mice synchronized to LD12:12 for 2 weeks and released into constant darkness (DD) by a continuation of D in 3 studies. Mice (6/study, 18 total) sampled every 4h for 24h beginning on day 3 in DD at previous L-onset in LD . Units = values normalized to corresponding control gene G3-PDH RNA level and expressed as % of maximum value, with highest value = 100%.

** Single cosinor analysis = fit of a 24h cosine to all data by least-squares linear regression. Cosine parameters = %R (percent rhythm) = % reduction by cosine of overall varaibility; p from zero-amplitude test; Mesor = 24h mean; Amp (amplitude) = distance from Mesor to peak or trough of cosine; Acrophase (aØ) = peak of best-fitting 24h cosine; 95% limits added if p≤0.05. Phase time units (hh:mm) in Circadian Time (CT), where L-onset = 00:00h.

Table 3: Metabolic and pathophysiological disorder development & regulation associated with Clock Gene (CG) disruption

Disorder	Clock Gene(s)	Parameter(s) of Study	Reference(s)
Aging-related Pathologies	*mPer2, mBmal1*	Impaired circadian expression with senescence	Kuneida et al., 2006 [97]
"	*mBmal1*	Premature aging, lifespan	Kondratov et al., 2006 [106]; Gibson et al., 2009 [107]
"	*mClock*	Degenerative processes. accelerated aging	Antoch et al., 2008 [108]; Gibson et al., 2009 [107]
Bipolar Disorders	*hBmal1[Arntl], hPer3*	haplotypes	Nievergelt et al., 2006 [109]
"	*hClock*	Allelic & haplotypic analyses	Shi et al., 2008 [110]
Breast Cancer	*hPer1*	Down-regulation in tumor vs. normal tissue	Gery et al., 2006 [111]
"	*hPer1,2*	Down-regulation in tumor vs. normal tissue	Winter et al., 2007 [112]
"	*hPer3*	Variant genotype as marker	Zhu et al., 2005 [113]
"	*hPer1,2,3*	Down-regulation in tumor vs. normal tissue	Chen et al., 2005 [114]
Colorectal Cancer	*hPer1*	DPD* reduction during tumor progression	Krugluger et al., 2006 [115]
"	*hPer1, hClock*	Down-regulation in tumor vs. normal tissue	Mostafaie et al., 2009 [116]
Endometrial Cancer	*hPer1*	Down-regulation in tumor vs. normal tissue	Yeh et al., 2005 [117]
Hepatocellular Cancer	*hPer1,2,3, hCry2, hTim*	Down-regulation in tumor vs. normal tissue	Lin et al., 2008 [118]
Lewis Lung & Mammary Cancer	*mPer2*	Overexpression & apoptosis	Hua et al., 2006 [119]
Lymphoma	*mPer2*	Tumor rate	Lee, 2006 [120]
Non-Hodgkin's Lymphoma	*hNPAS2*	Decreased risk with variant genotypes	Zhu et al., 2007 [121]
"	*nCry1*	NHL development biomarker	Hoffman et al., 2009 [122]
Non-Small Cell Lung Cancer	*hPer1*	Down-regulation in tumor vs. normal tissue	Gery et al., 2006, 2007 [111,123]
Ovarian Cancer	*hPer1,2,3, hBmal1, hClock, hCry1,2, hCKIε*	Down-regulation in tumor vs. normal tissue	Tokunaga et al., 2008 [124]
Cardiovascular Disease(CVD)/Control	*mBmal1, mClock, mNpas2*	Thrombogenesis	Westgate et al., 2008 [125]
"	*mBmal1, mPer2, mCry1,2*	Blood pressure, heart rate	Wang et al., 2008 [103]
"	*mClock*	Blood pressure, heart rate	Sei et al., 2008 [102]
"	*mDBP, mBmal1*	Blood pressure, heart rate, activity	Su et al., 2008 [126]
"	*mPer2, mBmal1*	Induced cardiac hypertrophy	Martino et al, 2007 [127]
"	*mRev-erbα*	CVD risk factors	Fontaine & Staels, 2007 [128]
Diabetes, Obesity, Metabolic Syndrome	*hBmal1, hPer1, hCry1*	Downregulation in adipose tissue	Gómez-Abellán et al., 2008 [129]
"	*hClock*	Symptoms development	Scott et al., 2008 [130]
"	*hClock, hBmal1, hPer1,2,3*	Dampened rhythm in leukocytes	Ando et al., 2009 [61]
"	*mBmal1, mClock*	Glucogenesis	Rudic et al., 2004 [131]
"	*mClock*	Weight, metabolic markers	Oishi et al., 2005 [27]; Turek et al., 2005 [132]
Hepatotoxicity	*mPer2*	Protection from chemical toxicants	Chen et al., 2009 [133]
Reproductive Performance	*mClock*	Litter size, cycle length, breeding characteristics	Kennaway et al., 2004 [134]; Miller et al., 2004 [135]; Boden & Kennaway, 2006 [136]
Seasonal Affective Disorder	*hPer2, hBmal1, hNpas2*	Sequence variations, polymorphisms	Partonon et al., 2007 [137]
Sleep Apnea	*hPer1*	Induction of CG by glucocorticoid agonist	Burioka et al., 2008 [138]
Advanced Sleep Phase Syndrome	*hPer2, hCKIδ*	Missense mutation	Toh et al., 2003 [139]; Xu et al., 2005 [140]
Delayed Sleep Phase Syndrome	*hPer3*	# of structural polymorphisms	Ebisawa et al., 2001 [141]; Archer et al., 2003 [142]; Pereira et al., 2005 [143]

*DPD = dihydropyrimidine dehydrogenase.
For an additional list of CG defects & biological consequences, see Table 2 in Ko & Takahashi, 2006 [19] and Table 3 in Borgs et al., 2008 [9].

the field [157], including 'chronobiology' in 1969 [158], and continues to investigate all oscillations (from ultra-low to ultra-high) found on earth to the outer fringes of the solar system as a universal panacea [153]. At the cellular level, Halberg anticipated the endogenous mechanisms of molecular clocks more than 50 years ago with the demonstration of built-in nucleic acid rhythms in the cell that could be manipulated by the lighting regimen [159,160] and that persisted under conditions of light and continuous darkness [161].

REFERENCES

1. Kondo T, Strayer CA, Kulkarni RD, et al. Circadian rhythms in prokaryotes: luciferase as a reporter of circadian gene expression in cyanobacteria. Proc Natl Acad Sci USA 1993; 90: 5672–76.
2. Reppert SM, Weaver DR. Molecular analysis of mammalian circadian rhythms. Ann Rev Physiol 2001; 63: 647–76.
3. Gachon F, Nagoshi E, Brown SA, Ripperger J, Schibler U. The mammalian circadian timing system: from gene expression to physiology. Chromosoma 2004; 113: 103–12.
4. Bell-Pedersen D, Cassone VM, Earnest DJ, et al. Circadian rhythms from multiple oscillators: lessons from diverse organisms. Nat Rev Genet 2005; 6(7): 544–56.
5. Looby P, Loudon SI. Gene duplication and complex circadian clocks in mammals. Trends Genet 2005; 21(1): 46–53.
6. Sandrelli F, Costa R, Kyriacou CP, Rosato E. Comparative analysis of circadian clock genes in insects. Insect Mol Biol 2008; 17(5): 447–63. Review.
7. Velarde E, Haque R, Iuvone PM, et al. Circadian clock genes of goldfish, *Carassius auratus*: cDNA cloning and rhythmic expression of *period* and *cryptochrome* transcripts in retina, liver, and gut. J Biol Rhythms 2009; 24(2): 104–13.
8. Harmer SL. The circadian system in higher plants. Ann Rev Plant Biol 2009; 60: 357–77.
9. Borgs L, Beukelaers P, Vandenbosch R, et al. Cell "circadian" cycle: new role for mammalian core clock genes. Cell Cycle 2009; 8(6): 832–7.
10. Cassone VM, Paulose JK, Whitfield-Rucker MG, Peters JL. Time's arrow flies like a bird: Two paradoxes for avian circadian biology. Gen Comp Endocrinol 2009 doi:10.1016/j.ygcen.2009.01.003
11. Reppert SM. Interaction between the circadian clocks of mother and fetus. Ciba Found Symp 1995; 183: 198–207.
12. Kováciková Z, Sládek M, Bendová Z, Illnerová H, Sumová A. Expression of clock and clock-driven genes in the rat suprachiasmatic nucleus during late fetal and early postnatal development. J Biol Rhythms 2006; 21(2): 140–8.
13. Seron-Ferre M, Valenzuela GJ, Torres-Farfan C. Circadian clocks during embryonic and fetal development. Birth Defects Res C Embryo Today 2007; 81(3): 204–14.
14. Sakamoto K, Oishi K, Nagase T, Miyazaki K, Ishida N. Circadian expression of clock genes during ontogeny in the rat heart. Neuroreport 2002; 13(10): 1239–42.
15. Sládek M, Jindráková Z, Bendová Z, Sumová A. Postnatal ontogenesis of the circadian clock within the rat liver. Amer J Physiol Regul Integr Comp Physiol 2007; 292(3): R1224–9.
16. Nagoshi E, Saini C, Bauer C, et al. Circadian gene expression in individual fibroblasts: cell-autonomous and self-sustained oscillators pass time to daughter cells. Cell 2004; 119(5): 693–705.
17. Welsh DK, Yoo SH, Liu AC, Takahashi JS, Kay SA. Bioluminescence imaging of individual fibroblasts reveals persistent, independently phased circadian rhythms of clock gene expression. Curr Biol 2004; 14(24): 2289–95.
18. Mihalcescu I, Hsing W, Leibler S. Resilient circadian oscillator revealed in individual cyanobacteria. Nature 2004; 430(6995): 81–5.
19. Ko CH, Takahashi JS. Molecular components of the mammalian circadian clock. Hum Mol Genet 2006; 15: R271–7. Review.
20. Dardente H, Cermakian N. Molecular circadian rhythms in central and peripheral clocks in mammals. Chronobiol Int 2007; 24: 195–213.
21. Yamazaki S, Numano R, Abe M, et al. Resetting central and peripheral circadian oscillators in transgenic rats. Science 2000; 288: 682–5.
22. Ruan GX, Zhang DQ, Zhou T, Yamazaki S, McMahon DG. Circadian organization of the mammalian retina. Proc Natl Acad Sci USA 2006; 103: 9703–08.
23. Yoo SH, Yamazaki S, Lowrey PL, et al. PERIOD2:LUCIFERASE real-time reporting of circadian dynamics reveals persistent circadian oscillations in mouse peripheral tissues. Proc Natl Acad Sci USA. 2004; 101(15): 5339–46.
24. Davidson AJ, London B, Block GD, Menaker M. Cardiovascular tissues contain independent circadian clocks. Clin Exp Hypertens 2005; 27(2–3): 307–11.
25. Fukuhara C, Tosini G. Peripheral circadian oscillators and their rhythmic regulation. Front Biosci 2003; 8: d642–651. Review.
26. Chen YG, Mantalaris A, Bourne P, Keng P, Wu JH. Expression of *mPer1* and *mPer2*, two mammalian clock genes, in murine bone marrow. Biochem Biophys Res Commun 2000; 276: 724–8.
27. Oishi K, Fukui H, Ishida N. Rhythmic expression of BMAL1 mRNA is altered in Clock mutant mice: differential regulation in the suprachiasmatic nucleus and peripheral tissues. Biochem Biophys Res Commun 2000; 268: 164–171.
28. Storch KF, Lipan O, Leykin I, et al. Extensive and divergent circadian gene expression in liver and heart. Nature 2002; 417: 78–83.

29. Yamamoto T, Nakahata Y, Soma H, et al. Transcriptional oscillation of canonical clock genes in mouse peripheral tissues. BMC Mol Biol 2004; 5: 18 (9pp).
30. Alvarez JD, Sehgal A. The thymus is similar to the testis in its pattern of circadian clock gene expression. J Biol Rhythms 2005; 20: 111–21.
31. Furukawa M, Kawamoto T, Noshiro M, et al. Clock gene expression in the submandibular glands. J Dent Res 2005; 84: 1193–7.
32. Guillaumond F, Dardente H, Giguere V, Cermakian N. Differential control of *Bmal1* circadian transcription by REV-ERB and ROR nuclear receptors. J Biol Rhythms 2005; 20: 391–403.
33. Noshiro M, Furukawa M, Honma S, et al. Tissue-specific disruption of rhythmic expression of *Dec1* and *Dec2* in clock mutant mice. J Biol Rhythms 2005; 20: 404–18.
34. Peirson SN, Butler JN, Duffield GE, et al. Comparison of clock gene expression in SCN, retina, heart, and liver of mice. Biochem Biophys Res Commun 2006; 351: 800–7.
35. Tsinkalovsky O, Filipski E, Rosenlund B, et al. Circadian expression of clock genes in purified hematopoietic stem cells is developmentally regulated in mouse bone marrow. Exp Hematol 2006; 34: 1248–60.
36. Hoogerwerf WA, Sinha M, Conesa A, et al. Transcriptional profiling of mRNA expression in the mouse distal colon. Gastroenterol 2008; 135(6): 2019–29.
37. Liu S, Cai Y, Sothern RB, Guan Y, Chan P. Chronobiological analysis of circadian patterns in transcription of seven key clock genes in six peripheral tissues in mice. Chrono Intl 2007; 24(5): 793–820.
38. Zvonic S, Ptitsyn AA, Kilroy G, et al. Circadian oscillation of gene expression in murine calvarial bone. J Bone Miner Res 2007; 22(3): 357–65.
39. Bebas P, Goodall CP, Majewska M, et al. Circadian clock and output genes are rhythmically expressed in extratesticular ducts and accessory organs of mice. FASEB J 2009; 23(2): 523–33.
40. Cai Y, Liu S, Li N, et al. Postnatal ontogenesis of molecular clock in mouse striatum. Brain Res 2009; 1264: 33–8.
41. Takekida S, Yan L, Maywood ES, Hastings MH, Okamura H. Differential adrenergic regulation of the circadian expression of the clock genes *Period1* and *Period2* in the rat pineal gland. Eur J Neurosci 2000; 12(12): 4557–61.
42. Asai M, Yoshinobu Y, Kaneko S, et al. Circadian profile of *Per* gene mRNA expression in the suprachiasmatic nucleus, paraventricular nucleus, and pineal body of aged rats. J Neurosci Res 2001; 66(6): 1133–9.
43. Young ME, Razeghi P, Taegtmeyer H. Clock genes in the heart: characterization and attenuation with hypertrophy. Circ Res 2001; 88(11): 1142–50.
44. Kennaway DJ, Varcoe TJ, Mau VJ. Rhythmic expression of clock and clock-controlled genes in the rat oviduct. Mol Hum Reprod 2003; 9(9): 503–7.
45. Mühlbauer E, Wolgast S, Finckh U, Peschke D, Peschke E. Indication of circadian oscillations in the rat pancreas. FEBS Lett 200; 564(1–2): 91–6.
46. Simonneaux V, Poirel VJ, Garidou ML, et al. Daily rhythm and regulation of clock gene expression in the rat pineal gland. Brain Res Mol Brain Res 2004; 120(2): 164–72.
47. Bendová Z, Sumová S. Photoperiodic regulation of PER1 and PER2 protein expression in rat peripheral tissues. Physiol Res 2006; 55(6): 623–32.
48. Wang GQ, Fu CL, Li JX, Du YZ, Tong J. Circadian rhythms and different photoresponses of *Clock* gene transcription in the rat suprachiasmatic nucleus and pineal gland. Acta Physiol Sinica 2006; 58: 359–64.
49. Fukuhara C, Tosini G. Analysis of daily and circadian gene expression in the rat pineal gland. Neurosci Res 2008; 60(2): 192–8.
50. Kolker DE, Fukuyama H, Huang DS, et al. Aging alters circadian and light-induced expression of clock genes in golden hamsters. J Biol Rhythms 2003; 18(2): 159–69.
51. Tong Y, Guo H, Brewer JM, et al. Expression of *haPer1* and *haBmal1* in Syrian hamsters: heterogeneity of transcripts and oscillations in the periphery. J Biol Rhythms 2004; 19(2): 113–25.
52. Crawford FI, Hodgkinson CL, Ivanova E, et al. Influence of torpor on cardiac expression of genes involved in the circadian clock and protein turnover in the Siberian hamster (*Phodopus sungorus*). Physiol Genomics 2007; 31(3): 521–30.
53. Maronde E, Pfeffer M, Glass Y, Stehle JH. Transcription factor dynamics in pineal gland and liver of the Syrian hamster (*Mesocricetus auratus*) adapts to prevailing photoperiod. J Pineal Res 2007; 43(1): 16–24.
54. Yasuo S, von Gall C, Weaver DR, Korf HW. Rhythmic expression of clock genes in the ependymal cell layer of the third ventricle of rodents is independent of melatonin signaling. Eur J Neurosci 2008; 28(12): 2443–50.
55. Bjarnason GA, Jordan R, Wood PA, et al. Circadian expression of clock genes in human oral mucosa and skin: association with specific cell cycle phases. Amer J Path 2001; 158(5): 1793–1801.
56. Takimoto M, Hamada A, Tomoda A, et al. Daily expression of clock genes in whole blood cells in healthy subjects and a patient with circadian rhythm sleep disorder. Am J Physiol Regul Integr Comp Physiol 2005; 289(5): R1273–9.
57. James FO, Boivin DB, Charbonneau S, Bélanger V, Cermakian N. Expression of clock genes in human peripheral blood mononuclear cells throughout the sleep/wake and circadian cycles. Chronobiol Int 2007; 24(6): 1009–34.

58. Tsinkalovsky O, Smaaland R, Rosenlund B, et al. Circadian variations of clock gene expression in CD34+ progenitor cells in the human bone marrow. J Biol Rhythms 2007; 22(2): 140–150.
59. Archer SN, Viola AU, Kyriakopoulou V, von Schantz M, Dijk DJ. Inter-individual differences in habitual sleep timing and entrained phase of endogenous circadian rhythms of *BMAL1*, *PER2* and *PER3* mRNA in human leukocytes. Sleep 2008; 31(5): 608–17.
60. Kusanagi H, Hida A, Satoh K, et al. Expression profiles of 10 circadian clock genes in human peripheral blood mononuclear cells. Neurosci Res 2008; 61(2): 136–42.
61. Ando H, Takamura T, Matsuzawa-Nagata N, et al. Clock gene expression in peripheral leucocytes of patients with type 2 diabetes. Diabetologia 2009; 52(2): 329–35.
62. Leibetseder V, Humpeler S, Svoboda M, et al. Clock genes display rhythmic expression in human hearts. Chronobiol Intl 2009; 26(4): 621–36.
63. Damiola F, Le Minh N, Preitner N, et al. Restricted feeding uncouples circadian oscillators in peripheral tissues from the central pacemaker in the suprachiasmatic nucleus. Genes Dev 2000; 14: 2950–61.
64. Stokkan KA, Yamazaki S, Tei H, Sakaki Y, Menaker M. Entrainment of the circadian clock in the liver by feeding. Science 2001; 291(5503): 490–3.
65. Filipski E, Innominato PF, Wu M, et al. Effects of light and food schedules on liver and tumor molecular clocks in mice. J Natl Cancer Inst 2005; 97(7): 507–17.
66. Lamont EW, Diaz LR, Barry-Shaw J, Stewart J, Amir S. Daily restricted feeding rescues a rhythm of period2 expression in the arrhythmic suprachiasmatic nucleus. Neuroscience 2005; 132(2): 245–8.
67. Horikawa K, Minami Y, Iijima M, Akiyama M, Shibata S. Rapid damping of food-entrained circadian rhythm of clock gene expression in clock-defective peripheral tissues under fasting conditions. Neuroscience 2005; 134(1): 335–43.
68. Hoogerwerf WA, Hellmich HL, Cornélissen G, et al. Clock gene expression in the murine gastrointestinal tract: endogenous rhythmicity and effects of a feeding regimen. Gastroenterol 2007; 133(4): 1250–60.
69. Jin X, Shearman LP, Weaver DR, et al. A molecular mechanism regulating rhythmic output from the suprachiasmatic circadian clock. Cell 1999; 96(1): 57–68.
70. Ripperger JA, Shearman LP, Reppert SM, Schibler U. CLOCK, an essential pacemaker component, controls expression of the circadian transcription factor DBP. Genes Dev 2000; 14(6): 679–89.
71. Baggs JE, Green CB. Nocturnin, a deadenylase in Xenopus laevis retina: a mechanism for posttranscriptional control of circadian-related mRNA. Curr Biol 2003; 13(3): 189–98.
72. Schibler U, Ripperger J, Brown SA. Peripheral circadian oscillators in mammals: time and food. J Biol Rhythms 2003; 18(3): 250–60.
73. Ptitsyn AA, Zvonic S, Conrad SA, et al. Circadian clocks are resounding in peripheral tissues. PLoS Comput Biol 2006; 2(3): e16 (9pp).
74. Ptitsyn AA, Zvonic S, Gimble JM. Digital signal processing reveals circadian baseline oscillation in majority of mammalian genes. PLoS Comput Biol 2007; 3(6): e120 (7pp).
75. Stratmann M, Schibler U. Properties, entrainment, and physiological functions of mammalian peripheral oscillators. J Biol Rhythms 2006; 21(6): 494–506.
76. Durgan DJ, Hotze MA, Tomlin TM, et al. The intrinsic circadian clock within the cardiomyocyte. Amer J Physiol Heart Circ Physiol 2005; 289(4): H1530–41.
77. Young ME. Circadian rhythms in cardiac gene expression. Curr Hypertens Rep 2003; 5(6): 445–53.
78. Young ME. The circadian clock within the heart: potential influence on myocardial gene expression, metabolism, and function. Amer J Physiol Heart Circ Physiol 2006; 290(1): H1–16. Review.
79. Reilly DF, Westgate EJ, FitzGerald GA. Peripheral circadian clocks in the vasculature. Arterioscler Thromb Vasc Biol 2007; 27(8): 1694–705.
80. Bray MS, Young ME. Diurnal variations in myocardial metabolism. Cardiovasc Res 2008; 79(2): 228–37.
81. Durgan DJ, Young ME. Linking the cardiomyocyte circadian clock to myocardial metabolism. Cardiovasc Drugs Ther 2008; 22(2): 115–24. Review.
82. Bray MS, Shaw CA, Moore MW, et al. Disruption of the circadian clock within the cardiomyocyte influences myocardial contractile function, metabolism, and gene expression. Amer J Physiol Heart Circ Physiol 2008; 294(2): H1036–47.
83. Katinas GS, Halberg F, Cornélissen G, Otsuka K, Bakken EE. Time microscopy for all kinds of data including circadian clock biology. Biomed Pharmacother 2005; 59(Suppl 1): S20–23.
84. Halberg F, Cornélissen G, Wang Z, et al. Chronomics: circadian and circaseptan timing of radiotherapy, drugs, calories, perhaps nutriceuticals and beyond. J Exp Ther Oncol 2003; 3(5): 223–60. Review.
85. Sothern RB, Cornélissen G, Yamamoto T, Takumi T, Halberg F. Time microscopy of circadian expression of cardiac clock gene mRNA transcription: chronodiagnostic and chronotherapeutic implications. Clin Ter 2009; 160(2): e25-e34.
86. Nelson W, Tong YL, Lee JK, Halberg F. Methods for cosinor rhythmometry. Chronobiologia 1979; 6: 305–23.
87. Mojón A, Fernández JR, Hermida R. Chronolab: an interactive software package for chronobiologic time series analysis written for the Macintosh computer. Chronobiol Intl 1992; 9: 403–12.

88. Honma K, Hashimoto S, Nakao M, Honma S. Period and phase adjustments of human circadian rhythms in the real world. J Biol Rhythms 2003; 18: 261–70.
89. Roenneberg T, Daan S, Merrow M. The art of entrainment. J Biol Rhythms 2003; 18: 183–94.
90. Sothern RB. Time of day versus internal circadian timing references. J Infus Chemother 1995; 5: 24–30.
91. Koukkari WL, Sothern RB. General features of rhythms: terminology and characteristics. In: Introducing Biological Rhythms. New York: Springer, 2006: 19–65.
92. Gotter AL. A Timeless debate: resolving TIM's noncircadian roles with possible clock function. Neuroreport 2006; 17(12): 1229–33.
93. Morse D, Cermakian N, Brancorsini S, Parvinen M, Sassone-Corsi P. No circadian rhythms in testis: Period1 expression is clock independent and developmentally regulated in the mouse. Mol Endocrinol 2003; 17: 141–51.
94. Durgan DJ, Trexler NA, Egbejimi O, et al. The circadian clock within the cardiomyocyte is essential for responsiveness of the heart to fatty acids. J Biol Chem 2006; 281(34): 24254–69.
95. Sumová A, Kováciková Z, Illnerová H. Dynamics of the adjustment of clock gene expression in the rat suprachiasmatic nucleus to an asymmetrical change from a long to a short photoperiod. J Biol Rhythms 2007; 22(3): 259–67.
96. Goh BC, Wu X, Evans AE, et al. Food entrainment of circadian gene expression altered in PPARalpha$^{-/-}$ brown fat and heart. Biochem Biophys Res Commun 2007; 360(4): 828–33.
97. Kunieda T, Minamino T, Katsuno T, et al. Cellular senescence impairs circadian expression of clock genes in vitro and in vivo. Circ Res 2006; 98(4): 532–9.
98. Sumová A, Bendová Z, Sládek M, et al. Setting the biological time in central and peripheral clocks during ontogenesis. FEBS Lett 2006; 580(12): 2836–42.
99. Bingham C, Arbogast B, Cornélissen-Guillaume G, Lee JK, Halberg F. Inferential statistical methods for estimating and comparing cosinor parameters. Chronobiologia 1982; 9: 397–439.
100. Koukkari WL, Sothern RB. Chronobiometry: analyzing for rhythms. In: Introducing Biological Rhythms. New York: Springer, 2006: 577–602.
101. You S, Wood PA, Xiong Y, et al. Daily coordination of cancer growth and circadian clock gene expression. Breast Cancer Res Treat 2005; 91(1): 47–60.
102. Sei H, Oishi K, Chikahisa S, et al. Diurnal amplitudes of arterial pressure and heart rate are dampened in *Clock* mutant mice and adrenalectomized mice. Endocrinol 2008; 149(7): 3576–80.
103. Wang N, Yang G, Jia Z, et al. Vascular PPARγ controls circadian variation in blood pressure and heart rate through *Bmal1*. Cell Metab 2008; 8(6): 482–91.
104. Sothern RB, Roitman-Johnson B. Biological rhythms and immune function. In: Ader R, Felten DL, Cohen N, eds. Psychoneuroimmunology, 3rd ed, Vol 1. San Diego: Academic Press, 2001: 445–79.
105. Koukkari WL, Sothern RB. Clinical medicine. In: Introducing Biological Rhythms. New York: Springer, 2006: 426–525.
106. Kondratov RV, Kondratova AA, Gorbacheva VY, Vykhovanets OV, Antoch MP. Early aging and age-related pathologies in mice deficient in BMAL1, the core component of the circadian clock. Genes Dev 2006; 20(14): 1868–73.
107. Gibson EM, Williams WP 3rd, Kriegsfeld LJ. Aging in the circadian system: considerations for health, disease prevention and longevity. Exp Gerontol 2009; 44(1–2): 51–6. Review.
108. Antoch MP, Gorbacheva VY, Vykhovanets O, et al. Disruption of the circadian clock due to the Clock mutation has discrete effects on aging and carcinogenesis. Cell Cycle 2008; 7(9): 1197–204.
109. Nievergelt CM, Kripke DF, Barrett TB, et al. Suggestive evidence for association of the circadian genes PERIOD3 and ARNTL with bipolar disorder. Am J Med Genet B Neuropsychiatr Genet 2006; 141B(3): 234–41.
110. Shi J, Wittke-Thompson JK, Badner JA, et al. Clock genes may influence bipolar disorder susceptibility and dysfunctional circadian rhythm. Am J Med Genet B Neuropsychiatr Genet 2008; 147B(7): 1047–55.
111. Gery S, Komatsu N, Baldjyan L, et al. The circadian gene *per1* plays an important role in cell growth and DNA damage control in human cancer cells. Mol Cell 2006; 22(3): 375–82.
112. Winter SL, Bosnoyan-Collins L, Pinnaduwage D, Andrulis IL. Expression of the circadian clock genes *Per1* and *Per2* in sporadic and familial breast tumors. Neoplasia 2007; 9(10): 797–800.
113. Zhu Y, Brown HN, Zhang Y, Stevens RG, Zheng T. Period3 structural variation: a circadian biomarker associated with breast cancer in young women. Cancer Epidemiol Biomarkers Prev 2005; 14(1): 268–70.
114. Chen ST, Choo KB, Hou MF, et al. Deregulated expression of the *PER1*, *PER2* and *PER3* genes in breast cancers. Carcinogenesis 2005; 26(7): 1241–6.
115. Krugluger W, Brandstaetter A, Kállay E, et al. Regulation of genes of the circadian clock in human colon cancer: reduced period–1 and dihydropyrimidine dehydrogenase transcription correlates in high-grade tumors. Cancer Res 2007; 67(16): 7917–22.
116. Mostafaie N, Kállay E, Sauerzapf E, et al. Correlated downregulation of estrogen receptor beta and the circadian clock gene *Per1* in human colorectal cancer. Mol Carcinog 2009; 48(7): 642–7.

117. Yeh KT, Yang MY, Liu TC, et al. Abnormal expression of period 1 (PER1) in endometrial carcinoma. J Pathol 2005; 206(1): 111–20.
118. Lin YM, Chang JH, Yeh KT, et al. Disturbance of circadian gene expression in hepatocellular carcinoma. Mol Carcinog 2008; 47(12): 925–33.
119. Hua H, Wang Y, Wan C, et al. Circadian gene *mPer2* overexpression induces cancer cell apoptosis. Cancer Sci 2006; 97(7): 589–96.
120. Lee CC. Tumor suppression by the mammalian Period genes. Cancer Causes Control 2006; 17(4): 525–30. Review.
121. Zhu Y, Leaderer D, Guss C, et al. Ala394Thr polymorphism in the clock gene NPAS2: a circadian modifier for the risk of non-Hodgkin's lymphoma. Int J Cancer 2007; 120(2): 432–5.
122. Hoffman AE, Zheng T, Stevens RG, et al. Clock-cancer connection in non-Hodgkin's lymphoma: a genetic association study and pathway analysis of the circadian gene Cryptochrome 2. Cancer Res 2009 15; 69(8): 3605–13.
123. Gery S, Komatsu N, Kawamata N, et al. Epigenetic silencing of the candidate tumor suppressor gene *Per1* in non-small cell lung cancer. Clin Cancer Res 2007; 13(5): 1399–404.
124. Tokunaga H, Takebayashi Y, Utsunomiya H, et al. Clinicopathological significance of circadian rhythm-related gene expression levels in patients with epithelial ovarian cancer. Acta Obstet Gynecol Scand 2008; 87(10): 1060–70.
125. Westgate EJ, Cheng Y, Reilly DF, et al. Genetic components of the circadian clock regulate thrombogenesis in vivo. Circulation 2008; 117(16): 2087–95.
126. Su W, Guo Z, Randall DC, et al. Hypertension and disrupted blood pressure circadian rhythm in type 2 diabetic db/db mice. Am J Physiol Heart Circ Physiol 2008; 295(4): H1634–41.
127. Martino TA, Tata N, Belsham DD, et al. Disturbed diurnal rhythm alters gene expression and exacerbates cardiovascular disease with rescue by resynchronization. Hypertension 2007; 49(5): 1104–13
128. Fontaine C, Staels B. The orphan nuclear receptor *Reverbalpha*: a transcriptional link between circadian rhythmicity and cardiometabolic disease. Curr Opin Lipidol 2007; 18(2): 141–6.
129. Gómez-Abellán P, Hernández-Morante JJ, Luján JA, Madrid JA, Garaulet M. Clock genes are implicated in the human metabolic syndrome. Int J Obes (Lond) 2008; 32(1): 121–8.
130. Scott EM, Carter AM, Grant PJ. Association between polymorphisms in the *Clock* gene, obesity and the metabolic syndrome in man. Int J Obes (Lond) 2008; 32(4): 658–62.
131. Rudic RD, McNamara P, Curtis AM, et al. BMAL1 and CLOCK, two essential components of the circadian clock, are involved in glucose homeostasis. PLoS Biol 2004; 2(11): e377 (7pp).
132. Turek FW, Joshu C, Kohsaka A, et al. Obesity and metabolic syndrome in circadian *Clock* mutant mice. Science 2005; 308(5724): 1043–5.
133. Chen P, Li C, Pang W, et al. The protective role of *Per2* against carbon tetrachloride-induced hepatotoxicity. Am J Pathol 2009; 174(1): 63–70.
134. Kennaway DJ, Boden MJ, Voultsios A. Reproductive performance in female *Clock Delta19* mutant mice. Reprod Fertil Dev 2004; 16(8): 801–10.
135. Miller BH, Olson SL, Turek FW, et al. Circadian clock mutation disrupts estrous cyclicity and maintenance of pregnancy. Curr Biol 2004; 14(15): 1367–73.
136. Boden MJ, Kennaway DJ. Circadian rhythms and reproduction. Reproduction 2006; 132(3): 379–92.
137. Partonen T, Treutlein J, Alpman A, et al. Three circadian clock genes *Per2*, *Arntl*, and *Npas2* contribute to winter depression. Ann Med 2007; 39(3): 229–38.
138. Burioka N, Koyanagi S, Endo M, et al. Clock gene dysfunction in patients with obstructive sleep apnoea syndrome. Eur Respir J 2008; 32(1): 105–12.
139. Toh KL, Jones CR, He Y, et al. An hPer2 phosphorylation site mutation in familial advanced sleep phase syndrome. Science 2001; 291(5506): 1040–3.
140. Xu Y, Padiath QS, Shapiro RE, et al. Functional consequences of a CKIdelta mutation causing familial advanced sleep phase syndrome. Nature 2005; 434(7033): 640–4.
141. Ebisawa T, Uchiyama M, Kajimura N, et al. Association of structural polymorphisms in the human *period3* gene with delayed sleep phase syndrome. EMBO Rep 2001; 2(4): 342–6.
142. Archer SN, Robilliard DL, Skene DJ, et al. A length polymorphism in the circadian clock gene *Per3* is linked to delayed sleep phase syndrome and extreme diurnal preference. Sleep 2003; 26(4): 413–5.
143. Pereira DS, Tufik S, Louzada FM, et al. Association of the length polymorphism in the human *Per3* gene with the delayed sleep-phase syndrome: does latitude have an influence upon it? Sleep 2005; 28(1): 29–32.
144. Zhu Y, Zheng T, Stevens RG, Zhang Y, Boyle P. Does "clock" matter in prostate cancer? Cancer Epidemiol Biomarkers Prev 2006; 15(1): 3–5.
145. Lévi F, Altinok A, Clairambault J, Goldbeter A. Implications of circadian clocks for the rhythmic delivery of cancer therapeutics. Philos Transact A Math Phys Eng Sci 2008; 366(1880): 3575–98. Review.

146. Hastings MH, Reddy AB, Maywood ES. A clockwork web: circadian timing in brain and periphery, in health and disease. Nat Rev Neurosci 2003; 4(8): 649–61. Review.
147. Gachon F, Fonjallaz P, Damiola F, et al. The loss of circadian PAR bZip transcription factors results in epilepsy. Genes Dev 2004; 18(12): 1397–412.
148. Burioka N, Fukuoka Y, Takata M, et al. Circadian rhythms in the CNS and peripheral clock disorders: function of clock genes: influence of medication for bronchial asthma on circadian gene. J Pharmacol Sci 2007; 103(2): 144–9.
149. Hayasaka N, Yaita T, Kuwaki T, et al. Optimization of dosing schedule of daily inhalant dexamethasone to minimize phase shifting of clock gene expression rhythm in the lungs of the asthma mouse model. Endocrinol 2007; 148(7): 3316–26.
150. Cai Y, Liu S, Sothern RB, Xu S, Chan P. Expression of clock genes *Per1* and *Bmal1* in total leukocytes in health and Parkinson's Disease. (*submitted)*
151. Hua H, Wang Y, Wan C, et al. Inhibition of tumorigenesis by intratumoral delivery of the circadian gene *mPer2* in C57BL/6 mice. Cancer Gene Ther 2007; 14(9): 815–8.
152. Ptácek LJ, Jones CR, Fu YH. Novel insights from genetic and molecular characterization of the human clock. Cold Spring Harb Symp Quant Biol 2007; 72: 273–7. Review.
153. Halberg F, Cornélissen G, Katinas G, et al. Chronobiology's progress: season's appreciations 2004–2005. Time-, frequency-, phase-, variable-, individual-, age- and site-specific chronomics. J Appl Biomed 2006; 4: 1–38.
154. Halberg F. Temporal coordination of physiologic function. Cold Spring Harbor Symp Quant Biol 1960; 25: 289–310.
155. Halberg F, Cornélissen G, Katinas G, et al. Transdisciplinary unifying implications of circadian findings in the 1950s. J Circadian Rhythms 2003; 1: 2 (61pp).
156. Halberg F. Physiologic 24-hour periodicity; general and procedural considerations with reference to the adrenal cycle. Z für Vitamin-, Hormon u Fermentforsch 1959; 10(3/4): 225–96.
157. Halberg F, Carandente F, Cornélissen G, Katinas GS. Glossary of chronobiology. Chronobiologia 1977; 4(Suppl): 1–189.
158. Halberg F. Chronobiology. Ann Rev Physiol 1969; 31: 675–725. Review.
159. Halberg F, Barnum CP, Silber RH, Bittner JJ. 24-hour rhythms at several levels of integration in mice on different lighting regimens. Proc Soc Exp Biol (NY) 1958; 97: 897–900.
160. Halberg F, Halberg E, Barnum CP, Bittner JJ. Physiologic 24-hour periodicity in human beings and mice, the lighting regimen and daily routine. In: Withrow RB, ed. Photoperiodism and related phenomena in plants and animals. Ed Publ No. 55. Washington DC: AAAS; 1959: 803–78.
161. Halberg F, Barnum CP. Continuous light or darkness and circadian periodic mitosis and metabolism in C and D_8 mice. Amer J Physiol 1961; 201: 227–30.

CLINICAL RESEARCH ON THE ACCURACY IN DETERMINING THE PULSE WAVE RISING POINT

Yambe T.[1], Shiraishi Y.[1], Saijo Y.[1], Liu H.[1], Nitta S.[1], Imachi K.[2], Baba A.[2], Yamaguchi T.[3], Sugawara S.[3], Katahira Y.[3], Ohsawa N.[4],Mibiki Y.[4], Watanabe M.[4], Shibata M.[4], Sato N.[4], Kameyama T.[5], Akino N.[5], Munakata M.[6], Honda M.[7], Yoshizawa M.[8], Sugita N.[8]

[1] Department of Medical Engineering and Cardiology, Institute of Development, Aging and Cancer, Tohoku University, Japan
[2] Tohoku University Biomedical Engineering Research Organization, Japan
[3] Cardiovascular Center, Tohoku Kouseinenkin Hospital, Japan
[4] Miyagi Cardiovascular Respiratory Center, Japan
[5] Miyagi Shakaihoken Hospital, Japan
[6] Tohoku Rosai Hospital, Japan
[7] Sennan Hospital, Japan
[8] Information Synergy Center, Tohoku University, Japan

Received after revision July 2009

KEY WORDS

Pulse wave velocity
Cardio Ankle Vascular Index(CAVI)
Pulse wave rising point
Amplitude adaptive tangent method

CORRESPONDING AUTHOR

Yambe T.
Department of Medical Engineering and Cardiology, Institute of Development, Aging and Cancer, Tohoku University, Japan

ABSTRACT

In the diagnosis and treatment of cardiovascular disease, various pulse wave parameters such as augmentation index in pulse wave measurement, baPWV, ABI, and CAVI are likely to be used more generally in the clinical setting. A critical point in pulse wave measurement is represented by accuracy. Determining the rising point of pulse waves, in particular, has considerable importance in ensuring diagnostic accuracy. Various methodologies for determining the rising point of pulse waves have been proposed. To compare each method, 1902 cases of measurement carried out in the clinical setting were reviewed. The pulse wave rising point was determined using the bottom method, the 1/10 method, the first derivative method, the second derivative method, the single tangent method, the intersecting tangents method, the McDonald method, and the amplitude adaptive tangent method. Detailed examination showed that the standard deviation was the smallest when the amplitude adaptive tangent method was used. Since the clinical setting does not always provide an ideal environment that allows accurate analytical measurement, it is critical to obtain stable measurement results. This research confirmed that the amplitude adaptive tangent method could be used to obtain measurement results exhibiting an accurate pulse wave rising point. In view of the possibility that future preventive medicine practices will expand into various facilities other than hospitals, as suggested by the efforts being made

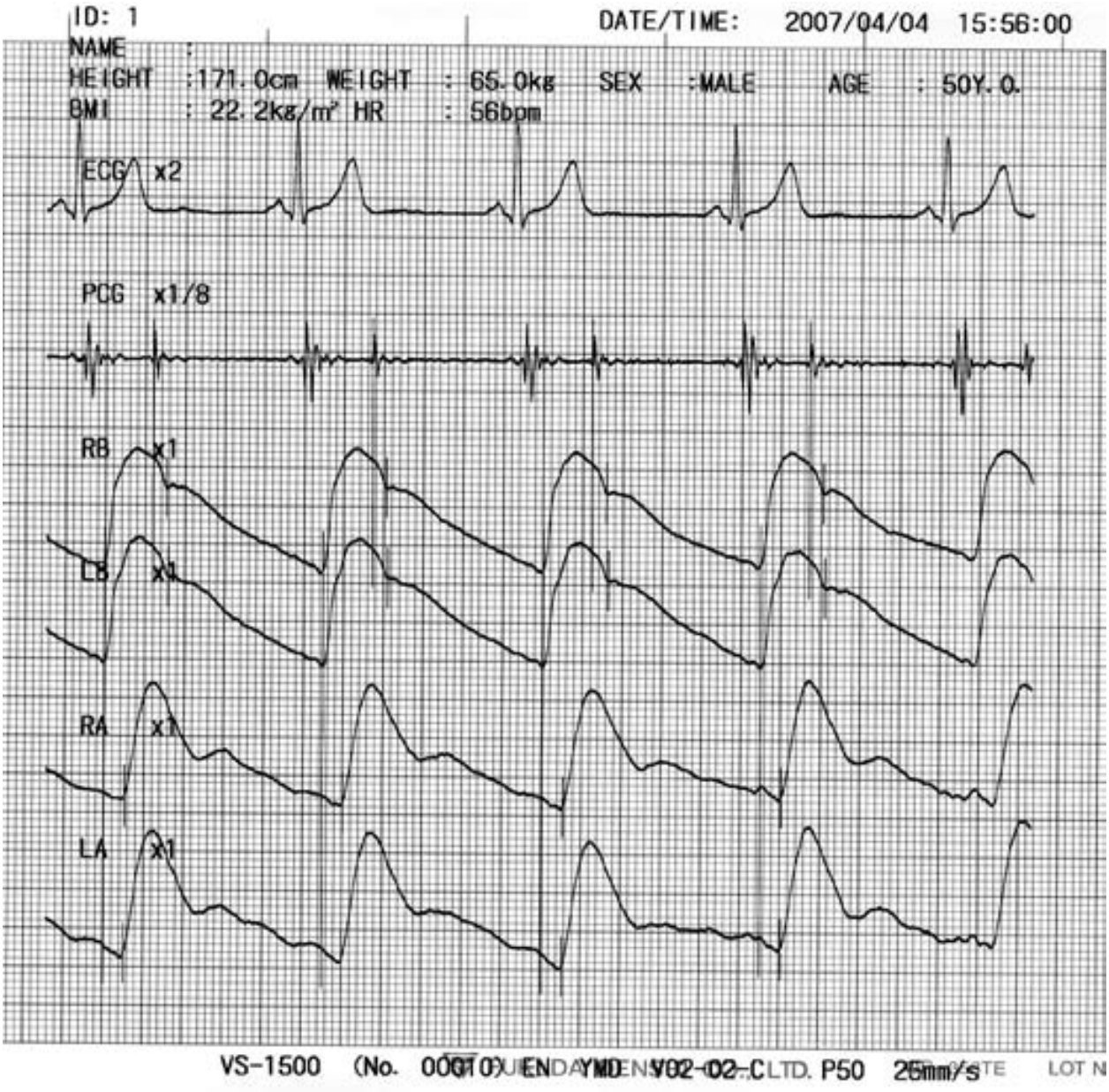

Figure 1
Pulse wave measurement record (electrocardiogram, phonocardiogram, and pulse pressure waveform at brachia and ankles and their rising points)

to fight metabolic syndrome, clinical research backed by practical footing will become increasingly important.

INTRODUCTION

It was not very long ago that Japanese people rarely developed myocardial infarction. However, with the change of dietary habits from Japanese to Western style in recent years, cardiovascular disease tends to account for a larger percentage in the Japanese disease structure. The upward trend of cardiovascular events is also found in the clinical setting, and the most common emergency treatment in major local hospitals is critical care for ischemic heart disease and stroke [1–3].

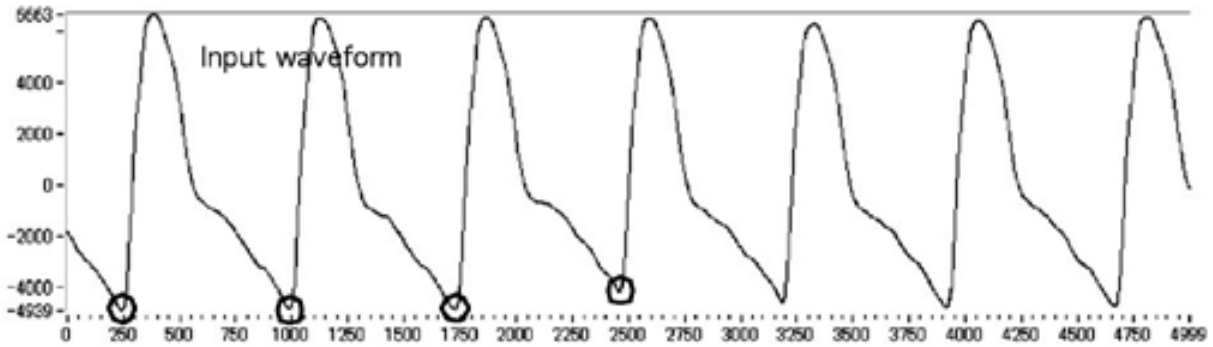

Figure 2
Pulse wave rising point determined by the bottom method

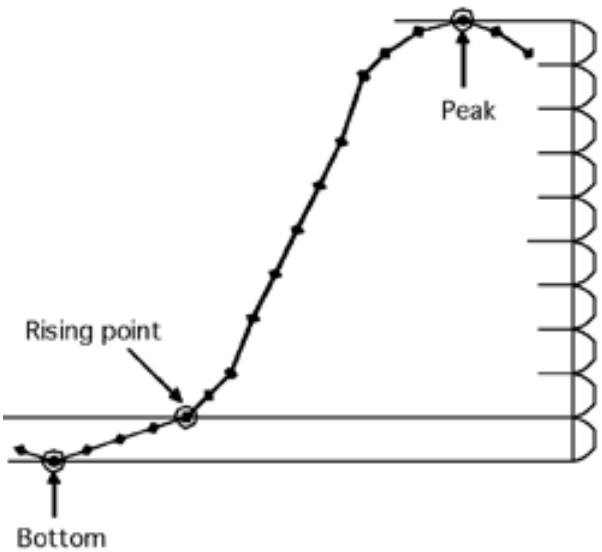

Figure 3
Pulse wave rising point determined by the 1/10 method

To break this trend and prevent increasing medical costs, the Japanese government is beginning to place more importance on preventive medicine, as shown by its efforts to fight metabolic syndrome. In the diagnosis and treatment of cardiovascular disease from the viewpoint of preventive medicine, various pulse wave parameters such as brachioankle Pulse Wave Velocity (baPWV), Ankle Brachial Index (ABI), and Cardio Ankle Vascular Index (CAVI) are now more commonly used in the clinical setting [4–7].

Many systems adopting various methodologies are offered on the market, including those that measure pulse waveforms only, those that measure pulse wave velocity from electrocardiograms and phonocardiograms, and those that quantitatively analyze arterial elasticity independently for diagnosis [8–13]. The critical point in pulse wave measurement using these systems is the accuracy of measurement. In pulse wave velocity (PWV) measurement or cardioankle vascular index (CAVI) measurement, in particular, determination of the pulse wave rising point has decisive importance in the accuracy of diagnosis [14–20].

Various methodologies for determining the pulse wave rising point have been proposed, and intellectual property rights for these methodologies have been claimed as well. The purpose of this research is to compare the accuracy of the bottom method, the 1/10 method, the first derivative method, the second derivative method, the single tangent method, the intersecting tangents method, the McDonald method, and the amplitude adaptive tangent method using each method [14–25].

MATERIAL AND METHODS

In stable measurement performed in an ideal measurement environment, relatively stable results are obtained for any of the methodologies used. However, in the clinical setting, stable measurement waveforms cannot always be obtained. Measurement can be affected by the movement of a patient with dementia, and the effect of external noise must always be taken into consideration in phonocardiography. Therefore, measurement data obtained in laboratories of forefront clinical hospitals was used for this research [20–22].

As shown in Figure 1, with the VaSera VS–1000 (Fukuda Denshi Co., Ltd.) used for this experiment, electrocardiographic and phonocardiographic measurement as well as pulse pressure waveform measurement can be performed.

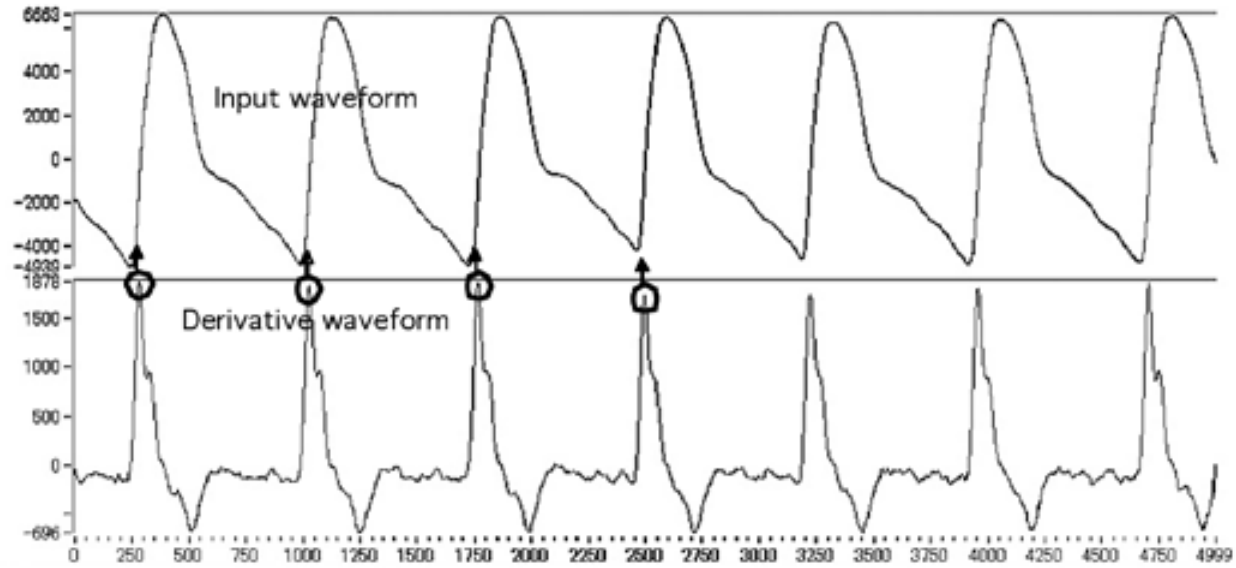

Figure 4
Rising point determined by the first derivative method

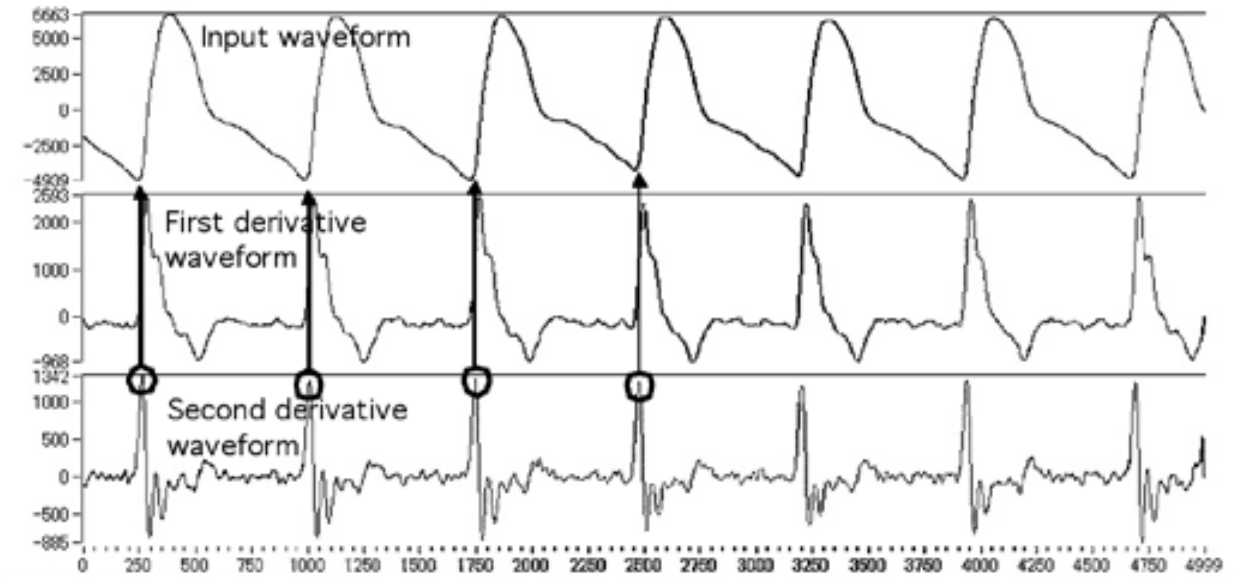

Figure 5
Rising point determined by the second derivative method

To study the accuracy of pulse wave measurement, the pulse wave rising point was identified, using the bottom method, the 1/10 method, the first derivative method, the second derivative method, the single tangent method, the intersecting tangents method, the McDonald method, and the amplitude adaptive tangent method.

As shown in Figure 2, the bottom method selected the lowest point of the pulse waveform and identified it as the rising point.

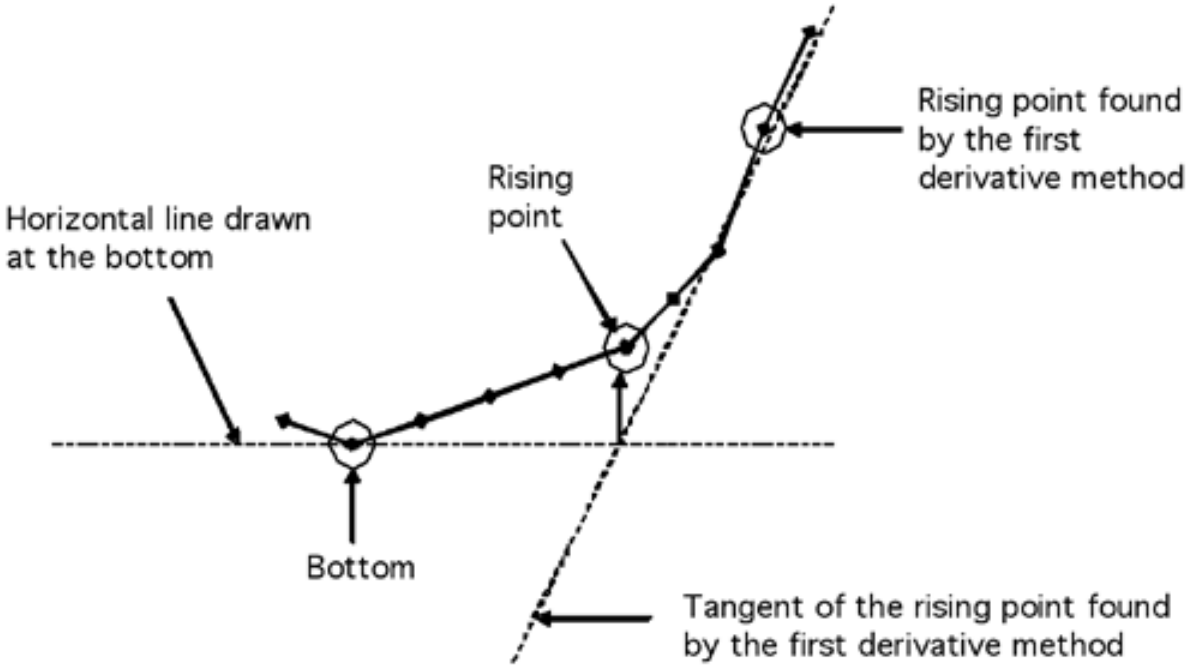

Figure 6
Rising point determined by the single tangent method

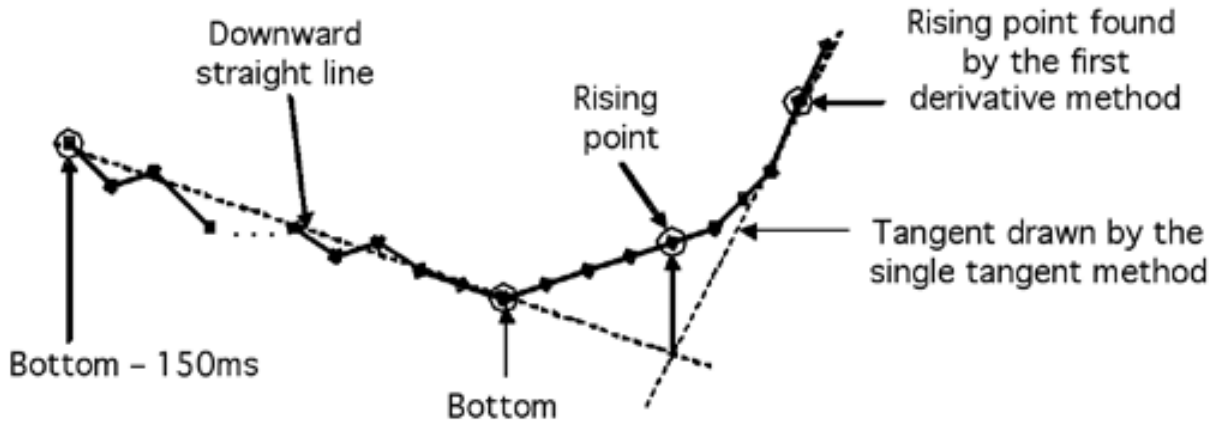

Figure 7
Rising point determined by the intersecting tangents method

With the 1/10 method, the amplitude of the pulse waveform was evenly divided by 10, and the place where the waveform reached from the bottom to 1/10 of the peak value was identified as the rising point. Figure 3 outlines this concept.

With the first derivative method, a differentiated waveform was calculated for the period of 5 ms before and after the target measurement point, and the point where the largest rising value was obtained was identified as the rising point (Figure 4).

With the second derivative method, a differentiated waveform was calculated for the period of 7 ms before and after the target measurement point, and the waveform was differentiated once again. The peak of the second derivative waveform, the time series curve created as a result of the second differentiation, was specified as the rising point (Figure 5).

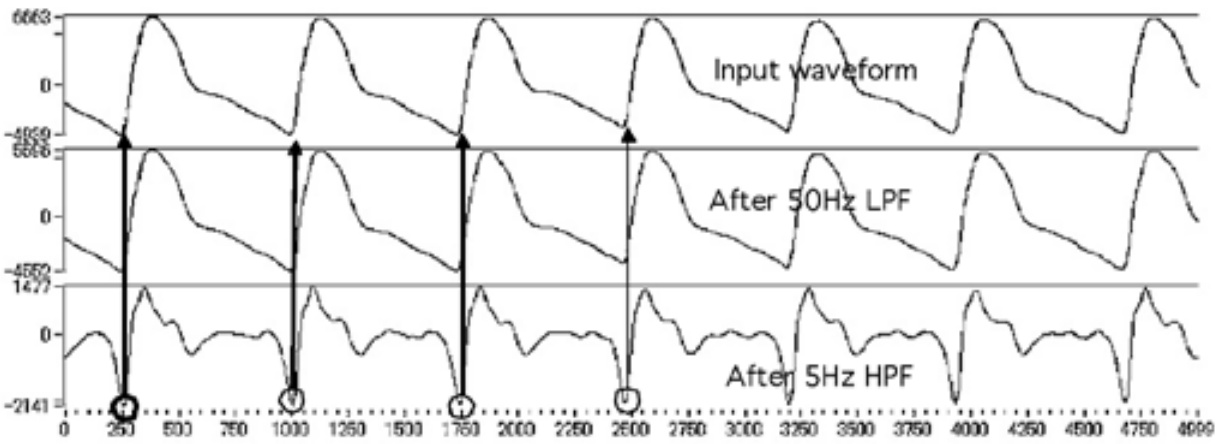

Figure 8
Rising point determined by the McDonald method

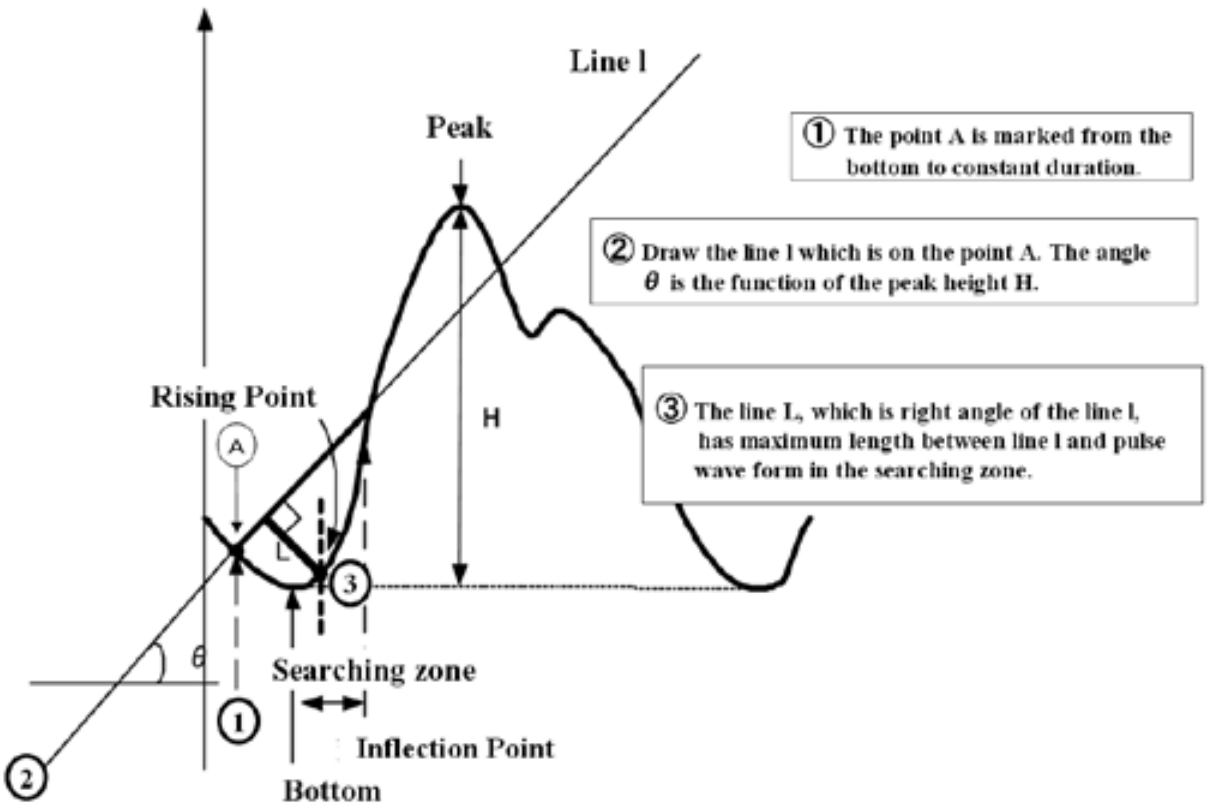

Figure 9
Rising point determined by the amplitude adaptive tangent method

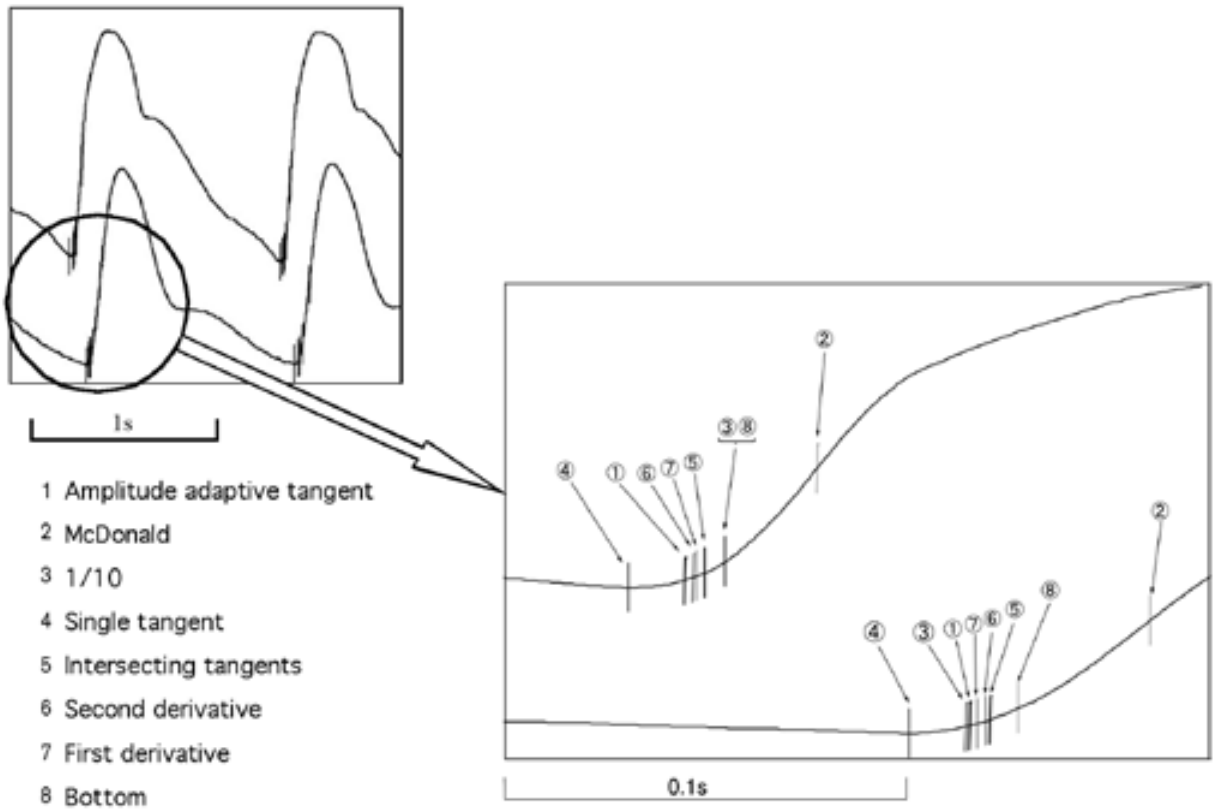

Figure 10
Example of determining pulse wave rising point

With the single tangent method, the tangent of the rising point found by the first derivative method was drawn, then a horizontal line was drawn at the bottom, and the point on the waveform that was on the vertical line drawn from the intersection of these two lines was identified as the rising point (Figure 6).

With the intersecting tangents method, the tangent of the downward pulse waveform before the bottom and that of the rising point identified by the first derivative method were drawn, and the point on the waveform that was on the vertical line drawn from the intersection of these two lines was identified as the rising point of the pulse waveform (Figure 7).

With the McDonald method, the pulse waveform underwent 50-Hz low-pass filtering, and then 5-Hz high-pass filtering, and the bottom point of the waveform obtained was identified as the rising point (Figure 8).

With the amplitude adaptive tangent method, a straight line was drawn on the point receding from the bottom by a certain time period empirically determined, at a predetermined angle, which was the function of the peak height H of the pulse pressure waveform. Another straight line was drawn perpendicular to the above line, and the intersection of that perpendicular line and the pulse waveform where the perpendicular line was the longest was identified as the rising point (Figure 9).

To perform a quantified comparison, the pulse wave rising point was determined using these methodologies, the pulse wave propagation time was calculated, and their standard deviations were compared. To be specific, the rising point was estimated from a phonocardiogram, and the propagation time between pulse wave rising points was calculated.

Of the 1902 continuous measurement data items collected during a one-month period using a blood pressure/pulse wave inspection device, data having an ABI of lower than 0.9, arrhythmia, and apparent artifact were excluded, and the

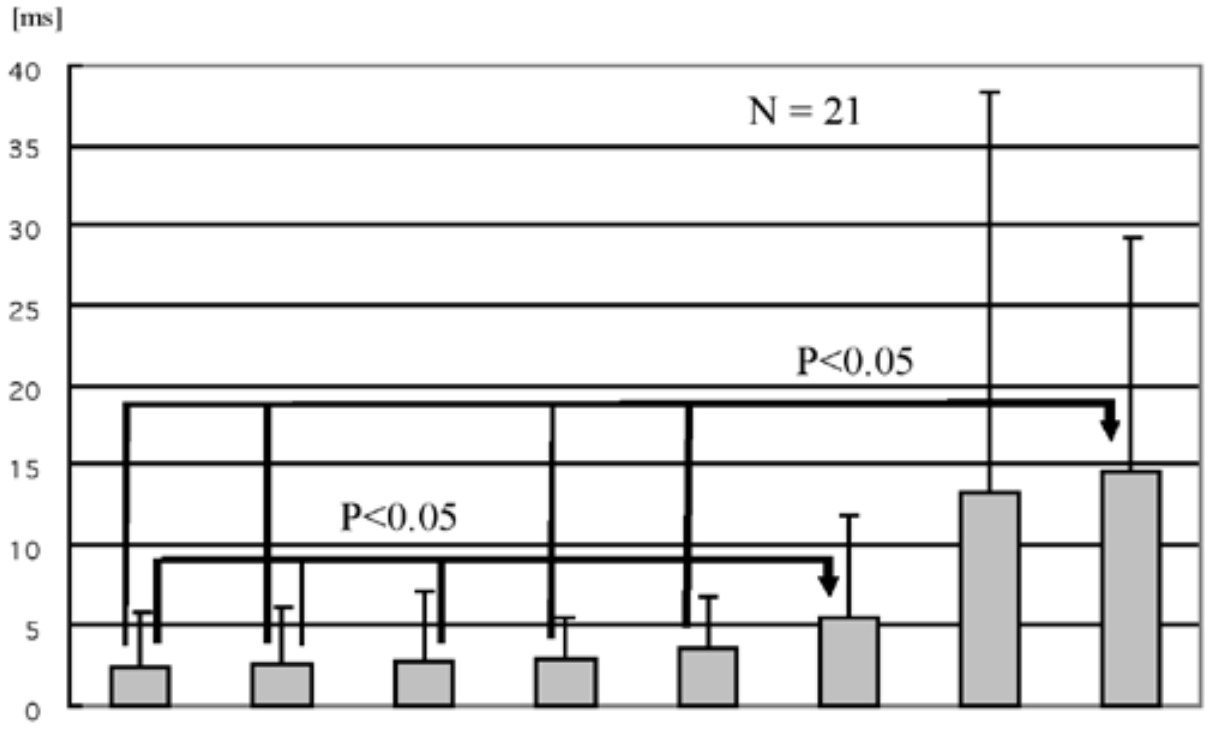

Figure 11
Comparison of standard deviation in each rising point determination method in 21 continuous examples

remaining 21 data items were used for analysis. To prevent fluctuation of measurements at medical facilities and to find a procedure to achieve stable measurement, the standard deviation of the typical four cases, in which stable determination of pulse wave propagation time was not made, was analyzed to compare each method.

RESULTS

Figure 10 is a typical example of the rising point determined using the bottom method, the 1/10 method, the first derivative method, the second derivative method, the single tangent method, the intersecting tangents method, the McDonald method, and the amplitude adaptive tangent method. It was found by enlarging the Figure in the direction of time that each method identified different points.

The ideal method for finding the pulse wave rising point is the one capable of making the measurement exhibit stable reproducibility even in the clinical setting. Therefore, of 1902 measurement examples taken in the examination rooms of clinical hospitals, 21 continuous data items that were collected in experienced hospitals and exhibited stable measurement results were selected. Their pulse wave velocity was calculated using the bottom method, the 1/10 method, the first derivative method, the second derivative method, the single tangent method, the intersecting tangents method, the McDonald method, and the amplitude adaptive tangent method. It was found that fluctuation (standard deviation) was relatively low with the amplitude adaptive tangent method, the intersecting tangents method, the McDonald method, and the 1/10 method (Figure 11).

Furthermore, with the four cases in which stable pulse waveform was displayed without indication of arrhythmia but pulse wave velocity measurement results fluctuated due to heart beat, pulse wave propagation time was diagnosed using the bottom method, the 1/10 method, the first derivative method, the second derivative method, the single tangent method, the intersecting tangents method, the McDonald method, and the amplitude adaptive tangent method. None of the methodologies provided stable results.

Figure 12 presents the standard deviation of pulse wave transmission time measurement in the four cases. In three of the cases, the amplitude adaptive tangent method provided the smallest standard deviation, and in the remaining case,

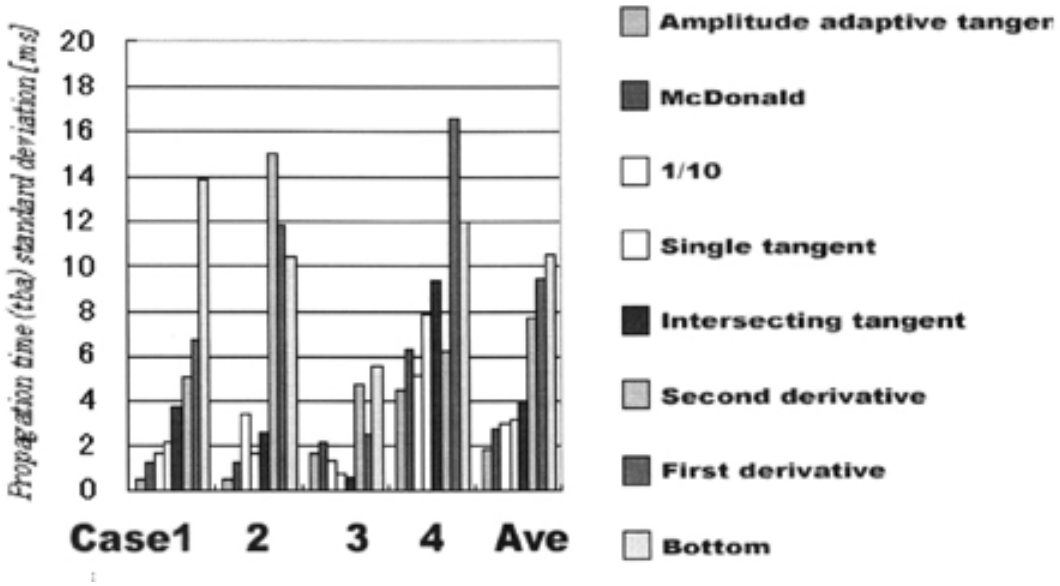

Figure 12
Comparison of standard deviations of propagation time measurement in the four cases exhibiting fluctuating measurement results

the intersecting tangents method provided the smallest deviation. With all of the cases, the amplitude adaptive tangent method provided the smallest standard deviation.

DISCUSSION

Increase of cardiovascular events due to arteriosclerotic disease is becoming a major problem in Japan as well, and quantitative pulse wave diagnosis is playing an increasingly important role in the field of preventive medicine [1–7]. New methodologies such as baPWV and CAVI, which ensures facilitated measurement conducted by simply wrapping cuffs around the patient's arms and ankles, are spreading rapidly in Japanese clinical settings [15–22]. The base of methodologies such as baPWV and CAVI is the measurement result of pulse wave propagation speed. Since the distance is nearly fixed in the calculation of pulse wave propagation speed in clinical diagnosis, it is not an exaggeration to say that the measurement of propagation time is everything, and the accuracy of measurement is critical. However, in clinical hospitals, where the most accurate diagnostic measurement cannot always be performed, it is important to obtain stable measurement results.

In view of such circumstances, this study compared the amplitude adaptive tangent method, the McDonald method, the 1/10 method, the single tangent method, the intersecting tangents method, the first derivative method, the second derivative method, and the bottom method in the clinical setting, and found as a result that the amplitude adaptive tangent method and the intersecting tangents method provided a relatively accurate pulse wave rising point.

Various physical parameters have been proposed as indices for arteriosclerosis, and it is a matter of course that diagnostic accuracy becomes a prerequisite of measurement [24–32]. It is apparent that studying and comparing various methodologies is necessary to find one capable of providing high measurement accuracy in the clinical setting.

The Ministry of Health, Labor and Welfare is beginning to place more importance on preventive medicine in the field of medical welfare, as suggested by their commitment to the fight against metabolic syndrome. They are promoting the expansion of medical welfare practices from hospitals to external facilities and, consequently, ensuring stable diagnostic measurement in places other than an ideal hospital environment is becoming increasingly important.

A blood pressure/pulse wave inspection device, which is capable of conducting 12-lead electrocardiographic measurement as well, is currently under development. If arteriosclerosis diagnosis would be added to the daily inspection items,

the device would become a very useful instrument in the field of preventive medicine.
Given the possibility that facilities other than hospitals would be used as sites for preventive medicine practices in the future, clinical study of pulse wave diagnosis performed from a practical point of view will become increasingly important. We plan to continue pursuing our study by reviewing as many cases as possible.

CONCLUSION

Various methodologies for determining the rising point in pulse wave measurement were compared. To perform precise quantitative diagnoses, a continuous comparative study of methodologies used in the clinical setting, such as hospitals, is indispensable.

ACKNOWLEDGEMENTS

This work was partly presented at 1st Brno-Sendai Symposium, Sept 4, 2007, in Brno. This work was partly supported by the Tohoku University Global COE Program "Global Nano-Biomedical Engineering Education and Research Network Centre", by the 21st century COE program: Future Medical Engineering based on Bio Nanotechnology, Research Grant for Cardiovascular Diseases from the Ministry of Health and Welfare, Research Grant from the Ministry of Education, Culture, Science and Technology, and Program for Promotion of Fundamental Studies in Health Science of Organizing for Drug ADR Relief, R&D Promotion and Product Review of Japan. It was also supported by a Research Grant from Mitsui Sumitomo Insurance Welfare Foundation, Nakatani Electronic Measuring Technology Association of Japan, Japan Epilepsy Research Foundation, Naito Foundation, and Fukuda Memorial Medical Research Foundation.

REFERENCES

1. Tsutani K, Igarashi A, Fujikawa K, et al. A health economic evaluation of aspirin in the primary prevention of cardiovascular disease in Japan. Intern Med 2007; 46(4): 157–62. Epub 2007 Feb 15.
2. Sakamoto K, Sakamoto T, Ogawa H. Kumamoto Joint Research on Hypercholesterolemia Investigators. The effect of 6 months of treatment with pravastatin on serum adiponectin concentrations in Japanese patients with coronary artery disease and hypercholesterolemia: a pilot study. Clin Ther 2006; 28(7): 1012–21.
3. Yoshimura T, Suzuki E, Egawa K, et al. Low blood flow estimates in lower-leg arteries predict cardiovascular events in Japanese patients with type 2 diabetes with normal ankle-brachial indexes. Diabetes Care 2006; 29(8): 1884–90.
4. Sasai H, Katayama Y, Numao S, Nakata Y, Okura T, Tanaka K. Effects of exercise training on metabolic syndrome and its component factors in Japanese middle-aged men: 1509: Board #272 May 30 9:30 AM – 11:00 AM. Med Sci Sports Exerc 2007; 39 (5 Suppl): S229. No abstract available.
5. Takahashi K, Bokura H, Kobayashi S, Iijima K, Nagai A, Yamaguchi S. Metabolic syndrome increases the risk of ischemic stroke in women. Intern Med 2007; 46(10): 643–8. Epub 2007 May 24.
6. Okamura T, Nakamura K, Kanda H, et al. The Health Promotion Research Committee of the Shiga National Health Insurance Organizations. Effect of combined cardiovascular risk factors on individual and population medical expenditures. Circ J 2007; 71(6): 807–13.
7. Ninomiya T, Kubo M, Doi Y, et al. Impact of metabolic syndrome on the development of cardiovascular disease in a general Japanese population. The Hisayama Study. Stroke 2007; May 24 [Epub ahead of print].
8. Fulton JS, McSwiney BA. The pulse wave velocity and extensibility of the brachial and radial artery in man. J Physiol 1930; 69(4): 386–92. No abstract available.
9. Hickson SK, McSwiney BA. The effect of variations in blood-pressure on pulse wave velocity in the brachial artery in man. J Physiol 1924; 59(2–3): 217–20.
10. Hayashi K, Maeda S, Iemitsu M, et al. Sex differences in the relationship between estrogen receptor alpha gene polymorphisms and arterial stiffness in older humans. Am J Hypertens 2007; 20(6): 650–656.
11. Protogerou AD, Safar ME. Dissociation between central augmentation index and carotid-femoral pulse-wave velocity: when and why? Am J Hypertens 2007; 20(6): 648–649.
12. Protogerou AD, Safar ME. Dissociation between central augmentation index and carotid-femoral pulse-wave velocity: when and why? Am J Hypertens 2007; 20(6): 648–649.
13. Vyas M, Izzo JL Jr, Lacourciere Y, et al. Augmentation index and central aortic stiffness in middle-aged to elderly individuals. Am J Hypertens 2007; 20(6): 642–647.
14. Patent application 2002–19370, Date of filing application: July 5, 2002, Publication number: Kokai number (2004) 33614, Date of publication: February 5, 2004, Patent applicant: Fukuda Denshi Co., Ltd., Inventor: T. Yamamoto, Name of invention: Pulse wave rising point detection device and procedures.
15. Yamashina A, Tomiyama H, Takeda K, et al. Validity, reproducibility, and clinical significance of noninvasive brachial-ankle pulse wave velocity measurement. Hypertens Res 2002; 25(3): 359–64.

16. Yambe T, Yoshizawa M, Saijo Y, et al. Brachio-ankle pulse wave velocity and cardio-ankle vascular index (CAVI). Biomed Pharmacother 2004; 58 (Suppl 1): S95–8. 17.
Yambe T, Kovalev YA, Milyagina IA, et al. A Japanese-Russian collaborative study on aging and atherosclerosis. Biomed Pharmacother 2004; 58 (Suppl 1): S91–4.
18. Flanigan DP, Keifer TJ, Schuler JJ, Ryan TJ, Castronuovo JJ. Experience with iatrogenic Paediatric vascular injuries. Incidence, etiology, management, and results. Ann Surg 1983; 198(4): 430–42.
19. Grossman PM, Mendelsohn F, Henry TD, et al. Results from a phase II multicenter, double-blind placebo-controlled study of Del–1 (VLTS–589) for intermittent claudication in subjects with peripheral arterial disease. Am Heart J 2007; 153(5): 874–80.
20. Yambe T, Meng X, Hou X, et al. Cardio-ankle vascular index (CAVI) for the monitoring of the atherosclerosis after heart transplantation. Biomed Pharmacother 2005; 59 (Suppl 1): S177–9.
21. Otsuka K, Norboo T, Otsuka Y, et al. Chronoecological health watch of arterial stiffness and neuro-cardio-pulmonary function in elderly community at high altitude (3524 m), compared with Japanese town. Biomed Pharmacother 2005; 59 (Suppl 1): S58–67.
22. Shirai K, Utino J, Otsuka K, Takata M. A novel blood pressure-independent arterial wall stiffness parameter; cardio-ankle vascular index (CAVI). J Atheroscler Thromb 2006; 13(2): 101–7.
23. Chiu YC, Arand PW, Shroff SG, Feldman T, Carroll JD. Determination of pulse wave velocities with computerized algorithms. Am Heart J 1991; 121(5): 1460–70.
24. Masanori Munakata. Accuracy in determining the pulse wave rising point-pulse wave velocity. Nakayama Shoten, Tokyo, 2006: pp 20–30.
25. McDonald DA. Regional pulse-wave velocity in the arterial tree. J Appl Physiol 1968; 24(1): 73–8.
26. Megnien JL, Simon A, Denarie N, et al. Aortic stiffening does not predict coronary and extracoronary atherosclerosis in asymptomatic men at risk for cardiovascular disease. Am J Hypertens 1998; 11(3 Pt 1): 293–301.
27. Asmar RG, Topouchian JA, Benetos A, Sayegh FA, Mourad JJ, Safar ME. Non-invasive evaluation of arterial abnormalities in hypertensive patients. J Hypertens Suppl 1997; 15(2): S99–107. Review.
28. Haidet GC, Wennberg PW, Finkelstein SM, Morgan DJ. Effects of aging per se on arterial stiffness: systemic and regional compliance in beagles. Am Heart J 1996; 132(2 Pt 1): 319–27.
29. Kidawa M, Krzeminska-Pakula M, Peruga JZ, Kasprzak JD, Trzos E. Cardiological syndrome X. Non-invasive assessment of endothelial function and arterial compliance. Kardiol Pol 2003; 59(11): 385–96.
30. Grey E, Bratteli C, Glasser SP, et al. Reduced small artery but not large artery elasticity is an independent risk marker for cardiovascular events. Am J Hypertens 2003; 16(4): 265–9.
31. Brooks B, Molyneaux L, Yue DK. Augmentation of central arterial pressure in type 1 diabetes. Diabetes Care 1999; 22(10): 1722–7.
32. Kubozono T, Miyata M, Ueyama K, et al. Clinical significance and reproducibility of new arterial distensibility index. Circ J 2007; 71(1): 89–94.

FINITE ELEMENT MODEL OF THE HUMAN HEAD VALIDATED BY THE RECONSTRUCTION OF A REAL CHILD SPORT ACCIDENT

Brichtová E., [1] **Jiroušek O.,** [2] **Gál P.** [1]

[1]Clinic of Paediatric Surgery, Orthopedics and Traumatology, Brno Faculty Hospital, Brno
[2]Institute of Theoretical and Applied Mechanics, Academy of Sciences, Prague

Received after revision July 2009

KEY WORDS

Paediatric brain injury
Finite element models
Head trauma
Injury models

CORRESPONDING AUTHOR

Brichtová E.
Clinic of Paediatric Surgery, Orthopedics
and Traumatology, Brno Faculty Hospital, Brno
Černopolní 9
613 00 Brno
Czech Republic

ABSTRACT

Reconstruction of a sport accident using detailed Finite Element (FE) model of the human head and explicit dynamics numerical simulation is presented in the paper. The sport accident involved a 13-year old boy on whom a handball cage fell during the school sport activity. FE model of the human head was developed using series of computer tomography (CT) scans. The FE model includes the skull, brain and subarachnoidal space. Rigid body model was used to assess initial conditions at the moment of the impact. The detailed FE model was imposed to the initial conditions obtained just before the head impacted the playground and differential equations of motion with explicit dynamics solver LS-DYNA (Livermore Software Dynamic Analysis) was used to determine the impact sequence. The pressure, shear stress response, von-Mises stress response and logarithmic strain values were evaluated in frontal, parietal, occipital and midbrain region. Head injury criteria were used to evaluate the injuries sustained. Results obtained from the numerical simulation of the accident showed good agreement with clinically observed head injuries and indicate the good ability of the FE model to simulate the impact situations and to investigate the brain injury mechanisms.

INTRODUCTION

Traumatic brain injury occurs most commonly as a result of a traffic accident, due to a fall or physical assault and it is one of the leading causes of death worldwide. In the Paediatric age group, traumatic brain injury is a leading cause of death and disability. Causes of injury vary with child developmental age, and sports related injuries are prominent among school aged children group. Children and adolescents spend up to 50% of their time at school and almost 40% of injuries occur during school sports activity. [1] Distortions and contusions are the most frequent diagnoses of all school activity related

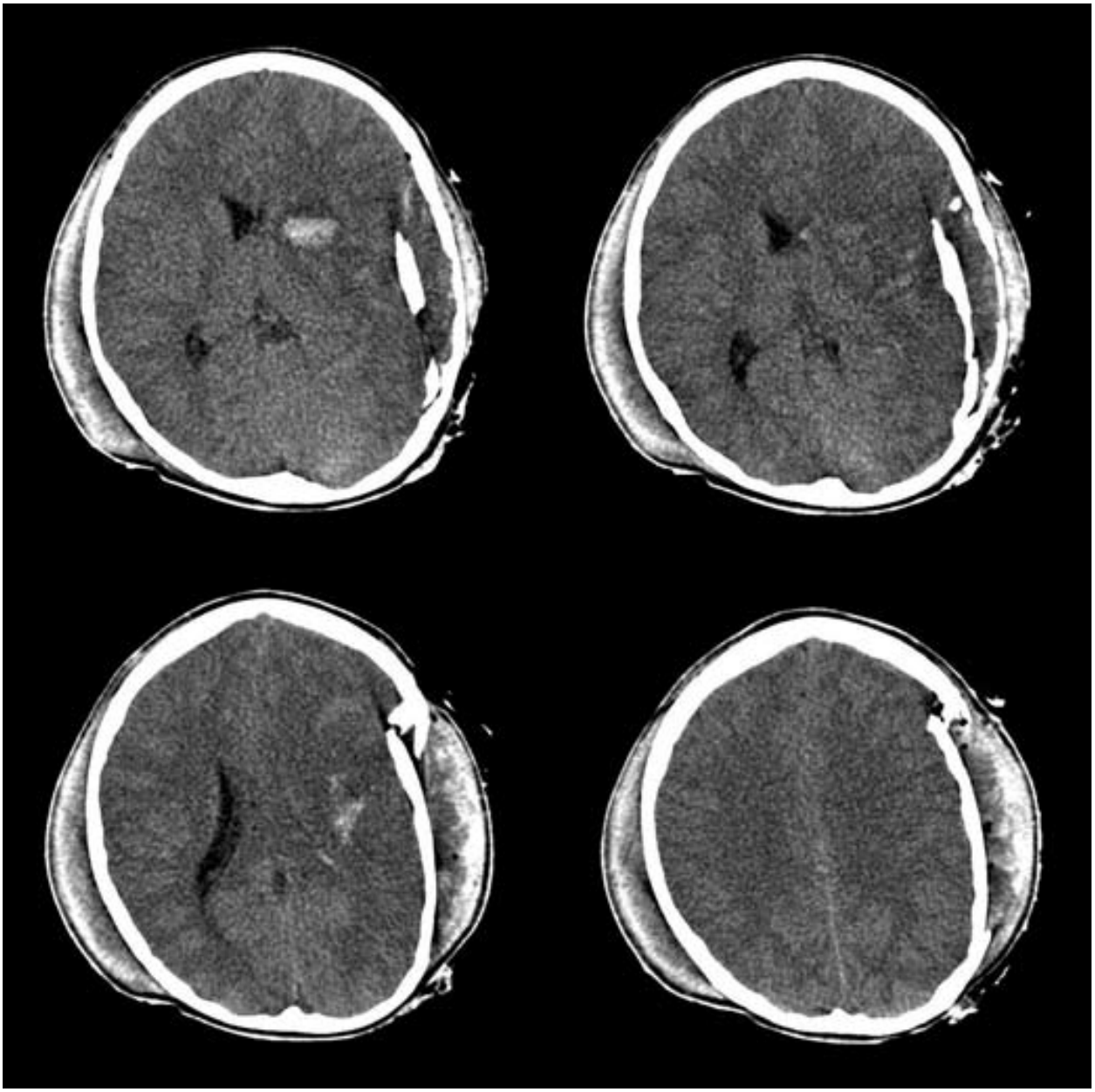

Figure 1
CT images after the accident.

injuries and head injuries from collective sport activities are frequently present. [2,3]

In the paper a detailed Finite Element (FE) model of human head is constructed using computer tomography (CT) scans of the patient's head. The geometry is constructed fully automatically on the basis of the medical imaging data. This make possible to use the model for "patient – specific" reconstruction of head injuries which is an important application of these FE models. Procedures used to develop the model need minimal user intervention. On one hand this approach creates the possibility to differentiate easily between individuals, on the other hand it makes impossible to render all the detailed structures. Presented model represents well the geometry of the skull, brain and subarachnoidal space using four material models. The sandwich construction of the human skull, composed by a thin shell of cortical bone filled with tetrahedral elements

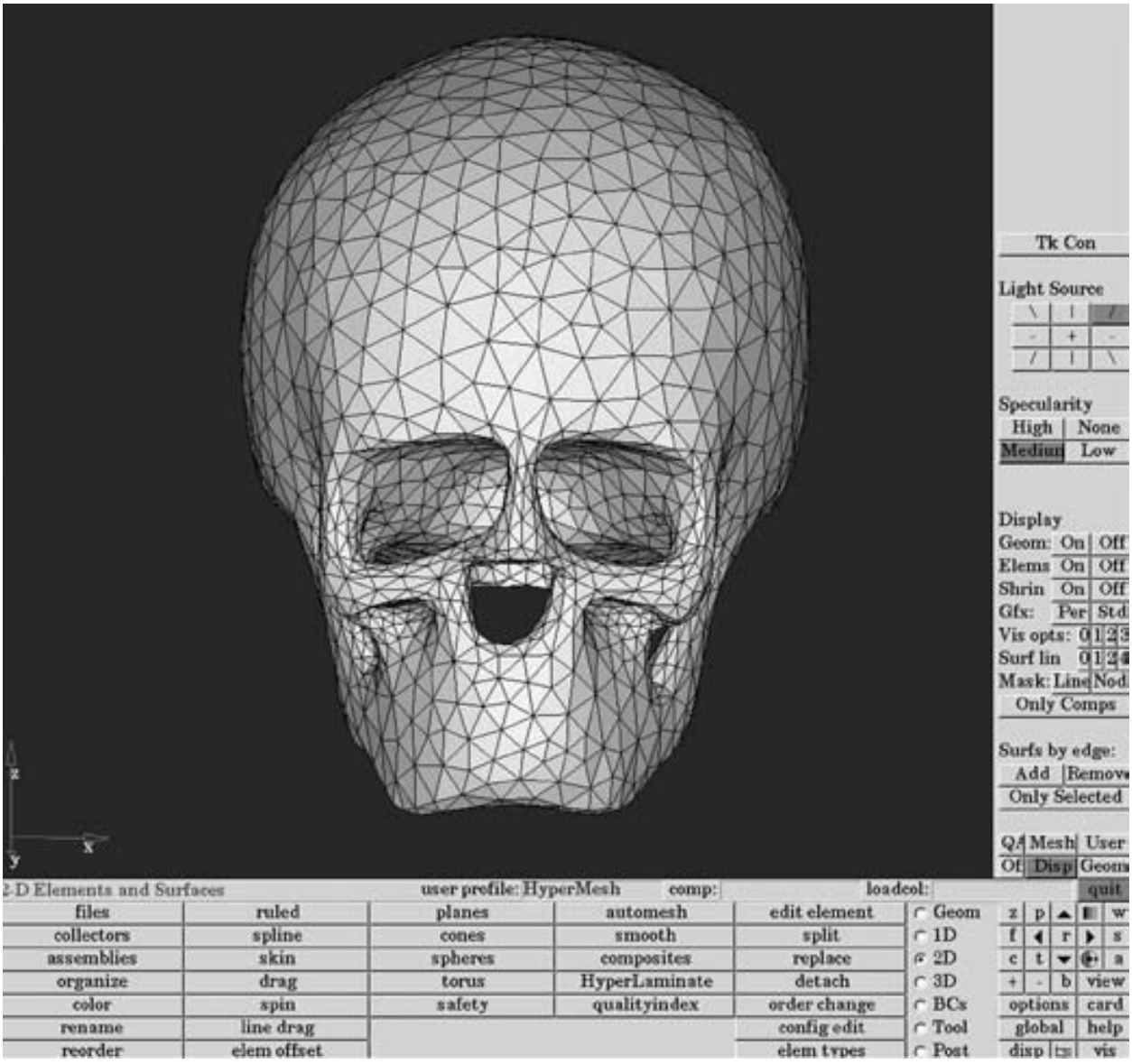

Figure 2
Skull FE model

(trabecular bone) is able to reflect the behavior of the real material. With the emphasis to minimize user intervention it is impossible to make difference between material properties of gray and white matter and therefore the same viscoelastic material properties are used for the entire brain.

MATERIALS AND METHODS

Reconstruction of a sport accident involved a 13-year old boy on whom a handball cage fell to the head during the school sport activity is presented. The 40kg weight, 1.58 m high boy was unconscious after the accident and comatose transported immediately by the rescue helicopter to specialized Paediatric trauma center in Brno Faculty Hospital. CT revealed impressive skull fracture, subdural haematoma and cerebral contusions in the left temporal – parietal region, corresponding to the impact of 70 kg weight handball cage. Extensive scalp contusions were found in the contralateral right temporal – parietal region. (Figure 1) The boy underwent acute neurosurgery and comprehensive intensive care unit treat-

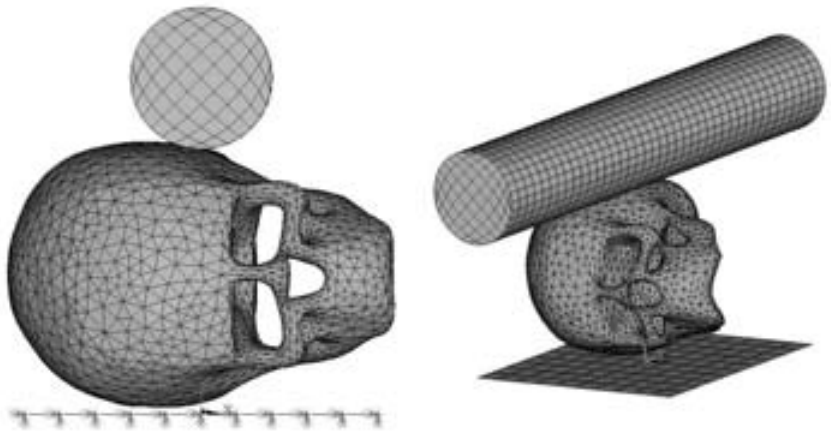

Figure 3
FE model of the impact situation

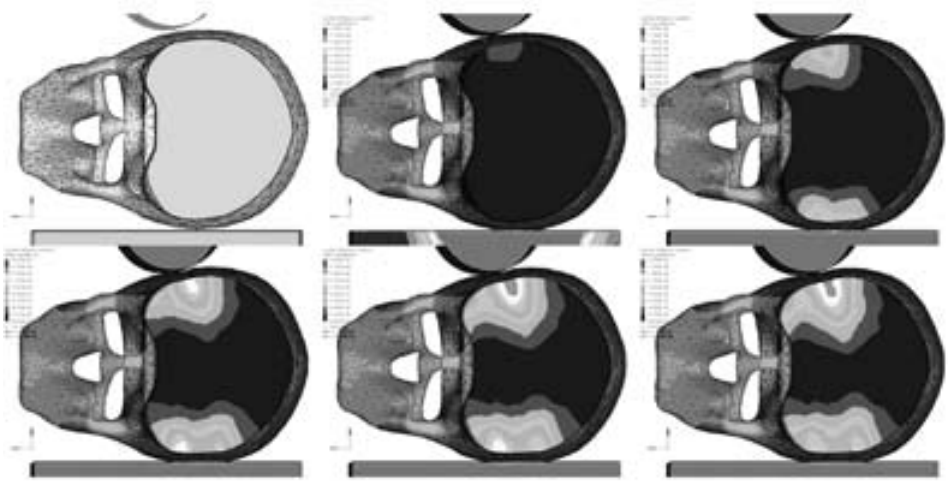

Figure 4
von Mises stress in the brain tissue in 0, 2, 4, 6, 10 ms intervals

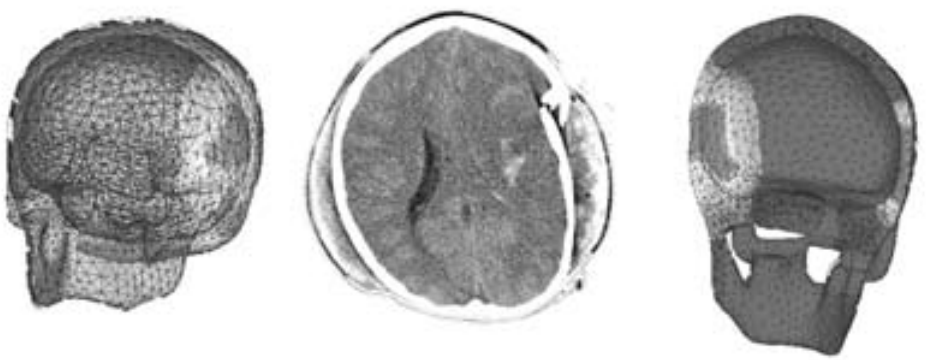

Figure 5
Comparison of CT and FE model results

ment, followed by the physiotherapy, psychology and logopedic care. With residual deficit the boy started to attend the school for disabled children one year after.

Detailed FE model of skull and brain was developed to reconstruct the accident. The geometry of the head was obtained from a series of CT images with the resolution of 512x512 pixels taken in 5 mm distances postsurgically. For the segmentation of the bone tissue from the CT images the intensity based segmentation method was used. For the brain tissue segmentation, the segmentation using active contours (region growing) was used. After the segmentation of both the skull and brain tissue, the inner and outer surfaces of both parts were reconstructed using the Marching Cubes Algorithm (MCA) [4]. The result of this algorithm is a set of triangles describing the surface of the domain of interest. For later use in the FE simulations, it is necessary to reduce the number of these triangles to a reasonable number using a decimation algorithm [5]. Out-of-plane distance decimation and border-distance decimation were used in order to reduce the density of the mesh surface and further optimization using energy minimization approach was used. Using these methods, the number of elements describing the skull was possible to reduce from original 1,500,000 triangles (both outer and inner surfaces reconstructed) to less than 5,000. (Figure 2)

After successful decimation the surface of the model is represented by a set of closed triangular elements. The last step is to create volumetric representation of the object from this surface representation. For the discretization of the volume Delaunay triangulation [6,7] in 3-D is used. Within the FE model of the head four different regions were defined: 1. skull (modeled as elastoplastic with defined material properties of tetrahedral volumetric elements for the spongional and cortical bone), 2. brain (modeled as viscoelastic material, with no differentiation between material properties of white and gray matter) and 3. subarachnoidal space (filled by tetrahedral elements with elastic isotropic material properties). The initial configuration of the head impacting the ground as well as the initial velocity of the steel cage was obtained from rigid-body modeling of the fall. For the rigid-body simulation Mathematical Dynamic Models (MADYMO) software package was used, with the female model (1.52 m and 49.8 kg) closest in weight and size to the boy injured (1.58 m and 40 kg). The components of velocity and acceleration at the time of impact obtained at the center of gravity of the pedestrian head were imposed on the detailed FE model. To determine the velocity and angular acceleration of the impacting handball cage a simple rigid model was used and the cage was supposed to fall from its indifferent equilibrium position. The situation modeled was set according the accident: the boy's head touching the ground and the cage cross-bar falling on the left part of the head. (Figure 3) The 70 kg weight cage, made of zinc-coated steel, was modeled as a bar of the same cross-sectional elasto-plastic material properties as the real one, but only the upper bar was modeled. The playground is covered with the Conipur material, which is an impact absorbing, permeable layer of polyurethane, often used for playground surfaces. This surface was modeled using three layers of solid elements with elasto-plastic material properties.

Differential equations of motion with explicit dynamics solver LS-DYNA (Livermore Software Dynamic Analysis) was used to determine velocity and angular acceleration of the upper bar of the cage at the moment it hit the boy's head. The components of velocity and acceleration determined from the equation of motion for the angle 84.5° (upper bar touching the skull) were used. Contact conditions were prescribed between the brain and inner surface of the skull as well as between the outer surface of the skull and the rigid plate. The pressure, shear stress response, von Mises stress response and logarithmic strain values were evaluated in frontal, parietal, occipital and midbrain regions and compared to injuries sustained. Von Mises stress was evaluated in left and right parietal regions and used for bone fracture predictions. In this work, the injury limits were set according to recent work of Baumgartner and Willinger [8]. The thresholds were derived from a FE modeling of 64 accident involving helmeted motorcyclists, American footballers and pedestrians. The limits were set to 20 kPa for concussion, and 40 kPa for severe brain neurological lesions. The limit for subdural and subarachnoidal haematoma sets the global strain energy of the subarachnoidal space to 5 J. A global strain energy of the skull of 2 J leads to skull fractures.

RESULTS

Von Mises stress in this study was evaluated at the side of impacting cage, at the opposite side (temporal regions) as well as at the occipital and parietal and midbrain regions. In the temporal regions the peak values of von Mises stress were 47 kPa and 23 kPa clearly predicting brain lesions and haematomas on both sides. Using these limits in our case of falling handball cage, the skull fracture was predicted with global strain energy of the skull reaching 4.3 J. The global strain energy of the subarachnoidal space was more than 8 J suggesting subdural haematomas. As an illustrative example of these results von Mises stress in the brain tissue in 0, 2, 4, 6, 10 ms time intervals are presented in Figure 4.

DISCUSSION

There are two possible methods for investigation of the dynamic response and the injury mechanism during an impact; experimental simulation (real car crash simulations and sled

tests) and numerical modeling. For the experimental simulations, the hybrid and Anthropomorphic Test Dummies (ATD) has become the industry standard for car collision testing in the last decades. Rapid advances in the computer technology and the numerical methods have enabled scientists to study problems described by a set of differential equations on very complex domains using the Finite Element method.

The aim of the study was to model the accident using explicit Finite Element model and to assess the possibilities of the existing injury criteria to describe the lesions caused by the falling cage. Results from the FE modeling were used for tissue thresholds. Most of the thresholds are used for axonal injury prediction rather than whether a particular type of injury would occur [9]. In recent years few works with injury thresholds based on von Mises stress appeared, particularly the work of Willinger et al. [10] and Baumgartner [8]. Prediction of skull fracture was based on Yoganandan et al. [11] experimental results, where the force necessary to fracture cadaver skulls ranged between 8.8 kN and 14.1 kN, with an average of 11.9 kN. The peak force from the rigid-body simulation was 7.4 kN indicating no skull fracture. This indicates that in case of free fall no skull fracture would occur. On the other hand, results from the finite element modeling show peak force more than double of that value clearly predicting skull fracture.

Remarkable observation in the study was the fact, that the skull was fractured at the side of the impact with the cage only, whereas on the opposite side, at the contact with ground it remained intact. Also brain injuries on the side opposite to cage impact were not so severe as on the opposite side. Obvious explanation of this phenomena is that the playground was covered with 16 mm layer of cushion material (Conipur) absorbing much of the deformation energy of the reverse side. The bone fracture was predicted at the impact side only showing good agreement with the real accident. Overall, the results from the numerical analysis were encouraging and showed good ability of the FE model to model the impact situation studied and to investigate the brain injury mechanisms in experimental conditions. In this way, FE model could be also used in forensic medicine cases. The graphical correlation between the CT findings and mathematical modeling based on FE model is shown in Figure 5.

CONCLUSIONS

The paper demonstrates the ability of detailed FE model of human head to quantify a head injury during traffic accident, sport injury or other traumatic event. The human skull is modeled as a sandwich construction, the subarachnoidal space is defined and the entire brain is modeled as viscoelastic material. The bone fracture was predicted at the impact side only showing good agreement with the real accident. The results from the numerical analysis showed good ability of the FE model to simulate the impact situations and to investigate the brain injury mechanisms, inclusive forensic medicine cases.

REFERENCES

1. Kraus R, Heiss C, Alt V et al. School accidents – an epidemiological assessment of injury types and treatment effort. Zentralbl Chir 2006; 131: 411–416.
2. Brichtová E. Kraniocerebrální poranění v dětském věku. [Craniocerebral injuries in childhood age.] Triton, 2008;124–128.
3. Kelm J, Ahlhelm F, Anagnostakos K et al. Gender – specific differences in school sports injuries. Sportverletz Sportschaden 2004; 18: 179–184.
4. Lorensen WE, Cline HE. Marching Cubes: A high resolution 3D surface construction algorithm. Computer Graphics 1987; 21: 155–168.
5. Schroeder WJ, Zarge JA. Decimation of Triangle Meshes. Computer Graphics 1992; 26: 65–70.
6. Fang TP, Piegl LA. Delaunay Triangulation in Three Dimensions. IEEE Computer Graphics and Applications 1995; 15: 62–69.
7. Fortune S. Voronoi diagrams and Delaunay triangulations. Algorithmica 1992; 1: 193–234.
8. Baumgartner D, Willinger R, Schewchenko N. et al. Tolerance limits for mild traumatic brain injury derived from numerical head impact replication. In International IRCOBI Conf. on the Biomechanics of Impacts, Isle of Man 2001; 353–355.
9. Morrison BI, Cater HL, Wang C et al. A tissue level tolerance criterion for living brain developed with an in vitro model of traumatic mechanical loading. Stapp Car Crush Journal 2003; 47: 93–105.
10. Willinger R, Baumgartner D, Chinn B et al. Head tolerance limits derived from numerical replication of real world accidents. IRCOBI Conf., Montpellier 2000; 209–221.
11. Yoganandan N, Pintar FA, Sances A et al. Biomechanics of skull fracture. J Neurotrauma 1995; 12: 659–668.

TREATMENT OF DEEP VENOUS THROMBOSIS WITH CONTINUOUS INTRAVENOUS INFUSION OF LOW-MOLECULAR-WEIGHT HEPARIN IN CHILDREN – A SAFE AND EFFICIENT ALTERNATIVE TO SUBCUTANEOUS APPLICATION

Fiamoli V.

Department of Clinical Haematology, Children's Faculty Hospital, Brno

Received after revision July 2009

KEY WORDS

Deep vein thrombosis
Low-molecular-weight-heparin (LMWH)
Risk of thrombosis
AntiXa

CORRESPONDING AUTHOR

Fiamoli V.
Department of Clinical Haematology, Children's Faculty Hospital, Brno
Černopolní 9,
613 00 Brno
Czech Republic

ABSTRACT

The incidence of thrombosis is age-dependent with the lowest risk in childhood. Children mostly suffer from venous thrombosis. The occurrence of thrombosis in children is 0.07/10 000, but it is higher among hospitalised children (3.5/10 000). Low-molecular-weight heparin (LMWH) is preferred in the treatment of deep venous thrombosis (DVT) in children. The most frequent form of application of LMWH is via subcutaneous injection. In this study we present a group of 33 children with DVT, who were treated with LMWH for their first thrombosis from 2003 to 2006. Twenty-one (63.6 %) patients were treated with LMWH by means of continuous infusion (CI) and 12 (36.3 %) patients by subcutaneous injection. Before starting the treatment our aim was to perform a full thrombophilia work-up and screening of acquired risks of thrombosis in all patients. The duration of the treatment with LMWH was modified in accordance with the course of thrombosis (monitored by Doppler ultrasound with compression). The average duration of the treatment in patients treated by continuous infusion was 18.7 days, median was 15 days. The average duration of treatment in the group of patients treated with subcutaneous (SC) injections was 28.2 days, median was 18.5 days. The average dose of LMWH for intravenous application was 250.7 IU/kg/24h, median was 240 IU/kg/24h, and the average dose of LMWH for SC application was 223.1 IU/kg/24h, median 215 IU/kg/24h. The dose of LMWH was modified according to the levels of antiXa. The required therapeutic range was 0.5–1 IU/ml.

The treatment with continuous infusion led to total recanalisation of the vein in 3 cases (14.3 %), partial recanalisation was achieved in 15 (71.4 %) patients. Three (14.3 %) patients were without any recanalisation. The treatment by subcutaneous injection led to total recanalisation of the vein in 4 cases (33.3 %), partial recanalisation was seen in 4 (33.3 %) patients. Three (33.3 %) patients were without any recanalisa-

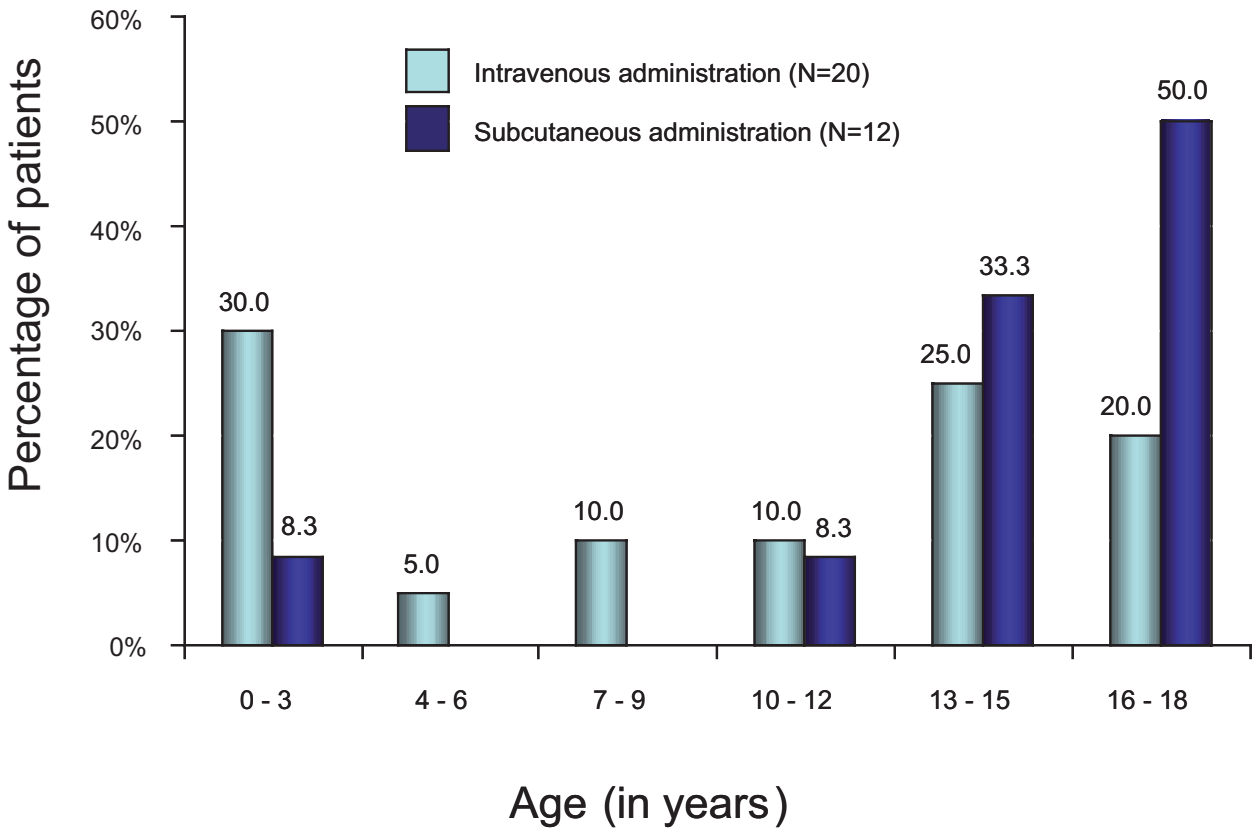

Figure 1
Age of patients according to administration of LMWH (percentage of patients)

Methods	Patients treated by continuous infusion	Patients treated by subcutaneous injection
FVL heterozygous	n = 21 / positive 5	n = 11 / positive 3
FIIG20210A heterozygous	n = 21 / positive 1	n = 11 / positive 1
MTHFR heterozygous	n = 21 / positive 11	n = 11 / positive 5
PC low plasmatic level	n = 15 / positive 4	n = 7 / positive 1
Hc high	n = 10 / positive 0	n = 7 / positive 1
Lp(a) high	n = 9 / positive 3	n = 5 / positive 3
AT low plasmatic level	n = 19 / positive 1	n = 9 / positive 1

Table 1
Hereditary prothrombotic risks

tion. The difference in the outcomes of the therapy between both groups appears to be statistically significant (p 0.041, tested by a non-parametric Mann-Whitney test). We have not noticed any bleeding as an adverse event of the treatment in any of our patients.

We would like to point out that the treatment of DVT with continuous infusion of LMWH in children might be an efficient and safe alternative to SC application under certain circumstances, especially in children with indwelling central venous lines or in those who are endangered by the risk of bleeding complications.

Key words: Deep venous thrombosis, LMWH, Risk of thrombosis, antiXa

Abbreviations: low-molecular-weight heparin (LMWH), deep venous thrombosis (DVT), subcutaneous (SC), continuous infusion (CI), pulmonary embolism (PE), venous thromboembolic event (VTE), thromboembolic disease (TED), central venous line (CVL), intravenous (IV)

1. INTRODUCTION

1.1. Incidence of thrombosis in children

The incidence of VTE – a venous thromboembolic event (deep venous thrombosis, pulmonary embolism) – is age-dependent with the lowest risk occurring in children [1,2,3]. The estimated incidence of deep venous thrombosis (DVT) and pulmonary embolism (PE) in the general paediatric population is 0.07/10 000 and 5.3/10 000 hospital admissions [4,5,6].

DVT/PE develop in children often as a secondary complication of other underlying disorders or in children with hereditary prothrombotic risks [7]. Idiopathic VTE occurs in less than 1% of newborns and in less than 5% of children compared to approximately 40% of adults [7,8,9,10]. Children under one year of age and teenagers are at the greatest risk of VTE [7,8,10].

1.2. Risk factors of thrombosis

Patients with hereditary prothrombotic risk factors in heterozygous form and without any other acquired prothrombotic risk factors that might potentiate each other, have very seldom their first thrombosis during childhood. Whereas patients with hereditary prothrombotic risk factors in homozygous form or with combination of the same in heterozygous form have thrombosis frequently during early childhood.

1.2.1. Hereditary prothrombotic risk

Clinically significant relationships have been confirmed between thromboembolic disease (TED) and deficiencies of antithrombin, protein C and protein S, as well as the presence of factor FV Leiden, prothrombin gene mutation G20210A, and some dysfibrinogenaemias in adults. The prevalence of congenital deficiencies of antithrombin, protein C and protein S is low, even in patients with a family history of thrombosis. In contrast, FV Leiden and prothrombin gene mutation G20210A are identified quite often as an inherited predisposing factor in patients with TED [11].

TED also appears more often, for example, in patients with an impaired fibrinolytic system, heparin co-factor II deficiency, FVIII increased level, FXII deficiency associated with significant lowering of FXII level caused by homozygous deficiency, hyperlipoproteinaemia and hyperhomocysteinaemia with or without methylenetetrahydrofolate reductase mutation, and in other conditions. However, to mention and analyse all of them in detail is far beyond the scope of this study.

1.2.2. Acquired prothrombotic risk factors

The most frequent acquired prothrombotic risk factors in children are malignancy, indwelling central venous lines (CVL), prematurity in neonates, sepsis, surgery – especially orthopaedic, injury or trauma including burns, hormonal therapy, vascular anomalies, autoimmune diseases, endocrine diseases, and nephrotic syndrome.

1.3. Clinical symptoms of thrombosis

Clinical symptoms of deep venous thrombosis depending on its location might involve swelling, pain and cyanosis of the limb, positive "plantar" or Homans' sign, thrombophlebitis, "vena cava superior" syndrome, collateral vascular bed, ascites in case of vena cava inferior obturation, inexplicable abdominal pain, and haematuria in renal vein occlusions [8,12,13,14]. Dyspnoea, tachypnoea, and respiratory failure might be present in patients with pulmonary embolism.

1.4. Treatment of deep venous thrombosis in children

Low-molecular-weight heparin (LMWH) has more predictable pharmacokinetics and a better bioavailability than unfractioned heparin [15]; therefore it is the current standard treatment of deep venous thrombosis in children. Other alternatives include unfractioned heparin, coumarins, pentasaccharides and, under specific circumstances, also thrombolytics.

2. PATIENTS AND METHODS

2.1. Patients

2.1.1. Demography

In the Children's Faculty Hospital in Brno there were 45 children treated for venous thrombosis with LMWH from 2004 to 2006. We excluded 3 children with superficial venous thrombosis, 5 children who died because of their underlying disease during the treatment, 1 patient who had not had thrombophilia screening done, 1 patient who was transferred

	N	Average	Median	Minimum	Maximum	p – level
Intravenous administration	21	18.7	15.0	5.0	44.0	0.726
Subcutaneous administration	12	28.2	18.5	6.0	94.0	

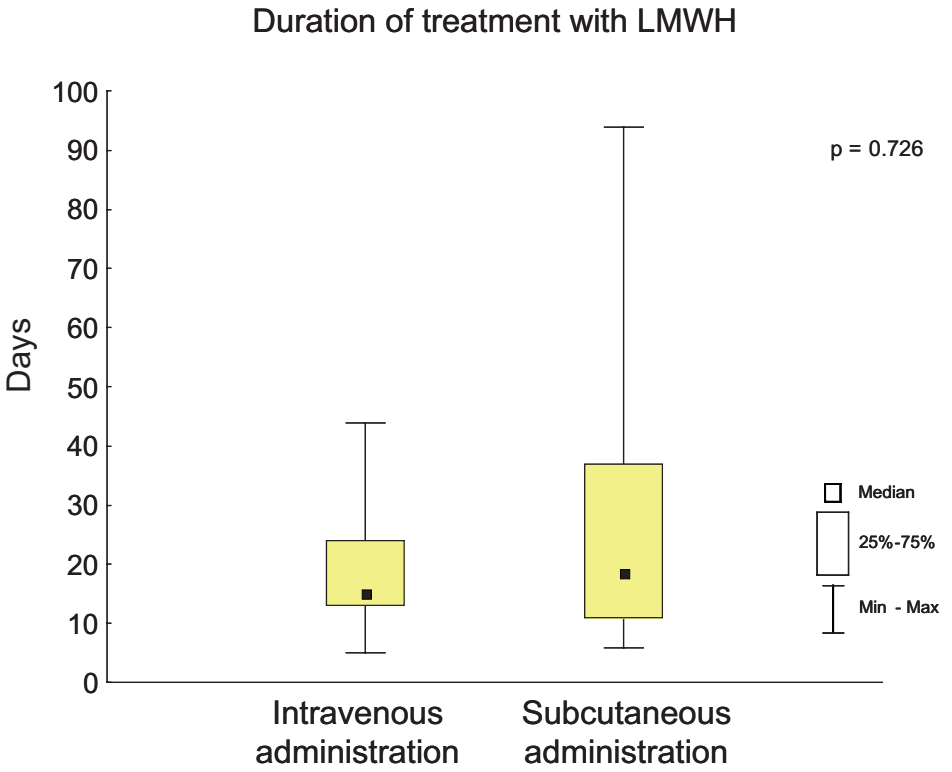

Figure 2
Summarisation of duration of treatment (in days) with LMWH

to another hospital with no sufficient feedback regarding his treatment outcome, 1 patient who was referred from a regional hospital and whose documentation was not complete, and 1 patient who was treated by local thrombolysis. We assessed 33 patients, who were treated by LMWH for deep venous thrombosis. Twenty-one of them were treated with continuous infusion (CI), 12 (57.1 %) were boys and 9 (42.9 %) were girls. Twelve patients were treated with subcutaneous (SC) application, 8 (66.7 %) girls and 4 (33.3 %) boys. The age range was from newborns to 18 years and was comparable in both groups (Figure 1).

The patients who were treated by CI were in-patients of the Department of Internal Medicine (52.4 %), Oncology Department (38.1 %), and surgical patients (9.5 %). Most of the patients who were treated by SC application were in-patients of the Department of Paediatric Oncology (52.4 %); some of them were also medical (25 %) or surgical patients (16.7 %).

2.2. Treatment with low-molecular-weight heparin

Low-molecular-weight heparin was administered to patients by intravenous (IV) pump Infusomat (Braun, Firana, Ivac) in a dose of 80 IU/kg/8h diluted in normal saline. The rate of infusion was 1 ml per hour. Continuous infusion was interrupted maximally for 2 hours and only in exceptional situations such as Doppler ultrasonography, et cetera. The chosen dose (240 IU/kg/24 h) was the recommended therapeutic dose for dalteparin, which we have used in all of our patients. In patients younger than 5 months we used the same initial dose. Further dosing was tailored individually for each patient to reach the required antiXa level.

2.3. Parameters monitored

2.3.1. Laboratory examination

Before starting the treatment our aim was to perform a full thrombophilia work-up in all patients. Blood samples were taken by qualified nurses into Sarstaedt tubes in accord with the Standard Operational Procedures valid in the Faculty Hospital in Brno at the time of the investigation. (The Faculty Hospital of Brno is certified in accord with the standard ISO 9000:2001.)

All genetic investigations were authorised by the local ethical committee.

The following tests were performed: antithrombin plasmatic level assessment (Accucolor AT III Kit, Trinity Biotech, Ireland); assessment of mutation FV Leiden by PCR method (East-Port Praha, Czech Republic); assessment of mutation FII G20210A by PCR method (East-Port Praha, Czech Republic); assessment of polymorphism methylenetetrahydrofolate reductase by PCR method (East-Port Praha, Czech Republic); protein C plasmatic level assessment (Sta Staclot protein C, Diagnostica Stago, France); protein S plasmatic level assessment (Asserachrom Total protein S, Sta Staclot Protein S, Diagnostica Stago, France); homocysteine plasmatic level assessment (Homocystein Bio-Rad, Bio-Rad Laboratories, USA); lipoprotein *a* plasmatic level assessment (Lpa Roche, Roche, Switzerland).

2.3.2. Diagnosis and monitoring of thrombosis and its treatment

Deep venous thrombosis was diagnosed with Doppler ultrasonography (Siemens, type Antarez, linear probe VFX 15–3, 10 MHZ), increased D-dimer level (STA Liatest D-Di, Diagnostica STAGO, France), and by clinical examination: tenderness at site of thrombosis, positive "plantar" sign and/or positive Homans' sign where applicable**.**

The efficiency of the treatment was monitored by the regression of clinical symptoms which were assessed and recorded during regular ward rounds, as well as by repeated Doppler ultrasonography (week 1, week 2, and week 6 after the diagnosis of the thrombosis) together with D-dimer testing. AntiXa levels (Coamatic Heparin, Chromogenix, Italy) were monitored at least during the first five days of the treatment, but the majority of the patients had longer monitoring of antiXa levels.

In patients treated by continuous infusion, samples for anti Xa level measurements were taken twelve hours after dose adjustment and/or change, and in patients treated by subcutaneous injection 3–4 hours after application following such a change. In accord with those levels the dose of LMWH was modified to keep antiXa levels in required intervals. The aim was to achieve as stable an anti Xa level as possible within the therapeutic range. This was the reason why the dose of LMWH was tailored individually to patient needs to reach interindividually comparable results.

We also monitored platelet levels during the whole time of the treatment to avoid possible bleeding complications in patients with low platelets treated with heparins. None of the patients in both groups had a kidney disorder; therefore no differences were supposed in antiXa clearance. Liver tests were not monitored regularly and/or intentionally in our patients. The treatment with LMWH was stopped when recanalisation of the vein was achieved or the thrombus was organised and unchanged during two consecutive Doppler ultrasound examinations. The patients were then switched to prophylactic treatment for at least 3 months to prevent re-occurrence of the thrombus. The safety of the treatment was clinically monitored by nurses, who recorded possible bleeding or other adverse events related to LMWH into the patients' charts.

No patients were treated with thrombolytics or other anticoagulants than those mentioned above.

2.4. Statistics – methods and data processing

Descriptive statistics such as mean, median, minimum, and maximum were used for comparison of the duration of treatment, the dose and the volume of anti-Xa. Differences between continuous variables were tested using a non-parametric Mann-Whitney test, whereas for assessment of associations between categorical variables the Spearman test for frequency tables was used. As a level of statistical significance, α=0.05 was used. Graphical visualisation was performed using box-plots prepared in the statistical programme STATISTICA for Windows 7.1.

3. RESULTS

3.1. Prothrombotic risks

3.1.1 Hereditary prothrombotic risk factors

In spite of the fact that we aimed to test all patients in our cohort for thrombophilia screening, we failed to achieve those results in some of the children. The reasons were mainly difficulties with sampling in severely ill and/or little children. We did not want to stress our patients with further repeated samplings as the results of the same were not the main output of this study. The table 1 shows the results available in our patients. We understand that this failure is limiting for drawing any significant results from those findings.

3.1.2. Acquired prothrombotic risk factors

Fifteen (71.4%) out of 21 patients who were treated with LMWH by CI had acquired prothrombotic risk factors. Eight (53.3%) out of them were hospitalised for malignancy, 7 (46.7%) had inserted CVL, 3 (20%) patients were treated

for sepsis or other serious infection, 2 (13.3 %) patients had thrombosis related to injury/trauma, 1 (6.7 %) girl used contraceptive pills, and 1 (6.7 %) neonate was born premature.
In the group of patients treated with LMWH by SC application, 10 (83.3 %) out of 12 patients had acquired prothrombotic risk factors. Seven of them (70 %) were hospitalised for malignancy, seven (70 %) patients had inserted CVL, two (20 %) patients had thrombosis related to injury/trauma, and 1 (10 %) girl used contraceptives.
None of the patients in both groups had thrombosis without any prothrombotic risk. Those who had no acquired risk had at least one inherited, despite the fact that screening for inherited risk factors was not complete.

3.2. Duration of treatment

The average duration of the_treatment in the patients on LMWH by CI was 18.7 days, the median was 15 days (ranging from 5 to 44 days). In the patients treated with LMWH by SC application the average duration of the treatment was 28.2 days, the median was 18.5 days (ranging from 6 to 97 days). The difference in the duration of the treatment between those two groups, however, was not statistically significant (Figure 2).

3.3. Weighted dose of LMWH during treatment

The average dose administered per kg per day to reach the required antiXa level in the group treated with LMWH by CI was 250.7 IU/kg/24h, median was 240 IU/kg/24h with the minimal dose of 200 IU/kg/24h and the maximal dose of 300 IU/kg/24h. In patients treated with LMWH by SC application the average dose administered per kg per day was 223.1 IU/kg/24h, median was 215 IU/kg/24h. With the minimal dose of 200 IU/kg/24h and the maximal dose of 282.5 IU/kg/24h.
In the case of the average weighted dose of LMWH administered per kg per day, we can see a statistically significant difference between the patients treated with LMWH by continual infusion and those treated with LMWH by subcutaneous applications (Figure 3).

3.4. Summarised anti Xa levels

The LMWH dose was adjusted to achieve and maintain the required anti Xa levels during the treatment. The therapeutic range of anti Xa level was 0.5 – 1 IU/ml. In the group of patients treated with LMWH by CI the average anti Xa level was 0.53 IU/ml, median was 0. 52 IU/ml with a minimal level of 0. 26 IU/ml and a maximal level of 0.87 IU/ml. In the patients who were treated with LMWH by SC application the average anti Xa level was 0.66 IU/ml, median was 0. 71 IU/ml with a minimal level of 0. 20 IU/ml and a maximal level of 0.93 IU/ml.
In the case of a summarised level of antiXa, a statistically significant difference between intravenous and subcutaneous administration of LMWH was observed (Figure 4).

3.5. Results of the treatment

3.5.1. Continuous intravenous infusion

In the group treated with LMWH by CI the treatment with the therapeutic dose led to complete recanalisation of the affected vein in 3 (14.3 %) patients and to partial recanalisation in 15 (71.4 %) patients. Only in 3 (14.3 %) patients on the therapeutic dose of LMWH the treatment did not lead to recanalisation (Figure 5).

3.5.2. Subcutaneous application

In the group of patients treated by subcutaneous application the treatment with the therapeutic dose of LMWH led to complete recanalisation in 4 (33.3 %) children. In 4 (33.3 %) patients this treatment led only to partial recanalisation and in 3 (33.3 %) patients it did not lead to recanalisation at all (Figure 5).
The above-mentioned results of the therapy seem to be statistically different when comparing patients treated with IV and SC administration of LMWH (Table 2).

3.6. Safety

In the group of patients treated by CI we have not recorded any adverse event, either any bleeding complication or a decreased platelet level, which could be related to heparin treatment.
In the group of patients treated by SC application we have recorded bruises after the application.

4. DISCUSSION

The aim of this pilot project is to point out an alternative way of treatment of thrombosis in children. In these days the standard treatment of DVT is subcutaneous application of LMWH. These well-established recommendations result especially from the REVIVE study, which has proved LMWH to be as effective as, and even safer than, unfractioned heparin.
We tried to compare the treatment of deep venous thrombosis with LMWH by CI and SC application. We assessed two groups of patients with similar age ranges and types of primary diagnoses. One group was treated with LMWH by CI and the other by SC application. In the group of patients treated with LMWH by CI the initial treatment with a full therapeutic dose of LMWH led to at least partial recanalisation of thrombosis in all children. In the group of patients treated with a similar dose of LMWH by SC application we were unable to recanalise the thrombosis in two (16.7 %) patients. The difference in the outcomes of the therapy between both groups

	N	Average	Median	Minimum	Maximum	p – level
Intravenous administration	21	250.7	240.0	200.0	300.0	0.024*
Subcutaneous administration	12	223.1	215.0	200.0	282.5	

*statistically significant result

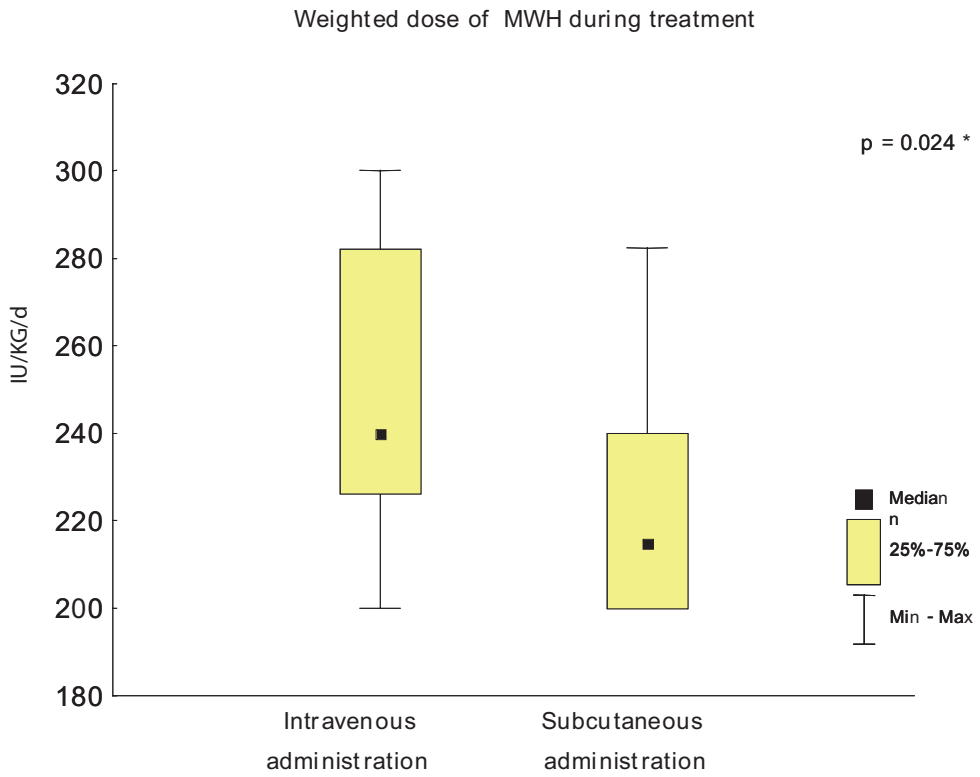

Figure 3
Weighted dose of LMWH (in IU/kg/d) during treatment

appears to be statistically significant (p 0.041, non-parametric Mann-Whitney test).

We can speculate that the reason for better results with CI could be perhaps a lower median dose of LMWH (IU/kg/day) and/or a wider range of antiXa levels and thereby a lower stability of antiXa levels in the plasma of patients treated with LMWH via SC application. The median of antiXa levels was higher in the group of patients treated by SC application, but we have to bear in mind that assessment of antiXa during SC treatment reflects only the maximal peaks of antiXa activity in vivo. On the contrary, monitoring of antiXa during CI aims to reflect the stable steady state of antiXa activity in the patients' plasma. Thus, the information provided is not fully comparable. On the other hand, it seems that, being guided by antiXa levels during treatment with LMWH via CI, we were able to reach better clinical results. To achieve the same or similar levels of antiXa we had to use different dosages for different ways of application of LMWH. Therefore, it is probably not correct just to extrapolate the dose of LMWH for CI from the dose of LMWH for SC application.

In any case, we should further assess what is more important for the successful treatment: whether the more stable antiXa levels or a higher median of the dose. A further and more detailed study of the pharmacodynamics of LMWH during CI administration might cast more light on that problem. However, based on currently available results of this study, it seems that the stability of antiXa levels in the patients' plasma will probably be more important for a favourable outcome of

	N	Average	Median	Minimum	Maximum	p – level
Intravenous administration	21	0.53	0.52	0.26	0.87	0.044*
Subcutaneous administration	12	0.66	0.71	0.20	0.93	

*statistically significant result

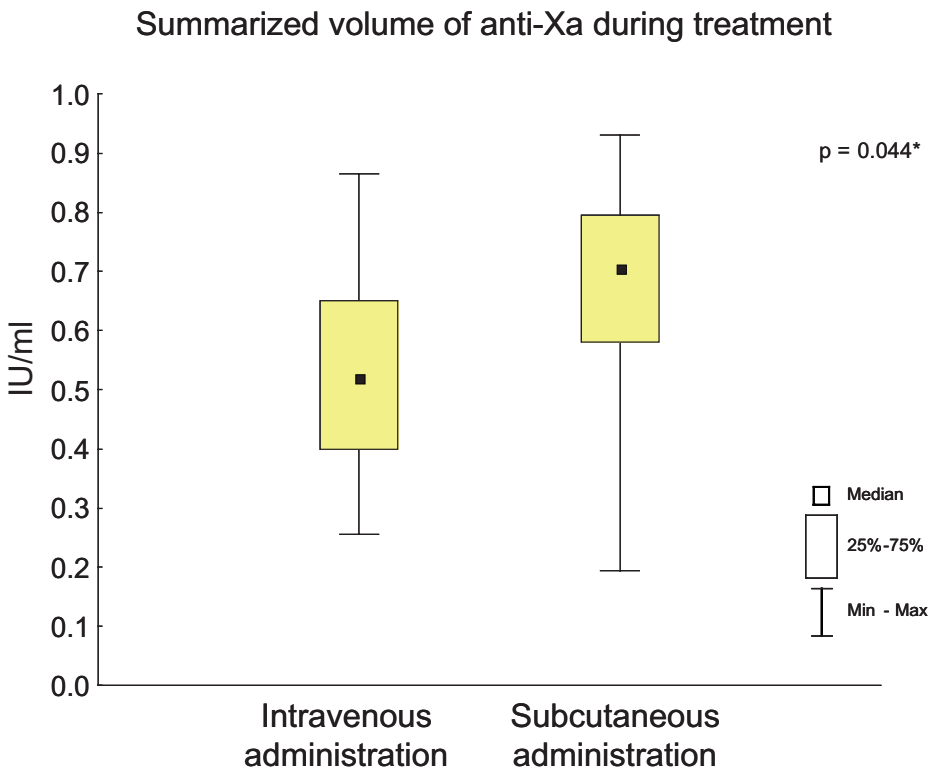

Figure 4
Summarised level of anti-Xa (in IU/ml) during treatment

the treatment. The duration of the treatment – average, minimal as well as maximal – was shorter in the group of patients treated by CI, which might be considered to be an advantage for the patients as well.

None of our patients had recurrent thrombosis; consequently we cannot confirm the results published by Italian or German authors showing evidence that carriers of combined prothrombotic risk factors [16,17] and patients who have experienced DVT which had not been fully recanalised remain in a higher risk of re-occurrence of DVT, mainly after withdrawal of anticoagulant treatment [18], compared to subjects with none or only one inherited prothrombotic defect or with complete thrombosis recanalisation. In contrast to the REVIVE study, we have not recorded any severe adverse events in any of our patients. In a certain way, this finding also corresponds with the results of U. Hoffman, showing that even i.v. bolus application of LMWH is as safe as SC administration and is not associated with any higher risk of adverse events [19].

A secondary endpoint of our study was to confirm the influence of prothrombotic risk factors on the development of thrombosis. As our data are incomplete, we cannot compare them relevantly with other published findings. Despite this weakness, over 70 % of our patients had at least one hereditary prothrombotic risk factor and so our results still cope with the findings that carriers of prothrombotic risk factors are at a higher risk of developing a first thrombotic event during childhood and early adolescence [20,21] and are consistent with the reports of German authors (Nowak-Göttl et al.) about the influence of hereditary prothrombotic risk factors in patients with primary thrombosis.

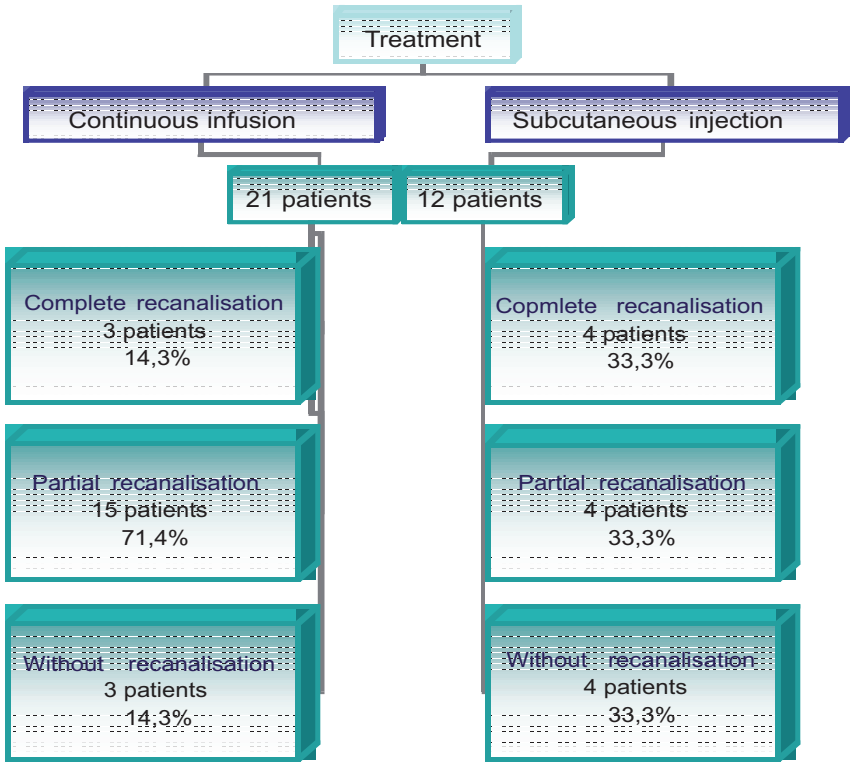

Figure 6
Results of treatment

At least half of the patients in both groups had also an inserted central venous line. The percentage of patients with CVLs was not different between both groups. This fact confirms the hypothesis that endothelial damage caused by the use of CVL might be an important cause of venous thrombosis in infants and children, especially when genetic risk factors are involved [22].

We understand that the results of this study do not enable us to draw any firm conclusions, mainly due to the small number of patients, and that it will be necessary to prove these results on a larger cohort study. In spite of that we believe to have shown that the treatment of DVT with LMWH by CI in our group of patients was an effective and safe alternative to SC application.

5. CONCLUSION

Based on the results mentioned above and according to facts coming up in the discussion we believe that in our group of patients the treatment of DVT with LMWH by continuous infusion was a promising alternative to the treatment by subcutaneous application.

In all patients the treatment with LMWH by CI led at least to partial recanalisation of DVT. The antiXa levels in these patients were more stable and the duration of treatment was even shorter than in the group treated by SC application. No patients had any adverse events. Thus, we can conclude that the treatment with LMWH by CI in our group of patients was at least equally as effective and safe as the treatment by SC application.

The treatment by CI is advantageous especially in those children admitted to hospital who have permanent intravenous access. By means of this treatment we can avoid repeated painful SC injections and thus increase the child's quality of life. In children with very low weight, it might be difficult to dose LMWH subcutaneously with enough precision due to the very small amount of the medication injected; moreover, little children and neonates have limited access to SC application. Further treatment by CI could be a great advantage in children with very low weight, in whom a titrate dose of IV application is easier than SC application. When administered by continuous infusion, LMWH has a shorter half-life and this could be useful especially in patients with a considerable risk of bleeding, for example patients with thrombocytopenia.

Table 2
Percentage of patients according to the result of the treatment with full therapeutic dose of LMWH

	Complete recanalisation	Partial recanalisation	No recanalisation	p – level
Intravenous administration (N = 21)	14.3 %	71.4 %	14.3 %	0.041*
Subcutaneous administration (N = 12)	33.3 %	33.3 %	33.3 %	

*statistically significant result

This table shows the percentage of patients in whom the treatment of LMWH in therapeutic doses led to complete recanalisation, partial recanalisation, or no recanalisation

Oncology patients with thrombocytopenia caused by chemotherapy in our group have not had any bleeding complications during the therapy. The parents did not object to the treatment by CI and appreciated that we were able to avoid painful SC applications. On the basis of our results we developed guidelines for the treatment of deep venous thrombosis for both the Department of Internal Medicine and the Department of Paediatric Oncology.

All our patients had at least one hereditary and/or acquired prothrombotic risk factor. We did not find any specific relation between any particular prothrombotic risk factor and the effect of the treatment. The number of patients in the groups was however low, which certainly decreases the power of the study to prove or rule out the same.

REFERENCES

1. Hirsh J. Heparin. N Eng J Med 1991; 324: 1565–74.
2. Collins R, Serimgeour A, Yusuf S, et al. Reduction in fatal pulmonary embolism and venous thrombosis by perioperative administration of subcutaneous heparin: overview of results of randomized trials in general, orthopedics and urologic surgery. N Eng J Med 1988; 318: 1162–73.
3. Clagett GP, Reisch JS. Prevention in thromboembolism in surgical patients. Ann Surg 1988; 208: 227–40.
4. Castaman C, Roderghiero F, Dini E. Thrombotic complication during L-asparaginase treatment for acute lymphoblastic leukemia. Haematologica 1990; 75: 567–69.
5. Wise RC, Todd JK. Spontaneous lower-extremity venous thrombosis in children. Am J Dis Child 1973; 126: 766–69.
6. Bernstein D, Coupy S, Schouberg SK. Pulmonary embolism in adolescent. Am J Dis Child 1986; 140: 667–71.
7. Andrew M, David M, Adams M, et al. Venous thromboembolic complications (VTE) in children: first analyses of the Canadian registry. Blood 1994; 83: 1251–57.
8. Schmidt B, Andrew M. Neonatal thrombosis: report of a prospective Canadian and international registry. Paediatrics 1995; 96: 939–43.
9. Monagle P, Adams M, Mahoney M, et al. Long-term outcome of Paediatric thromboembolic disease: a report from the Canadian Childhood Thrombophilia Registry. Pediatr Res 1999;
10. David M, Andrew M. Venous thromboembolism complications in children: a critical review of the literature. J Pediatr 1993; 123: 337–46.
11. Andrew M, Monagle P, Brooker L. Thromboembolic complications during infancy and childhood. Decker, Hamilton, Ontario, Canada 2000.
12. Nowak-Göttl U, von Kries R, Göbel U. Neonatal symptomatic thrombosis in Germany: two years survey. Arch Dis Child Fetal Neonatal Ed 1997; 76: F163–7.
13. Mocan H, Beattie TJ, Mureny AV. Renal venous thrombosis in infancy: long-term follow-up. Pediatr Nephrol 1991; 5: 45–9.
14. Bökenkamp A, von Karies R, Nowak-Göttl U, Göbel U, Hoyer PF. Neonatal venous renal thrombosis in Germany between 1992 and 1994: epidemiology, treatment and outcome. Eur J Pediatr 2000; 159: 44–8.
15. Monagle P, Chalmers E, Chan A, et al. Antithrombotic therapy in neonates and children: American College of Chest Physicians evidence. Based Clinical Practice Guidelines, 8th ed. Chest 2008; 133: 887–968.
16. Lindmarker P, Schulman S, Sten-Linder M, et al. The risk of recurrent venous thromboembolism in carriers and non-carriers of the G1691A allele in the coagulation factor V gene and the G20210A allele in the prothrombin gene. Thromb Haemost 1999; 81:684–89.
17. Stefano de V, Martinelli I, Mannucci PM, et al. The risk of recurrent deep venous thrombosis in heterozygous carriers of both factor V Leiden and the G20210A prothrombin mutation. N Engl J Med 1999; 34: 801–6.

18. Streif W, Andrew M, Marzinotto V, et al. Analysis of Warfarin therapy in paediatrics patients: a prospective cohort study of 319 patients. Blood 1999; 94: 3007–14.
19. Hoffman U, Harenberg J, Bauer K, et al. Bioequivalence of subcutaneous and intravenous body-weight-independent high-dose low-molecular-weight heparin Certoparin on anti-Xa, Geotest, and tissue factor pathway inhibitor activity in volunteers. Blood Coagulation and Fibrinolysis 2002; 13: 289–96.
20. Salomon O, Steinberg DM, Zivelin A, et al. Single and combined prothrombic factors in patients with idiopathic venous thromboembolism – prevalence and risk assessment. Arteriol Thromb BASF Biol 1999; 19: 511–18.
21. Ehrenforth S, von Depka Prondsinski M, Aygoren-Pursun E, Nowak-Göttl U, Scharrer I, Ganser A. Study of the prothrombin gene 20210GA variant in FV:Q506 carriers in relationship to the presence or absence of juvenile venous thromboembolism. Arterioscler Thromb BASF Biol 1999; 19: 276–80.
22. Nowak-Göttl U, Dübbers A, Kececioglu D, et al. Factor V Leiden, protein C and lipoprotein (a) in catheter-related thrombosis in childhood – a prospective study. J Pediatr 1997; 131: 608.

MUTATIONS IN EGFR SIGNAL PATHWAY IN CORRELATION WITH RESPONSE TO TREATMENT OF HEAD AND NECK CANCERS

Neuwirthová J.[1], Smilek P.[1], Rottenberg J.[1], Kostřica R.[1], Berkovcová J.[2], Hajdúch M.[2]

[1] Department of Otorhinolaryngology and Head and Neck Surgery, Masaryk University and St. Anne's Faculty Hospital, Brno
[2] Laboratory of Experimental Medicine, Department of Paediatrics, Palacký University and Faculty Hospital, Olomouc

Received after revision July 2009

KEY WORDS

Head and neck cancer
EGFR
Predictive marker

CORRESPONDING AUTHOR

Neuwirthová J.
Department of Otorhinolaryngology and Head and Neck Surgery, Masaryk University and St. Anne's Faculty Hospital, Brno
Pekařská 53
656 91 Brno
Czech Republic

ABSTRACT

The prognostic and predictive value of the epidermal growth factor receptor (EGFR) expression and some genetic alterations in the EGFR signal pathway, such as EGFR amplification, EGFR-activating tyrosine kinase mutations or the k-ras gene mutation, were investigated in our study. The aim of the research was to evaluate the occurrence of the above-mentioned biomarkers in correlation with the therapeutic response and survival in patients with spinocellular head and neck cancers. The presence of activating mutations in the EGFR tyrosine kinase domain, the k-ras mutation, and the correlation between EGFR gene amplification and receptor expression were proved.

ABBREVIATIONS USED

HNSCC – head and neck squamous cell cancer
EGFR (HER1) – epidermal growth factor receptor
FISH – fluorescence in situ hybridisation

INTRODUCTION

Surgical resection is the standard therapy of an advanced head and neck squamous cell carcinoma (HNSCC). Radiotherapy or chemoradiotherapy is frequently added to the treatment scheme to target the remaining tumour cells and to induce programmed cell death (apoptosis). However, HNSCC tumours regularly exhibit resistance to apoptosis induction. Some genetic alterations detected from tumour cells could predict the response to treatment or could be helpful in deciding which type and how aggressive therapy should be selected for a patient. The aim of investigating predictive factors is to individualise the therapy.

The epidermal growth factor receptor (EGFR) is a well-characterised proto-oncogene which is present in multiple cancers where – as will be shown – it promotes tumour progression. The EGFR (HER1) is a member of the family of transmembrane receptors which also include HER2/neu (ErbB–2), Her3 (ErbB–3), and Her4 (ErbB–4). The EGFR has an extracellular ligand-binding domain, a transmembrane region, and an intracellular domain which includes a kinase domain and autophosphorylation sites. The EGFR is ubiquitously distributed on normal epithelial tissues and is overexpressed in several cancers. The EGFR plays a critical role in the control of cellular proliferation, differentiation, and survival. A series of EGFR ligands has been identified, with most studies implicating the transforming growth factor alpha as a predominant autocrine growth factor in head and neck cancers. The binding ligand to EGFR triggers homodimerisation with the EGFR or heterodimerisation of the EGFR with another receptor from its family, resulting in autophosphorylation and downstream signalling. Abnormalities in the signalling of the EGFR pathway are found in a wide range of cancers. Targeted therapy directed against the EGFR represents a new approach in oncology.

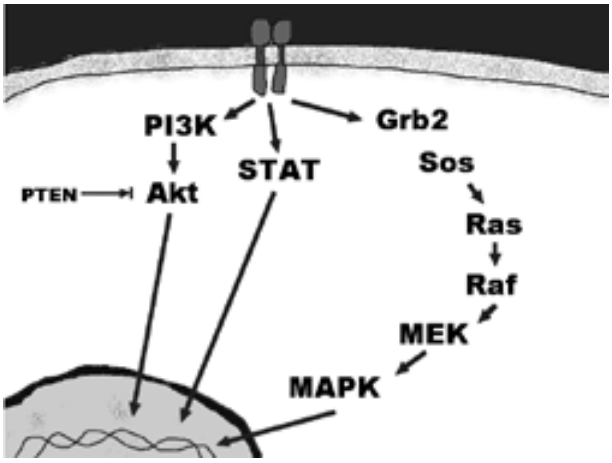

Figure 1
Signal transducers in EGFR signal pathway

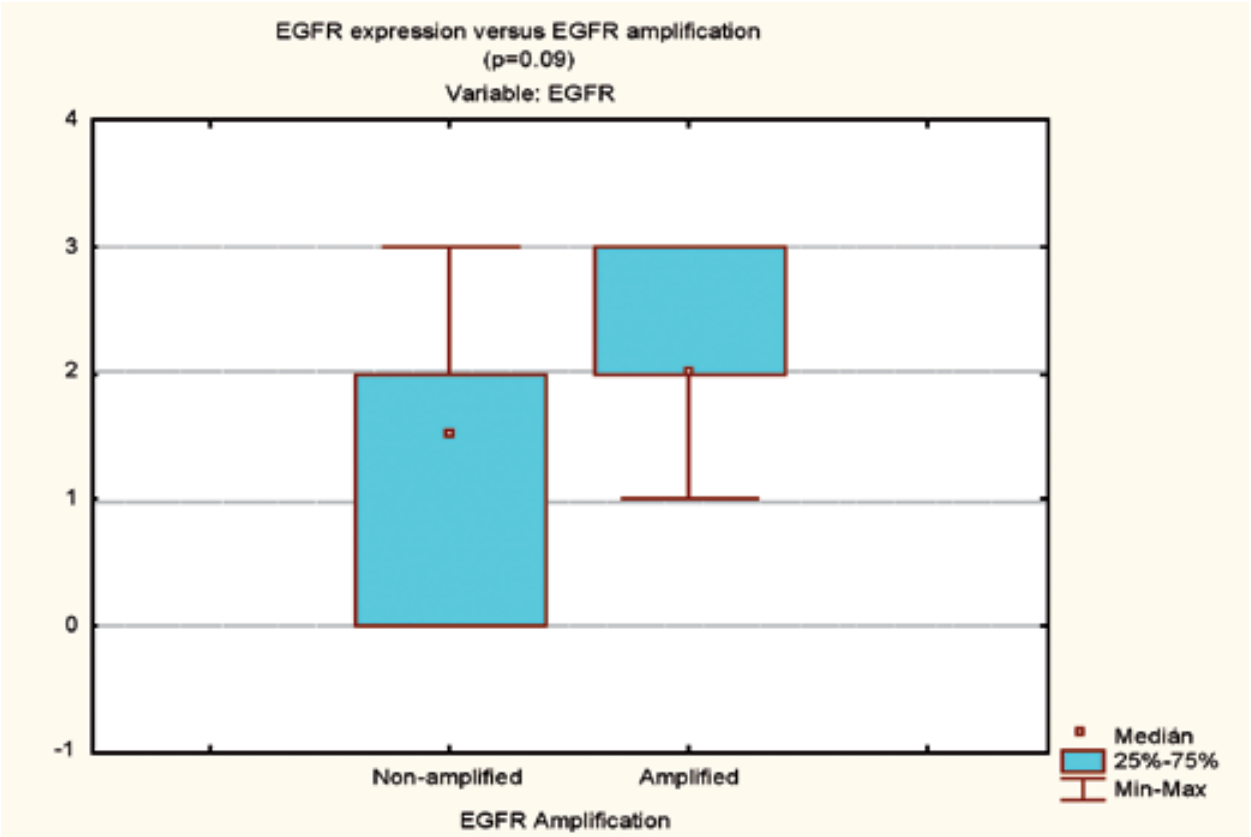

Figure 2
Correlation between EGFR gene amplification and protein expression

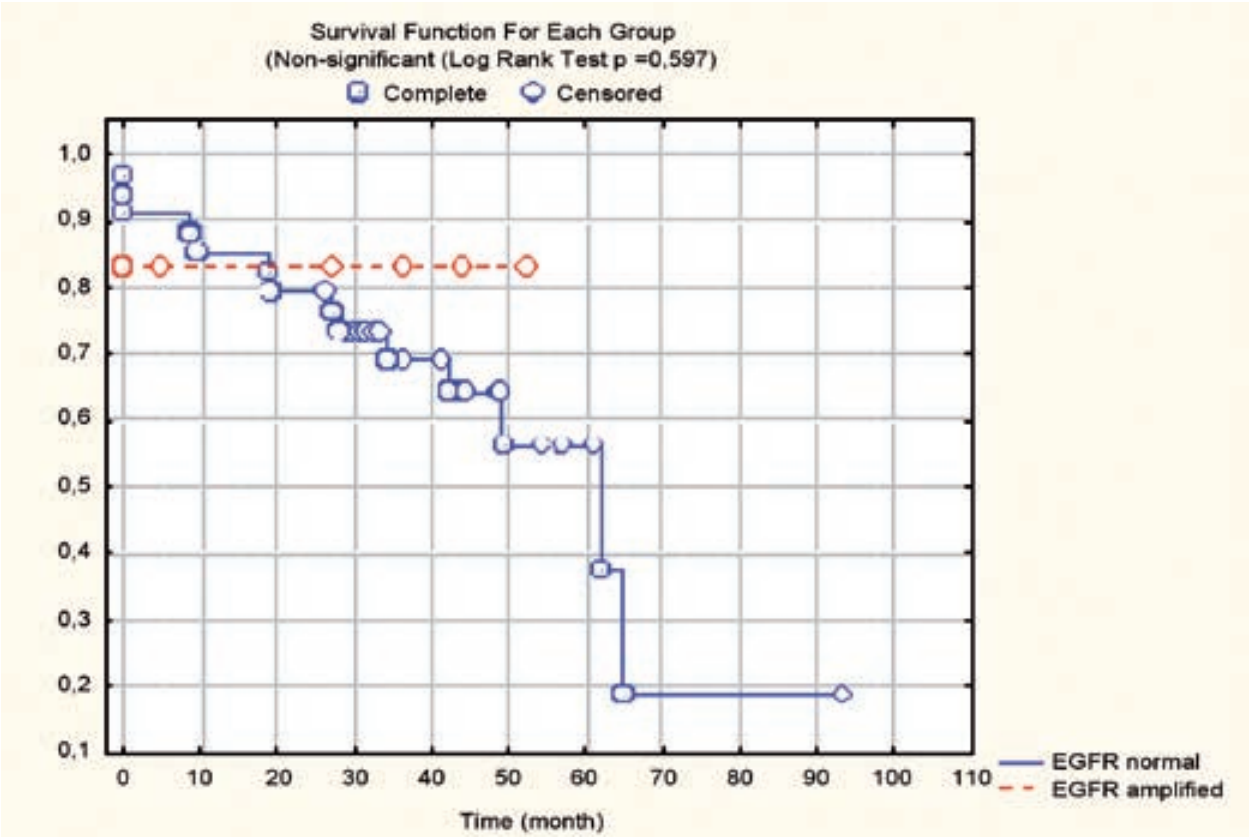

Figure 3
Survival of EGFR non-amplified vs. amplified group (non-significant)

Monoclonal antibodies and tyrosine kinase inhibitors, acting extracellularly and intracellularly, respectively, comprise two classes of agents currently available for use. Various genetic alterations predict the response to EGFR inhibitors activating especially mutations of intracellular transuders in the EGFR signal pathway (Figure 1). Some of these mutations are clinically used before the selection of patients convenient for this treatment in various types of tumours, but not all of them were studied in HNSCC. Activating mutations in the EGFR signal pathway cause a more aggressive phenotype which could influence the response to chemotherapy and radiotherapy. However, indicating these mutations as predictive markers for clinical use requires strong association with the therapeutic response and enough representation in specific tumours.

MATERIALS AND METHODS

Forty-five tumour samples from patients with HNSCC of oropharynx, hypopharynx, oral cavity, or larynx were evaluated. The patients were treated by chemoradiotherapy / radiotherapy as a primary definitive treatment (20 patients), or as an adjuvant treatment after the surgical resection of the tumour (25 patients). Surgical resection was preferred in resectable cases while definitive chemoradiotherapy or radiotherapy was selected in unresectable cases or if preservation of the organ was preferred. Dividing patients into two groups was caused by a well-known reason: patients with primary surgical resection have better therapeutical results and a better chance of surviving than patients with definitive chemoradiotherapy. All clinical stages were represented in these 2 groups of patients, with stage IVA being represented mostly. The following genetic alterations of tumour cells from paraffin blocks were evaluated: EGFR expression, ras gene mutation, EGFR gene amplification, and activating mutations of the EGFR gene. The EGFR expression was evaluated by an international scoring system 0, 1+, 2+, 3+ (Novocastra). The activating mutation of the ras gene mutation was detected in exon 1, the other cases were non-

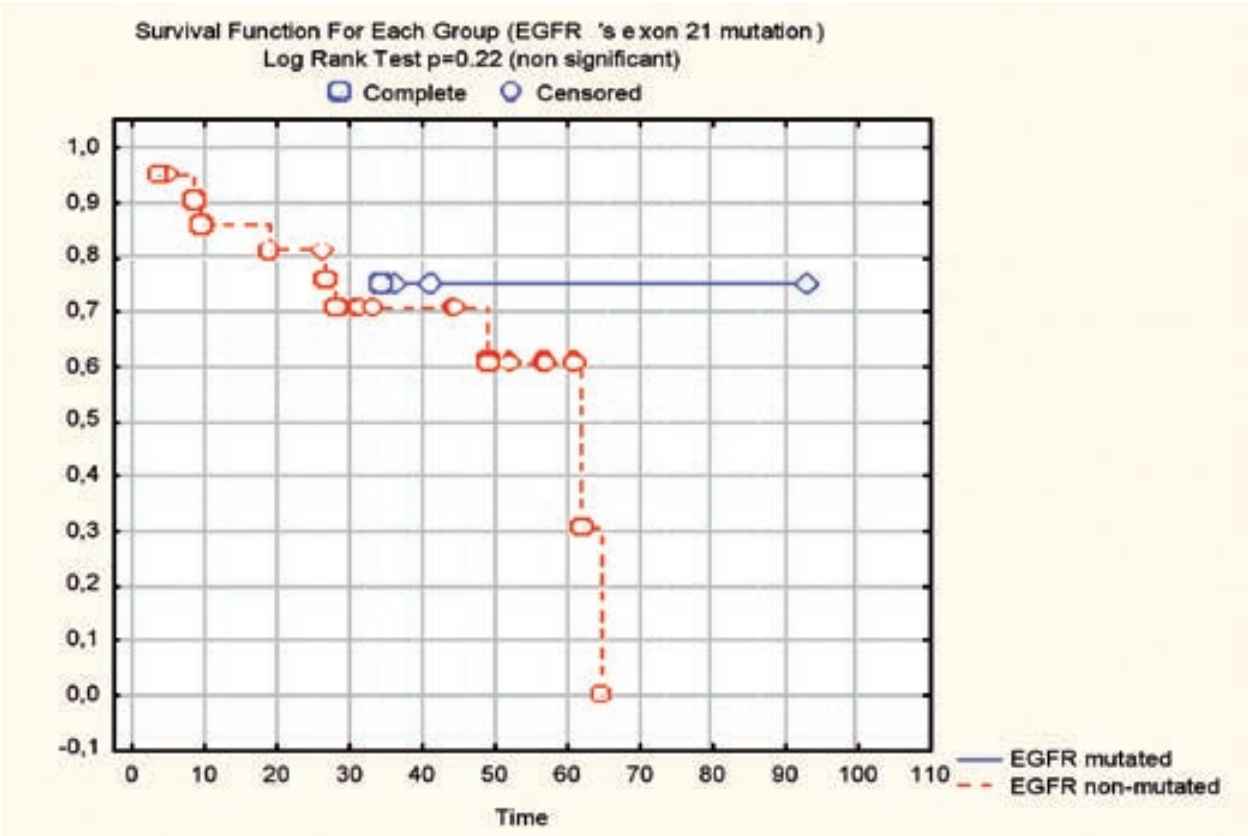

Figure 4
Survival of EGFR non-mutated vs. mutated in exon 21 group (non-significant)

mutated (wild type). Activating mutations of the EGFR gene were detected in exons 19 and 21. The gene amplification was defined as a ratio of EGFR signals to a chromosome 7 copy number of 1.5 or more.

Tumour samples were taken mostly from peripheral active parts of tumours. The receptor expression was detected by immunohistochemical staining. The paraffin sections were assessed by laser capture microdissection. The polymerase chain reaction (PCR) was used to identify mutations; fluorescence in situ hybridisation (FISH) was used for EGFR gene amplification.

Kaplan-Meier analysis and the Gehan-Wilcoxon test were used for the survival evaluation; the χ^2 test and the Fischer test were used for the evaluation of the EGFR expression dependence on clinical stages; and the Mann-Whitney test was used for the relation between EGFR expression and gene amplification. Statistical analysis was carried out with the help of Statistica for Windows 6.0 software.

RESULTS

In our study, 91 % of the patients achieved complete remission; five-year survival was recorded in 70 %. These results were influenced by patients with the first stage of glottic cancer.

The EGFR expression was positive in 72 % and negative in 28 % of the patients.

The EGFR amplification was present in 15 % and was associated with the higher EGFR protein expression (Figure 2).

Four mutations in the tyrosine kinase domain in exon 21 were found; however, no mutation in exon 19 was discovered. No significant correlation between the mutations or amplification of the EGFR gene and the patients' survival was proved in spite of the fact that only data of patients with definitive chemo/radiotherapy (organ preservation protocols) (Figures 3, 4) were analysed. The ras gene mutation, which is known as a negative predictive and prognostic marker, was only seen in 1 patient (laryngeal cancer of

glottis T3N0M0), and this case was associated with a negative prognosis.

DISCUSSION

It has been observed that there are discrepancies between the results of studies comparing EGFR amplification and EGFR expression; some authors have reported a correlation while others have not. The detection of EGFR expression depends partly on the specificity and sensitivity of the available immunohistochemical sets [1]. Furthermore, there are differences in EGFR expression inside a tumour; the highest expression, e.g. the most active parts, can be found in the periphery, whereas in the central parts the expression could be very low or negative. The FISH has been used as a reference method for the assessment of gene amplification for many years; however, there are several ways to analyse the gene expression by the FISH and not all authors differentiate true gene amplifications from chromosomal polysomy. This could be the reason why in the literature there are studies with low percentage of FISH positivity, e.g. 17 % [2], whereas other studies present 58 % [3] or 63 % [4] in HNSCC. The association between the true EGFR gene amplification and the EGFR protein overexpression was found in our study.

The mutations of the tyrosine kinase domain of the EGFR gene in exons 19 and 21 are known to affect sensitivity to the EGFR inhibitors; at the same time, they can be used as positive predictive markers during the therapy with intracellular inhibitors [5, 6]. In our group of patients, several cases of EGFRex21 were found.

The ras gene mutation is a negative predictive and prognostic marker. This mutation is strongly associated with a negative response to the EGFR inhibitors, and it is used as a negative predictive marker in some types of tumours. The ras gene mutation is rare in HNSCC [7]. Only 1 ras gene mutation was found in our group of patients and this case had a highly negative prognosis.

CONCLUSIONS

The study suggests that in spite of the fact that the ras gene mutation was not found in a representative percentage in HNSCC, its presence can be associated with negative prognosis. Furthermore, EGFR tyrosine kinase mutations which could be useful for the prediction of the response to EGFR inhibitors were detected.

Not enough cases of the EGFR genetic alterations for analysing their importance as predictive factors in clinical use were found. However, they do not seem to be as useful for the prediction of the response to chemo/radiotherapy as EGFR inhibitors. Therefore, the monitoring of predictive factors during the EGFR inhibitor therapy will continue.

ACKNOWLEDGEMENTS

This study was supported by the following grants: IGA MZCR No. NC 7602–3/2003 and MSM Nos. 6198959216, LC07017.

REFERENCES

1. Kersting C, Packeisen J, Leidinger B, et al. Pitfalls in immunohistochemical assessment of EGFR expression in soft tissue sarcomas. J Clin Pathology 2006; 59: 585–90.
2. Temam S, Kawaguchi H, El-Naggar AK, et al. Epidermal growth factor receptor copy number alterations correlate with poor clinical outcome in patients with head and neck squamous cancer. J Clin Oncol 2007; 25: 2164–70.
3. Chung CHH, Ely K, McGavran L, et al. Increased epidermal growth factor receptor gene copy number is associated with poor prognosis in head and neck squamous cell carcinomas. J Clin Oncol 2006; 24: 4170–76.
4. Chung CH, Ely K, Carter J, et al. High gene copy number of epidermal growth factor receptor by fluorescence in situ hybridisation is frequent in head and neck squamous cell carcinomas and associates with worse recurrence-free survival. ASCO Annual Meeting Proceedings Part I. J Clin Oncol 2006; 24 (Suppl 18): 5502.
5. Paez JG, Janne PA, Lee JC, et al. EGFR mutations in lung cancer: correlation with clinical response to gefitinib therapy. Science 2004; 304: 1497–500.
6. Lynch TJ, Bell DW, Sordella R, et al. Activating mutations in the epidermal growth factor receptor underlying responsiveness of non-small-cell lung cancer to gefitinib. N Engl J Med 2004; 350: 2129–39.
7. Sheikh AM, Gunduz M, Nagatsuka H, et al. Expression and mutation analysis of epidermal growth factor receptor in head and neck squamous cell carcinoma. Cancer Sci 2008; 99: 1589–94.

QT DYNAMICITY AND TIME TO ARTERY OPENING IN PATIENTS WITH MYOCARDIAL INFARCTION WITH ST ELEVATIONS

Dohnalová I.[1], Novotný T.[1], Šišáková M.[1], Poloczek M.[1], Kyselová I.[1], Dostálová L.[1], Floriánová A.[1], Kala P.[1], Toman O.[1], Vít P.[2], Špinar J.[1]

[1] Department of Internal Medicine and Cardiology, Faculty Hospital Brno and Faculty of Medicine, Masaryk University, Brno

[2] 2nd Department of Paediatrics, Faculty Hospital Brno and Faculty of Medicine, Masaryk University, Brno

Received after revision July 2009

KEY WORDS

QT dynamicity
Myocardial infarction
Sudden cardiac death

CORRESPONDING AUTHOR

Dohnalová I.
Department of Internal Medicine and Cardiology,
Faculty Hospital Brno and Faculty of Medicine,
Masaryk University, Brno
Jihlavská 20
625 00 Brno
Czech Republic

ABSTRACT

QT dynamicity is a marker of ventricular repolarisation used in risk stratification of cardiac death. The aim of this study was to correlate QT dynamicity parameters with time to artery opening, and Q wave evolution after myocardial infarction with ST elevations (STEMI).

A 24-hour ECG monitoring was performed in 112 patients 48–72 hours after acute STEMI (treated with direct angioplasty). The QT dynamicity (slope of linear QT/RR regression line) was automatically analysed from 24-hour ECG recordings (QT Guard, MARS Unity Workstation, GE Medical). The occurrence of pathological Q wave was assessed on 12-lead ECG 48 hours after STEMI.

Infarction artery was opened 120 minutes from the beginning of symptoms in 10 patients (group A), 121–240 min in 53 patients (group B), 241–360 min in 31 patients (group C), and more than 360 min in 18 patients (group D). QT/RR slopes in all these groups were not different (A: 0.168±0.045, B: 0.216±0.076, C: 0.225±0.095, D: 0.206±0.089. A vs B: p=0.066, A vs C: p=0.058, A vs D: p=0.27, B vs C: p=0.638, B vs D: p=0.44, C vs D: p=0.258). Pathological Q wave evolved in 86 patients; in 46 patients no Q wave was observed. The QT/RR slope was significantly steeper in patients with Q wave evolution after STEMI compared to the patients with nonQ MI (0.229±0.118 vs 0.181±0.099, p=0.007).

No simple relationship between time to artery opening and QT dynamicity was found. The QT/RR slope is steeper in patients with Q wave evolution after STEMI, confirming that they are high-risk individuals.

ABBREVIATIONS USED

ECG – electrocardiography
STEMI – myocardial infarction with ST elevations
MI – myocardial infarction
dPCI – direct percutaneous coronary intervention
PVC – premature ventricular complexes

Table 1
Clinical characteristics of patients

n	112
Age	62.6±11.1
Female/male	26/86
LV EF	48.5±12.1 %
Diabetes	25 (22.3 %)
Hypertension	64 (57 %)
Beta blocker	101 (90.2 %)

LVEF – left ventricle ejection fraction

Table 2
n = 112 Values of "slope" individual groups

Time to artery opening	n	slope (a)
A 0–120 min	11	0.168±0.045
B 121–240 min	52	0.216±0.076
C 241–360 min	31	0.225±0.095
D >360 min	18	0.206±0.089

Table 3
The comparison of "slope" between groups

		p
A vs B	0.168±0.045 vs 0.216±0.076	0.066
A vs C	0.168±0.045 vs 0.225±0.095	0.058
A vs D	0.168±0.045 vs 0.206±0.089	0.270

A: Group of patients with time to artery opening until 120 min from chest pain beginning
B: Group of patients with time to artery opening from 121 to 240 min from chest pain beginning
C: Group of patients with time to artery opening from 241 to 360 min from chest pain beginning
D: Group of patients with time to artery opening later than 360 min from chest pain beginning

INTRODUCTION

It is well established that ventricular repolarisation abnormalities are associated with the risk of arrhythmic death after myocardial infarction (MI) [1]. The aim of many studies is the risk stratification after MI using non-invasive methods based on electrocardiography (ECG). The QT interval on surface ECG is usually considered a surrogate of ventricular action potential duration. Introduction of digital ECG has brought new methods for quantitative evaluation of ventricular repolarisation. One of these new markers is the slope of linear QT/RR regression line – QT dynamicity. It reflects the influence of heart rate and the autonomic nervous system on the QT interval [2]. The aim of this study was to correlate QT dynamicity parameters with time to artery opening, and Q wave evolution after myocardial infarction with ST elevations (STEMI).

METHODS

Patients with the diagnosis of acute MI with ST elevation (STEMI) were hospitalised at the Department of Internal Medicine and Cardiology, Faculty Hospital Brno and Faculty of Medicine, Masaryk University, Brno. A direct percutaneous coronary intervention (dPCI) was carried out in all patients who fulfilled the indication criteria. The initial flow through the infarction-related artery was classified according to TIMI classification: TIMI 0 – stop; TIMI 1 – minimal flow through artery occlusion; TIMI 2 – partial recanalisation, slow flow; TIMI 3 – normal flow [3]. There were the following exclusion criteria: rhythm other than sinus, >50 premature ventricular complexes (PVCs)/hour, left bundle branch blockade, artificial pulmonary ventilation, and cardiogenic shock. The 24-hour ECG monitoring (MARS Unity Workstation, GE Medical Information Technologies) was performed 48–72 hours after acute STEMI in all patients who fulfilled the inclusion criteria. Recordings shorter than 20 hours were not assessed. QT dynamicity (assessed as the slope of the linear regression line QT=aRR+b, where "a" is the slope and "b" is the point of intersection with the *y*-axis) was automatically analysed from 24-hour ECG recordings (QT Guard software of MARS Unity Workstation, GE Medical) (Figure 1) [4]. The occurrence of the pathological Q wave was assessed on 12-lead ECG 48 hours after STEMI. The program Statistica 6 was used for statistical data analysis.

RESULTS

The 24-hour ECG monitoring was performed in 112 patients. Clinical characteristics are summarised in Table 1. The patients were divided into 4 groups (A – D) according to the time to in-

farction artery opening from chest pain beginning (Table 2). QT/RR slopes in all these groups were not different (Table 3). To further enhance the precision of analysis, patients with the initial TIMI flow greater than 1 (i. e. with opened artery) were excluded from the groups A, B, C, D (Table 4). A statistically significant difference was found only between groups A vs B, other values were not different (Table 5). The QT/RR slope was significantly steeper in patients with Q wave evolution after STEMI, confirming (Q: 0.229±0.118 vs. nonQ: 0.181±0.099, p=0.007) that there are high-risk individuals also with lower EF (Q: 45.30±11.96 % vs. nonQ: 53.12±9.86 %, p=0.0001) (Table 6).

DISCUSSION

QT dynamicity is considered to be a surrogate of action potential physiology at the cellular level. It reflects the influence of various factors such as heart rate, balance of autonomous innervation, drug treatment, the metabolic state of the myocardial cell, etc. [2]. The basic physiology information about QT/RR relationship, and diurnal [5] or gender differences of QT dynamicity [6] was found thanks to the development of Holter ECG monitoring. The pathological behaviour in patients with congenital LQTS was published [7]. Later smaller studies indicated that the risk stratification of sudden cardiac death using QT dynamicity may be possible [8].

Several studies assessed the benefit of QT dynamicity for risk stratification during the last years: two of them reported on patients after acute MI [9, 10], another one about patients with chronic heart failure [11]. Another alternate paper used the registry of an EMIAT study (European Myocardial Infarct Amiodarone Study) [12], while comparing QT dynamicity in patients who had cardiac death and in survivors. In all these studies the QT/RR slopes were significantly steeper in those who died; nevertheless, the values of this parameter notably overlapped.

In this article we present results on the correlation of QT dynamicity parameters with time to infarction artery opening. These are partial data obtained within the frame of a research project supported by the Internal Grant Agency of the Ministry of Health [13, 14]. The mortality follow-up has not been finished yet.

It was repeatedly shown that the worst prognosis of patients after acute MI corresponds with ischaemia duration [15]. Thus we hypothesised that with longer ischaemia the QT/RR slope would get steeper. The slope was really significantly lower in patients with dPCI performed up to 120 minutes, but only if compared to patients with dPCI during the 121st to 240th minute. No statistically significant difference was found compared to the patients in whom the infarction artery was opened 241 minutes and later since chest pain beginning.

Table 4
Values of "slope" in individual groups restricted only to patients with initial TIMI flow 0–1

Time to artery opening	n	slope (a)
A 0–120 min	11	0.168±0.045
B 121–240 min	33	0.225±0.074
C 241–360 min	22	0.219±0.108
D >360 min	13	0.197±0.049

Table 5
The comparison of "slope" between groups restricted only to patients with initial TIMI flow 0–1

		p
A vs B	0.168±0.045 vs 0.225±0.074	0.018*
A vs C	0.168±0.045 vs 0.219±0.108	0.136
A vs D	0.168±0.045 vs 0.197±0.049	0.156

A: Group of patients with time to artery opening until 120 min from chest pain beginning
B: Group of patients with time to artery opening from 121 to 240 min from chest pain beginning
C: Group of patients with time to artery opening from 241 to 360 min from chest pain beginning
D: Group of patients with time to artery opening later than 360 min from chest pain beginning
* statistically significant difference

Table 6
Values of "slope" in patients with Q and nonQ myocardial infarction

Q wave	n	slope (a)	LV EF
Yes	66	0.229+0.118	45.30 %
No	46	0.181+0.099	53.12 %
p		0.007	0.0001

LV EF left ventricle ejection fraction

Afterwards, we correlated QT dynamicity parameters with Q wave evolution after myocardial infarction with ST elevation. The QT/RR slope was significantly steeper in patients with Q wave evolution after STEMI, confirming that they are high-risk individuals. They had also more marked systolic dysfunction.

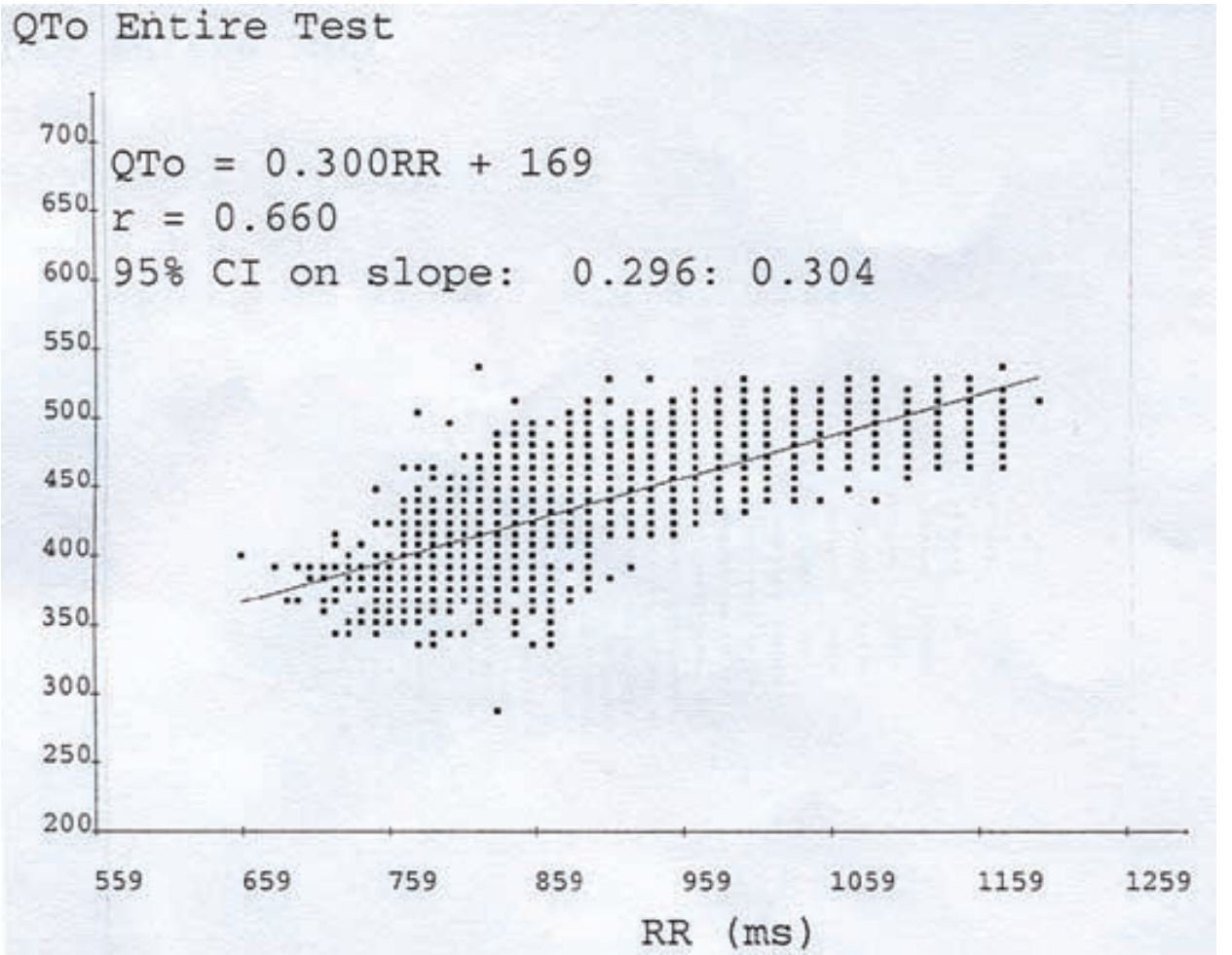

Figure 1
Graphical output of QT dynamicity results from MARS Unity Workstation: x-axis: RR interval in ms, y-axis: QT interval duration in ms (QTo – QT offset), "QTo = 0.300RR + 169" is the mathematical expression of linear regression, where 0.300 is the slope and 169 is the intersection with the y-axis. The "r" is the correlation coefficient

Thus, no simple relation was found between the time to infarction artery opening and QT dynamicity. One of the possible explanations of this fact could be independence of QT dynamicity as a risk marker. On the other hand, the results may be distorted by many factors: previous myocardial infarction, presence of coronary artery collaterals, infarction size, etc.

An important limitation of QT dynamicity analysis is the necessity of selection of patients eligible for the examination. The QT dynamicity analysis cannot be done in potentially high-risk patients with atrial fibrillation, left bundle branch blockade, and with frequent premature ventricular ectopies. Our protocol also excluded haemodynamically unstable patients with the need for catecholamine administration, hence risk patients again. This group could have been investigated if the Holter recording had been done later. Another limitation of QT dynamicity evaluation is also posed by availability of technical equipment.

There are many technical limitations of ECG morphological analysis. The problem is not only identification of the T wave end [16] but also identification of the QRS complex onset [17]. The relationship between QT/RR is not linear, thus making the use of linear regression problematic [18]. Detailed discussion of these features exceeds the scope of this article.

Despite high expectation, the importance of QT dynamicity as a risk factor remains uncertain. By all means, research

into this domain has brought a great deal of information about the relation between repolarisation and heart rate in different situations, and it became a springboard for the use of new generation methods, like evaluation of the angle of QRS complex and T wave vectors or T wave residue [19]. The role of these methods in risk stratification remains yet to be established.

ACKNOWLEDGEMENT

Supported by IGA MH CR NR/8060–3 and NR/8374–3.

REFERENCES

1. Schwartz PJ, Wolf MD. QT interval prolongation as predictor of sudden death in patients with myocardial infarction. Circulation 1978; 57: 1074–1077.
2. Coumel P, Maison-Blanche P. QT dynamicity as a predictor for arrhythmia development. In: Oto A, Breithardt G, eds. Myocardial repolarization: from gene to bedside. Armonk, NY: Futura Publishing Co, 2001: 173–186.
3. The TIMI Study Group. Special Report. The thrombolysis myocardial infarction (TIMI) trial. N Engl J Med 1985; 312: 932–936.
4. QT intervals in Mars Unity Workstation. GE Medical Information Technologies. 12-Mar–01 Rev. 1.0.
5. Lecocq B, Lecocq V, Jaillon P. Physiologic relation between cardiac cycle and QT duration in healthy volunteers. Am J Cardiol 1989; 63: 481–486.
6. Extramiana F, Maison-Blanche P, Badilini F, et al. Circadian modulation of QT rate dependence in healthy volunteers: gender and age differences. J Electrocardiol 1999; 32: 33–43.
7. Merri M, Moss AJ, Benhorin J, et al. Relation between ventricular repolarization duration and cardiac cycle length during 24-hour Holter recordings. Findings in normal patients and patients with long QT syndrome. Circulation 1992; 85: 1816–1821.
8. Yi G, Guo X, Reardon M, et al. Circadian variation of the QT interval in patients with sudden cardiac death after myocardial infarction. Am J Cardiol 1998; 81: 950–956.
9. Chevalier P, Burri H, Adeleine P, et al. QT dynamicity and sudden death after myocardial infarction. J Cardiovasc Electrophysiol 2003; 14: 227–233.
10 Jensen BT, Abildstrom SZ, Larroude CE, et al. QT dynamics in risk stratification after myocardial infarction. Heart Rhythm 2005; 2: 357–364.
11. Pathak A, Curnier D, Fourcade J, et al. QT dynamicity: a prognostic factor for sudden cardiac death in chronic heart failure. Eur J Heart Failure 2005; 7: 269–275.
12. Milliez P, Leenhardt A, Maison-Blanche P, et al. Usefulness of ventricular repolarization dynamicity in predicting arrhythmic deaths in patients with ischemic cardiomyopathy (from the European Myocardial Infarct Amiodarone Study). Am J Cardiol 2005; 95: 821–826.
13. Šišáková M, Toman O, Floriánová A, et al. Analysis of QT dynamicity behaviour in relationship to the risk of sudden cardiac death – a pilot study. Scripta Medica 2005; 78: 171–176.
14. Novotný T, et al. QT dynamicity in risk stratification in patients after myocardial infarction. Vnitr Lek 2007: 53 (9): 964–967.
15. Aschermann M, et al. Cardiology. Part 1. 1st ed. Praha: Galén, 2004: 753 pp.
16. Camm AJ, Malik M, Yap YG. Measurement of QT interval and repolarization assessment. In: Camm AJ, Malik M, Yap YG. Acquired long QT syndrome. Oxford: Blackwell Futura, 2004: 24–59.
17. Laguna P, Thakor NV, Caminal P, et al. New algorithm for QT interval analysis in 24-hour Holter ECG: performance and applications. Med Biol Eng Comp 1990; 28: 67-73.
18. Batchvarov VN, Ghuran A, Smetana P, et al. QT-RR relationship in healthy subjects exhibits substantial intersubject variability and intrasubject stability. Am J Physiol Heart Circ Physiol 2000; 282: H2356-H2363.
19. Smetana P, Batchvarov V, Hnatkova K, et al. Ventricular gradient and nondipolar repolarisation components increase at higher heart rate. Am J Physiol Heart Circ Physiol 2004; 286: H131-H136.

REGRESSION OF HISTOPATHOLOGICAL MYOPATHIC CHANGES IN PATIENTS WITH CRITICAL ILLNESS NEUROMUSCULAR DISORDERS

Lukáš Z.[1], Maňák J.[2], Bednařík J.[3], Schreiber M.[4]

[1] Department of Pathology, Masaryk University and Faculty Hospital Brno
[2] Medical Intensive Care Unit, Department of Gerontology and Metabolism, Charles University Faculty Hospital Hradec Králové
[3] Department of Neurology, Masaryk University and Faculty Hospital Brno
[4] Department of Neurology, Charles University Faculty Hospital Hradec Králové

Received after revision July 2009

KEY WORDS

Critical illness polyneuropathy
Critical illness myopathy
Diagnosis
Biopsy
Follow-up study

CORRESPONDING AUTHOR

Lukáš Z.
Department of Pathology, Masaryk University and Faculty Hospital Brno
Jihlavská 20
625 00 Brno
Czech Republic

ABSTRACT

Histopathological analysis of 52 muscle biopsies from 43 adult critically ill patients was performed to determine the differential diagnosis and course of neuromuscular involvement in critically ill patients suffering from critical illness polyneuropathy or myopathy.

The first histopathological examination in all 43 patients revealed signs of neuropathy in 2 biopsies, myopathy in 19 biopsies, and neuromyopathy in 18, including type 2 fibre atrophy.

A repeat study of 9 patients showed that the histopathological features changed in all cases. A second biopsy performed several months or years after the first revealed that myopathic features had regressed and either recovery to normal histopathological findings had occurred or evidence of a persistent neurogenic lesion was found. The results indicate that muscle involvement in critically ill patients is reversible.

ABBREVIATIONS USED

ATPase – adenosinetriphosphatase
CIM – critical illness myopathy
CIP – critical illness polyneuropathy
CK – creatine kinase
CMAP – compound muscle action potentials
dMHC – developmental myosin heavy chain
DMS – direct muscle stimulation
EM – electron microscopy (-ic)
EMG – electromyography(-ic)
HLA 1 – human leukocyte antigen 1
ICU – intensive care unit
N-CAM – neural cell adhesion molecule

MODS – multiple organ dysfunction syndrome
NMBA – neuromuscular blocking agent
OFA – sepsis-related organ failure assessment
SIRS – systemic inflammatory response syndrome
SNAP – sensory nerve action potentials

INTRODUCTION

Neuromuscular disorders in critically ill patients have been recorded with increasing frequency. The classification of intensive care unit (ICU) neuromuscular disorders distinguishes critical illness polyneuropathy (CIP) and critical illness myopathy (CIM). The diagnosis and differential diagnosis of these types of ICU neuromuscular disorders is the subject of discussion in a number of papers [1–7]. Correct interpretation and classification of the elementary features of the histopathological findings in muscle biopsies (atrophy, degeneration, necrosis, and regeneration) is a prerequisite for correct classification of the disease.

Follow-up clinical, electrophysiological and histopathological examination may assess or predict the future quality of life for ICU patients. The follow-up studies reported [8–10] refer to electrophysiological evidence of chronic partial denervation of muscle, consistent with previous critical illness polyneuropathy, which could be found within up to 5 years after intensive care unit discharge. These electrophysiological data were not correlated with the histopathological findings.

In this report, we present a histopathological analysis of muscle biopsy findings – in addition to clinical and electrodiagnostic examination – in critically ill patients with initial signs of CIP/CIM, focused on the course of neuromuscular involvement.

PATIENTS AND METHODS

Patients

The study group consisted of 43 consecutive critically ill patients – 19 men and 24 women aged 21–79 (mean 57) years, who had been admitted to a medical or neurological ICU in two Faculty hospitals and developed generalized severe muscle weakness (Table 1). Only patients with severe muscle weakness defined as score 2 or less of the Medical Research Council scale [11] were enrolled into the study. Patients with previous history of neuromuscular disease were not included. The examination of the patients was performed from 1997 to 2003.

The sepsis-related organ failure assessment (SOFA) score was used [12–14] for the evaluation of organ dysfunction or failure. Creatine kinase (CK) activity was measured on admission and then routinely once a week. Additional CK measurements were performed as clinically indicated. SOFA measurements were performed daily and a maximum SOFA score (SOFA-max) was eventually calculated. Administration of drugs with known risk potential for the development of neuromuscular disorders, i.e. corticosteroids and neuromuscular blocking agents, was monitored.

After obtaining informed consent from the patient or their next of kin, skeletal muscle needle or open biopsies from the m. vastus lateralis were obtained. Sequential biopsies were performed in two patients (Table 2) and repeated biopsies were performed after several months or years in seven patients (Table 3). The study had the approval of the local ethics committees.

Histopathological examination

Muscle biopsies were deep-frozen in a propane-butane mixture cooled with liquid nitrogen. Cryostat sections of all biopsies were processed using a set of conventional histological and histochemical methods including myosin ATPase (pH 9.4) [15]. In order to prevent misinterpretation of the histopathological findings, the methods were supplemented with markers for regenerating skeletal muscle [16–20]. The antibodies were visualized with a biotinylated anti-mouse secondary antibody followed by streptavidin Amersham) conjugated with peroxidase. Electron microscopic examination to investigate possible loss of myosin filaments was performed in 11 biopsies in which irregular reactivity to myosin ATPase had been noted.

Muscle disorders were classified as neuropathy, myopathy (simple or cachectic myopathy), myosin loss myopathy, and necrotizing myopathy. Neuropathy involves signs of denervation and/or reinnervation, myosin loss myopathy and necrotizing myopathy are well defined; simple (cachectic) myopathy comprises mild fibre atrophy, variation of fibre diameters, occasional increase of inner nuclei and myofibre splitting without profound structural alteration of the myofibres. Even a normal histopathological finding is compatible with the diagnosis of CIM [1, 21, 22]. The presence of scattered, fascicular, diffuse or single-fibre atrophy had been described as a sign of possible myogenic and/or neurogenic lesions [6, 22]. Fibre 2 atrophy [disuse atrophy) is a feature of neurogenic as well as non-neurogenic disorders. Increased basophilia, increased reactivity to desmin, or expression of a developmental myosin-heavy chain [dMHC), CD56 or HLA1 in small myofibres were taken as signs of regeneration or maturation [20].

Electrophysiological investigation

An electrophysiological investigation was performed in 36 patients during the fifth week of critical illness and consisted of a repetitive stimulation test, conduction studies, and nee-

Patient No.	Sex	Day of biopsy	Age	Clinical diagnosis	SOFAmax	CK	Pipecuronium	Corticosteroid dosage	Histopathology	Electrophysiology	DMS
1	F	7	30	Bronchopneumonia	8	15.8	0	0	Simple myopathy	ND	ND
2	M	8	43	Aortic dissection, rhabdomyolysis	16	21.2	73	0	Normal	ND	ND
3 (+seq)	M	12	66	Aortic valve replacement	14	3.8	28	X	Necrotizing myopathy, atrophy 2	Myopathy	ND
4 (+seq)	M	13	67	Myocardial revascularization	12	546.7	134	0	Simple myopathy, neuropathy	Neuromyopathy*	ND
5	F	14	73	Myocardial revascularization	8	4.1	26	0	Myosin loss myopathy	ND	ND
6	M	14	72	Myocardial revascularization	15	8.8	8	X	Normal	ND	ND
7	M	19	54	GI bleeding	14	6.1	0	0	Neuropathy	Normal	Normal
8	F	20	65	Urosepsis	14	17.1	0	0	Simple myopathy, neuropathy	ND	ND
9	M	21	71	Aortic dissection	16	15.1	18	X	Necrotizing myopathy, neuropathy	Neuromyopathy*	ND
10 (+seq)	F	22	49	Malignant lymphoma	20	2.4	0	T	Simple myopathy	Myopathy	ND
11	F	23	20	Intra-abdominal sepsis	17	8.9	4	S	Myosin loss myopathy	Myopathy	ND
12	M	25	47	Atrial septal defect	6	1.3	20	0	Simple myopathy, atrophy 2	Neuromyopathy*	Normal
13	F	25	69	Myocardial revascularization	8	2.1	22	X	Simple myopathy, atrophy 2	Neuromyopathy*	DME
14	F	25	77	Peritonitis	18	74.6	0	0	Normal	ND	ND
15	F	26	54	Cholangitis	14	3.5	20	S	Simple myopathy	Neuromyopathy*	ND
16	M	26	64	Myocardial infarction	15	246.7	0	0	Necrotizing and myosin loss myopathy	Myopathy	ND
17	F	30	64	Intracerebral hematoma	8	2.8	0	0	Simple myopathy, neuropathy	Neuromyopathy	DME
18	M	31	59	Brain contusion	12	2.8	260	T	Simple myopathy	Neuromyopathy	DME
19	F	31	78	Brain ischemia	12	3.1	0	0	Simple myopathy, neuropathy	Neuromyopathy	DME
20	M	31	72	Aortic valve replacement	13	13.7	40	0	Necrotizing myopathy	Neuromyopathy*	ND
21	F	31	48	Acute pancreatitis	10	4.1	0	0	Simple myopathy	Neuromyopathy*	DME
22 (+seq)	F	33	51	Pulmonary embolism	12	4.3	0	0	Necrotizing myopathy, neuropathy	Neuromyopathy*	ND
23	M	33	69	Brain ischemia	10	3.1	0	0	Simple myopathy	Myopathy	DME
24	F	35	35	Meningoencephalitis	11	0.1	224	T	Simple myopathy, neuropathy	Myopathy	DME
25 (+seq)	M	36	43	Mediastinitis	14	5.4	12	0	Necrotizing myopathy, atrophy 2	Neuromyopathy*	ND
26	F	36	55	Pulmonary abscess	11	12.2	16	S	Necrotizing myopathy	Myopathy	ND
27	F	36	67	Ileus – peritonitis	9	9.1	2	0	Simple myopathy, atrophy 2	Neuromyopathy*	DME
28	F	37	62	Septic shock	17	20.1	68	T	Simple myopathy, neuropathy	Polyneuropathy	DNE
29 (+seq)	F	39	70	Pancreatitis	7	1.1	0	0	Simple myopathy	Neuromyopathy*	ND
30	F	41	72	Bacterial pericarditis	20	1.1	16	0	Myosin loss myopathy	ND	ND
31 (+seq)	M	43	45	Aortic valve replacement	18	7.2	90	X	Necrotizing myopathy	Neuromyopathy*	ND
32	M	45	22	Basilar thrombosis	6	30.1	0	0	Normal	Myopathy	DME
33	F	48	78	Acute pancreatitis	17	1.1	0	0	Simple myopathy, neuropathy	Neuromyopathy*	ND
34	F	51	66	Cardiac arrest	13	5.1	16	0	Simple myopathy, neuropathy	Myopathy	DME
35	M	51	51	Subarachnoid hemorrhage	9	2.1	216	T	Simple myopathy	Polyneuropathy	DNE
36	M	55	70	Acute pancreatitis	19	0.1	0	0	Myosin loss myopathy	Neuromyopathy*	ND
37	F	57	57	Intracerebral hematoma	11	11.2	0	0	Simple myopathy	Myopathy	Normal
38	F	57	54	Acute pancreatitis	15	13.1	32	X	Simple myopathy, neuropathy	Neuromyopathy*	Normal
39 (+seq)	M	58	62	Aortic valve replacement	14	2.1	24	X	Simple myopathy, neuropathy	Neuromyopathy*	ND
40	F	62	30	Brain ischemia	10	10.1	0	0	Neuropathy	Neuromyopathy	DME
41	F	62	62	Aortic valve replacement	15	4.1	12	0	Simple myopathy	Neuromyopathy*	ND
42 (+seq)	M	65	44	Acute pancreatitis	10	24.1	0	0	Simple myopathy	Polyneuropathy	DNE
43	M	77	47	Gastrointestinal bleeding	11	1.1	88	0	Simple myopathy, neuropathy	Neuromyopathy*	ND

Abbreviations
No. – number
(+seq) – patient with two biopsies
Day of biopsy, interval between beginning of ICU disease and date of first biopsy
Atrophy 2 – atrophy of type 2 fibre
CK – creatine kinase
ND – not done
Minimal – minimal changes
Pipecuronium – non-depolarizing neuromuscular blocking agent, cumulative dose in milligrams
DMS – direct muscle stimulation
DME – decreased muscle excitability
DNE – decreased nerve excitability
Neuromyopathy* – the assumption of a myopathic component was based on the presence of electrophysiological motor syndrome, while in cases not marked with asterisks it was proven by DMS.

Steroid dosage was classified as
O – No steroids or periprocedural single boluses, e.g. extubation
T – Therapeutic use – therapy of underlying condition, pharmacological doses
S – Substitution therapy in patients with proven adrenal insufficiency or history of chronic steroid therapy. Daily dose <300 mg hydrocortisone or equivalent
X – Short-term steroid therapy in severe septic shock in presumed relative adrenal insufficiency. Daily doses >300 mg hydrocortisone or equivalent.

dle EMG. Direct muscle stimulation (DMS) was performed in 18 cases.

All electrophysiological tests were performed at bedside with a Nicolet Viking IV apparatus. Administration of non-depolarizing muscle-blocking agents was stopped 24 hours before electrophysiological examination. As the first step, a motor nerve repetitive stimulation test was performed in the right ulnar nerve using a stimulation frequency of 2 Hz. Further electrophysiological evaluation followed only after the absence of any reproducible decrement, to exclude persistent neuromuscular blockade. If any reproducible decrement was found, electrophysiological testing was postponed for 24–48 hours, until normalization of the repetitive stimulation test was achieved.

Motor and sensory conduction studies were performed at six motor nerves (median, peroneal, and tibial nerves bilaterally) and four sensory nerves (ulnar and sural nerves bilaterally), using conventional techniques. Normal limits from the authors' neurophysiological laboratory were employed in the assessment. Abnormality of CMAP or SNAP amplitudes was considered significant if found in at least two nerves.

Needle EMG from four muscles (deltoid, first dorsal interosseus, tibial anterior, and abductor hallucis muscles on the right) was performed, with assessment of spontaneous activity and, if possible, recruitment and interference patterns. The presence of spontaneous activity was considered significant if found from a minimum of two muscles. Three more muscles (rectus femoris, vastus lateralis, and biceps brachii) were examined in 66 % of the patients; this lack of completion prevents the results being included here. Needle EMGs from these muscles showed the same non-specific abnormalities (abnormal spontaneous activity, simplified interference pattern, or lack of volitional activity) as from tibial anterior muscles and did not disclose any additional abnormality.

Direct muscle stimulation from the right tibial anterior muscle was applied, using the technique described by Rich et al. [23, 24]. A pair of subdermal electrodes was used for the recording. The ratio of CMAP amplitude evoked by nerve stimulation (neCMAP) to that evoked by direct muscle stimulation (dmCMAP) was calculated. DMS findings were classified into three groups: neuropathic with decreased ne/dmCMAP amplitude ratio below 0.5, myopathic with decreased absolute dmCMAP amplitude below the normal limit of 2 mV, and normal with the absolute dmCMAP amplitude above the normal limit and the ne/dmCMAP amplitude ratio above 0.5 [25].

RESULTS

Clinical state of the patients

The underlying clinical conditions are summarized in Table 1. All the patients were mechanically ventilated and fulfilled the criteria for septic shock and multiple organ dysfunction

Table 2
Patients with sequential examination, short intervals

Patient No.	Neurological finding (1) EMG (1) Biopsy (1)	Interval Bi1–Bi2	Neurological finding (2) Electrophysiology (2) Biopsy (2)
3	Quadruplegia EMG: Myopathy Histopathology: necrotizing myopathy, fibre type 2 atrophy	5 weeks	Marked improvement EMG: Polyneuropathy Histopathology: fibre type 2 atrophy
10	MOF, sepsis, quadruplegia EMG: Myopathy Histopathology: simple myopathy	8 days	Rhabdomyolysis, quadruplegia EMG: Myopathy Histopathology: severe necrotizing myopathy

or failure syndrome [12, 14, 26]. Corticosteroids were administered in some patients. Doses of less than 300 mg of hydrocortisone or equivalent were administered in three patients with proven adrenal insufficiency. Short-term corticosteroid therapy (hydrocortisone >300 mg/day or equivalent) was administered in 7 patients with septic shock refractory to catecholamines and stopped immediately upon achievement of hemodynamic stability. Five patients received pharmacological corticosteroid doses in response to underlying disease. The majority of the cases did not receive any corticosteroids at all.

Neuromuscular blocking agents (NMBA) were administered in 25 patients. The only agent used was pipecuronium (Arduan, Gedeon Richter Chemical Works, Budapest, Hungary), a long-acting, non-depolarizing neuromuscular blocker. It was administered on an intermittent basis if indicated, in order to facilitate mechanical ventilation, or in patients with increased intracranial pressure. A combination of corticosteroids and NMBAs was administered to 14 patients, while three of them received steroids in substitution doses due to proven adrenal insufficiency. Creatine kinase levels were high in all our patients with necrotizing myopathy, but a very pronounced fluctuation of values appeared among patients with CIM. The sensitivity of CK evaluation critically depends on the timing of evaluation [5], as CK level usually peaks several days after the onset of critical illness and decreases afterwards. It is no longer considered as a sensitive or specific indicator of CIM.

Electrophysiology

The results of the electrophysiological examination were abnormal in 35 of 36 patients examined. Two main types of electrophysiological abnormality were identified: pure motor syndrome (signs of abnormal CMAP amplitudes and/or abnormal spontaneous activity) and combination of motor syndrome and sensory polyneuropathy (abnormal SNAP amplitudes). With respect to the DMS findings, the abnormalities were classified as myopathy in 3 cases, axonal sensory-motor polyneuropathy in 4 cases, and neuromyopathy in 7 cases (Table 1, column Electrophysiology). The classification of neuromyopathy was based on combined electrophysiological patterns of the motor syndrome and sensory polyneuropathy in association with decreased sarcolemmic excitability in 4 cases, while in the remaining 18 cases the assumption of a myopathic component was based on the presence of electrophysiological motor syndrome [25].

Histopathology

The results of the first histopathological examination of all 43 patients (Table 1, column Histopathology) showed the presence of a clear-cut neurogenic lesion in 2 biopsies. A myogenic pattern was present in 19 patients (Figures 1a-d), and 18 patients had signs of neuromyopathy (Figure 1e), including type 2 fibre atrophy (Figure 1d).

Muscle fibre atrophy was recorded in all patients with the diagnosis of CIM, CIP, or of a combination of both. Foci of myosin deficiency in atrophic fibres were demonstrated in 3 patients [5, 30, 36]. A proportion of small ("atrophic") myofibres in biopsies with myopathy or neuromyopathy expressed d-MHC (Figure 1a), increased desmin reactivity, HLA1, NCAM (CD56), and other signs of regeneration.

Electron microscope investigation focused on possible loss of myosin filaments was performed in 11 biopsies (patients 3, 4, 5, 12, 13, 16, 29, 30, 35, 36, 42), where irregular reactivity to myosin ATPase had been noted. Multifocal myosin loss

Table 3
Patients with repeat examination, long intervals

Patient No.	Clinical, electrophysiological, and histopathological findings at the time of 1st biopsy	MRC	Interval Bi 1-Bi 2	Clinical, electrophysiological, and histopathological findings at the time of 2nd biopsy	MRC
4	Quadruparesis, Electrophysiology: neuromyopathy Histopathology: simple myopathy, neuropathy	2.3	31 months	Ambulatory with 1 stick, acral dysesthesia Electrophysiology: polyneuropathy Histopathology: neuropathy	3.4
22	Quadruplegia, Electrophysiology: neuromyopathy Histopathology: necrotizing myopathy, neuropathy	0.6	20 months	Fully ambulatory with peroneal paresis, acral paresthesia, Electrophysiology: polyneuropathy (improved) Histopathology: normal	3.8
25	Quadruparesis, Electrophysiology: neuromyopathy Histopathology: necrotizing myopathy, fibre type 2 atrophy	0.9	20 months	Fully ambulatory with peroneal paresis, acral paresthesia, Electrophysiology: polyneuropathy (improved) Histopathology: normal (minimal changes)	3.5
29	Quadruparesis, Electrophysiology: neuromyopathy Histopathology: simple myopathy	not done	21 months	Ambulatory with 2 sticks, MRCav Electrophysiology: polyneuropathy (improved) Histopathology: neuropathy	not done
31	Quadruplegia, Electrophysiology: neuromyopathy Histopathology: necrotizing myopathy	0.2	29 months	Fully ambulatory with peroneal paresis, acral paresthesia, Electrophysiology: persisting axonal polyneuropathy Histopathology: normal	4.5
39	Quadruparesis, Electrophysiology: neuromyopathy Histopathology: simple myopathy and neuropathy	0.9	20 months	Ambulatory with peroneal paresis, Electrophysiology: persisting axonal polyneuropathy Histopathology: normal (minimal changes)	4.0
42	Muscle weakness, Electrophysiology: polyneuropathy Histopathology: simple myopathy	3.0	11 months	Normal, Electrophysiology: persisting axonal polyneuropathy Histopathology: normal	5.0

Explanation to the abbreviations and symbols in Tabs. 2 and 3:
Bi (1), 1st biopsy, Bi (2), 2nd biopsy
MRC, Medical Research Council score, average values
For other symbols see Tab. 1
EMG: electrophysiological examination

Histopathological findings in patients with CIM/CIP

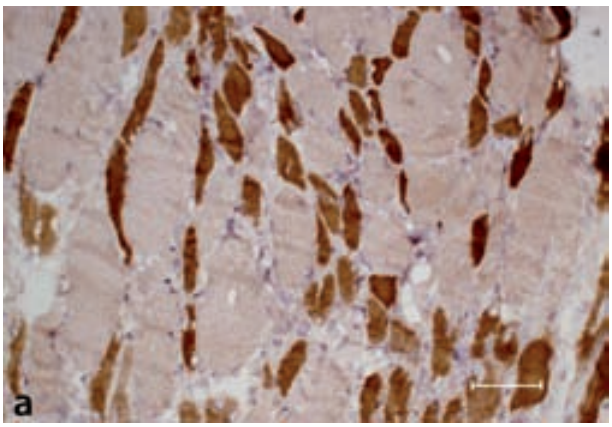

Figure 1a
Small regenerating myofibres in myopathy, d-MHC**.** Bar, 100μm.

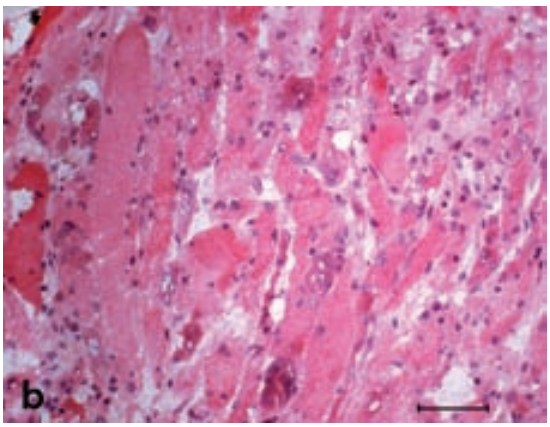

Figure 1b
Severe necrotizing myopathy, Hem&Eos, patient 10, 2nd biopsy. Bar, 100 μm.

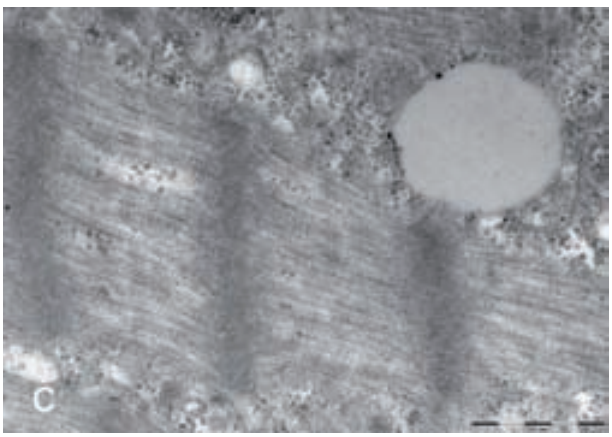

Figure 1c
Loss of thick filaments, patient 30. Bar, 1μm.

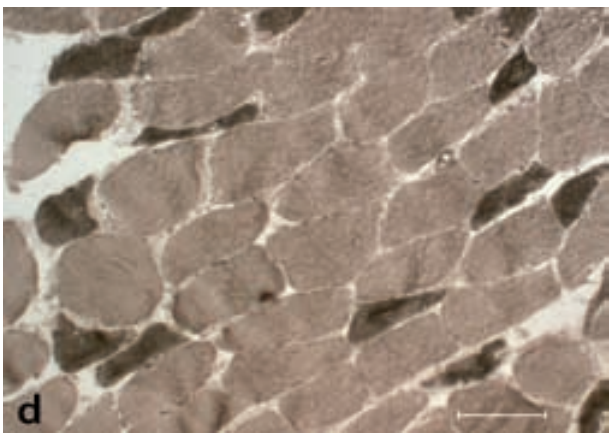

Figure 1d
Type 2 fibre atrophy, myo-ATPase, pH 9.4, patient 3. Bar, 100 μm.

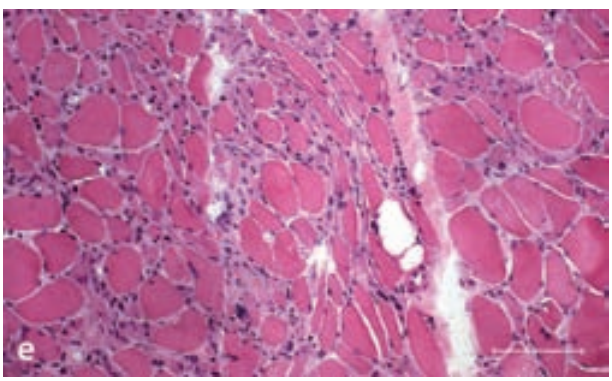

Figure 1e
Bundles of atrophic myofibres, a picture admitting neurogenic as well as myogenic lesion (EMG: myopathy and axonal polyneuropathy), patient 39. Bar, 100 μm.

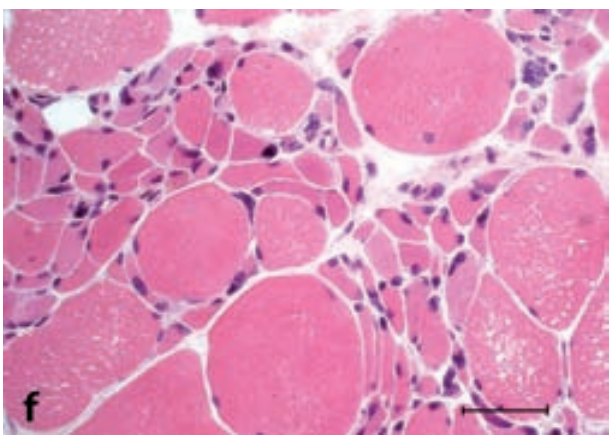

Figure 1f
Advanced neurogenic atrophy, Hem&Eos, patient 4, 2nd biopsy. Bar, 100 μm.

was proven by electron microscopy in 5 patients [5, 11, 16, 30, 36] (Figure 1c). It is of interest that only one of the five patients with multifocal myosin loss had been treated with corticosteroids.

The frequency of regenerating myofibres (not demonstrated) was proportional to the extent of structural alteration of the muscle: maximal values were recorded in patients with CIM (11 patients had 25 % or more regenerating myofibres). We found no correlation between the percentage of regenerating fibres and age, timing of the biopsy, or extent of organ failure expressed as maximum SOFA score.

Normal findings were recorded in 4 patients.

Discrepancies between the results of electrophysiological and histopathological examinations were not pronounced: contradictory or mutually exclusive results (i.e. "pure" EMG neuropathy versus "pure" histopathology myopathy) were recorded in only two patients [35 and 42], while patient 7 had signs of neuropathy in the biopsy but normal electrophysiology.

The course of the disease

All 43 patients were arranged in order of interval between the beginning of ICU disease and the date of the first biopsy (Table 1, column Day of biopsy).

Non-specific myopathic changes were found 7 days after the beginning of the disease. The longest interval between the onset of the disease and the finding of a severe necrotizing myopathy (Mn) was recorded in patient 30, six weeks [42 days) after the beginning of the disease. Beyond this period only mild structural changes in the myofibres were recorded.

The results of the examination of patients with two consecutive biopsies are summarized in Tables 2 and 3. The first biopsy of patient 10, with malignant lymphoma, was obtained 22 days after the beginning of the disease (and aggressive therapy) and revealed a picture of mild, simple myopathy (Figure 1a). Eight days after the first biopsy, the patient suffered an attack of rhabdomyolysis and the second biopsy revealed profound structural histopathological alterations corresponding to a necrotizing myopathy (Figure 1b). In patient 3, the first biopsy (day 12) revealed a picture of myopathy with several necrotic fibres and with lower type 2 fibre diameters. The second biopsy was obtained 5 weeks later, when the clinical finding showed improvement, and offered a similar picture with more pronounced fibre type disproportion (type 2 atrophy) (Figure 1d), but without necrotic myofibres.

When a second biopsy was performed several months or years after the first one, clinical improvement or recovery was recorded in all patients (Table 3).

Discrepancies between the results of electrophysiological and histopathological examinations in these patients were more pronounced than in the previous (first) biopsies.

Myogenic features, i.e. simple or necrotizing myopathy, were not found. Normal histological findings were recorded in patients 22, 25, 31, 39, and 42, with previous findings of neuromyopathy (patients 22, 25, 39), or myopathy (patients 31 and 42). The second biopsy in patients 4 and 29 revealed the presence of a developed denervation-reinnervation process (Figure 1f), against the first biopsy results of neuromyopathy (patient 4) and myopathy (patient 29). Electrophysiological (EMG) examination of all seven patients revealed persisting axonal polyneuropathy, with a regression of previous myogenic features in patients 25 and 29..

DISCUSSION

The diagnosis of CIP/CIM

The frequency and spectrum of neuromuscular changes in critically ill patients is a matter of debate since CIP was first described by Bolton et al. [27]. The term "critical illness polyneuromyopathy" was proposed by Op de Coul et al. [7], and a combination of neuropathy and myopathy was then documented by many authors [1, 6, 25, 28–30] including this paper.

The final diagnosis of CIP, CIM or both is critically dependent on the diagnostic method used. An electrophysiological pattern of acute axonal motor-sensory polyneuropathy is not difficult to discern, but differentiation between CIP and CIM is difficult or even impossible [25], while histopathological analysis can easily detect structural alteration of the muscle fibres [1, 15, 31].

The classification of essential muscle disorders in our patients studied revealed a predominant myogenic or mixed pattern of neuromuscular involvement, which is in concordance with recent reports [2, 3, 32, 33].

Myosin loss is a hallmark of CIM [1, 9, 21, 28, 34]. In our patients, myosin loss was suspected because of irregular reactivity to myo-ATPase in 11 patients and confirmed by electron microscopic examination in five of them. It is possible that the number of myosin-deficient patients is underdiagnosed (not only in this study) because of a sampling error. Experimentally, both atrophy and myosin filament loss have been produced in surgically denervated muscles exposed to corticosteroids [35–37]. On the other hand, none of our patients with myosin loss was treated with substantial doses of corticosteroids and NMBA (corticosteroids were administered in only one case as substitution for adrenal insufficiency). Similarly, Deconinck et al. [38] reported on three patients with acute quadriplegic myopathy with loss of myosin filaments, two of whom were not exposed to corticosteroids or neuromuscular blocking agents. These results indicate that myosin loss myopathy can occur independently of corticosteroids or neuromuscular blocking agents and that other pathogenetic factors may be involved.

The course of neuromuscular complications of critical illness

In the group presented, histopathological changes of CIP and CIM developed soon after the beginning of the disease. These findings correspond to the reports of early electrophysiological signs of neuromuscular involvement 1–2 weeks after the beginning of the disease [7, 28, 33, 39].

Similarly, some reports mention the presence of signs of CIP/CIM in muscle biopsies even immediately [40] or shortly [41] after the beginning of the disease. Lacomis et al. [2] found selective loss of thick filaments in ICU patients 2 weeks or more after intravenous corticosteroid exposure. In the animal denervation models, muscle fibre atrophy and myosin loss developed after seven days [35, 36].

Sequential biopsy findings deserve attention. A comparison of sequential biopsy findings in patients 3 and 10 offers evidence that the histopathological picture of the disease may change relatively quickly in the course of the disease.

When a second biopsy was performed several months or years after the first, the myogenic features, i.e. simple myopathy in four patients (patients 4, 29, 39, 42] and necrotizing myopathy in three patients (patients 22, 25, 31] subsided or disappeared: either recovery to norm (5 patients] or persistent neurogenic lesion (2 patients) was recorded. Electrophysiological signs of myopathy (6 out of 7 cases were classified as neuromyopathy) changed to persistent neuropathy in all 7 cases. Regression of histopathological changes, especially those of myopathy, correlated better with functional improvement in ambulatory patients, assessed by evaluation of muscle strength, than electrophysiology (Table 3). The number of the patients with repeat biopsies is too low to predict the patients' outcome but the retreat of myopathic features is a constant finding in all seven cases.

Regression of myopathic (myogenic) histopathological changes in our patients is in concordance with the conclusions of Lacomis and Campellone [3] that critical illness myopathy is generally reversible. Latronico, Shehu and Seghelini [42] summarized studies offering results of long-term outcomes of 263 patients: in most reports, CIP was the main diagnosis associated with persistent disability, while CIM was often associated with rapid and complete recovery. Recent reports [43, 44] also indicate that CIM has a better prognosis than CIP. However, incomplete recovery and dismal prognosis were also reported for CIM, and poor recovery of muscle strength in four patients with acute necrotizing myopathy was reported by Ramsay et al. [45]. The course and mortality in patients with CIM appears to be related to the underlying illness [3].

A follow-up examination of seven patients with CIP [9] (confirmed in three patients by muscle and nerve biopsy) was performed 3 months to 3.5 years after the onset of acute illness: five survivors showed clinical improvement or recovery, although signs of chronic neurogenic damage were demonstrated in all survivors electrodiagnostically. Similarly, Fletcher et al. [8] recorded clear history of severe weakness and electrophysiological evidence of chronic partial denervation on a 5-year follow-up in 21 of 22 patients, findings indicative of preceding axonal neuropathy. Residual neurogenic abnormalities in the patients reported were not confirmed by histological examination.

ACKNOWLEDGEMENTS

This work was supported by Research Plans No. MSM0021620819 and MSM0021622404 from the Czech Ministry of Education.

REFERENCES

1. Bolton CF. Neuromuscular manifestations of critical illness. Muscle Nerve 2005; 32: 140–163.
2. Lacomis D. Critical illness myopathy. Current Rheumatologic Reports 2002; 4: 403–408.
3. Lacomis D, Campellone JV. Critical illness neuromyopathies. Adv Neurol 2002; 88: 325–335.
4. Lacomis D, Giuliani MJ, Van Cott A, Kramer DJ. Acute myopathy of intensive care: clinical, electromyographic, and pathological aspects. Ann Neurol 1996; 40: 645–654.
5. Lacomis D, Zochodne DW, Bird SJ. Critical illness myopathy. Muscle Nerve 2000; 23: 1785–1788.
6. Latronico N, Fenzi F, Recupero D, et al. Critical illness myopathy and neuropathy. Lancet 1996; 347: 1579–1582.
7. Op de Coul AA, Verheul GA, Leyten AC, Schellens RL, Teepen JL. Critical illness polyneuromyopathy after artificial respiration. Clin Neurol Neurosurg 1991; 93: 27–33.
8. Fletcher SN, Kennedy DD, Ghosh IR, et al. Persistent neuromuscular and neurophysiologic abnormalities in long-term survivors of prolonged critical illness. Crit Care Med 2003; 31: 1012–1016.
9. Hund EF, Fogel W, Krieger D, DeGeorgia M, Hacke W. Critical illness polyneuropathy: clinical findings and outcomes of a frequent cause of neuromuscular weaning failure. Crit Care Med 1996; 24: 1328–1333.
10. Witt NJ, Zochodne DW, Bolton CF, et al. Peripheral nerve function in sepsis and multiple organ failure. Chest 1991; 99: 176–184.
11. De Jonghe B, Sharshar T, Lefaucheur JP, et al. Groupe de Réflexion et d'Etude des Neuromyopathies en Réanimation. Paresis acquired in the intensive care unit. A prospective multicenter study. JAMA 2002; 288: 2859–2867.
12. Bone RC, Sibbald WJ, Sprung CL. The ACCP/SCCM consensus conference on sepsis and organ failure. Chest 1992; 101: 1481–1483.

13. Ferreira FL, Bota DP, Bross A, Melot C, Vincent JL. Serial evaluation of the SOFA score to predict outcome in critically ill patients. JAMA 2001; 286: 1754–1758.
14. Vincent JL, Moreno R, Takala J, et al. The SOFA (Sepsis-related Organ Failure Assessment) score to describe organ dysfunction/failure. On behalf of the Working Group on Sepsis-Related Problems of the European Society of Intensive Care Medicine. Intensive Care Med 1996; 22: 707–710.
15. Dubowitz V. Sewry CA. Muscle biopsy. A practical approach. 3rd ed. London: Elsevier Saunders, 2007.
16. Cashman NR, Covault J, Wollman RL, Sanes JR. Neural cell adhesion molecule in normal, denervated and myopathic human muscle. Ann Neurol 1987; 21: 481–489.
17. Perl DP, Little BW. Acridine orange-nucleic acid fluorescence. Its use in routine diagnostic muscle biopsies. Arch Neurol 1980; 37: 641–644.
18. Sarnat HA. Vimentin/desmin immunoreactivity of myofibres in developmental myopathies. Acta Paediatr Jpn 1991; 33: 238–246.
19. Sartore S, Gorza L, Schiaffino S. Fetal myosin heavy chains in regenerating muscle. Nature 1982; 298: 294–296.
20. Winter A, Bornemann A. NCAM, vimentin and neonatal myosin heavy chain expression in human muscle diseases. Neuropathology and Applied Neurobiology 1999; 25: 417–424.
21. Hund EF. Neurological complications of sepsis: critical illness polyneuropathy and myopathy. J Neurol 2001; 48: 929–934.
22. Helliwell TR, Wilkinson A, Griffiths RD, et al. Muscle fibre atrophy in critically ill patients is associated with the loss of myosin filaments and the presence of lysosomal enzymes and ubiquitin. Neuropathol Appl Neurobiol 1998; 24: 507–517.
23. Rich MM, Teener JW, Raps EC, Schotland DL, Bird SJ. Muscle is electrically inexcitable in acute quadriplegic myopathy. Neurology 1996; 46: 731–736.
24. Rich MM, Bird SJ, Raps EC, McCluskey LF, Teener JW. Direct muscle stimulation in acute quadriplegic myopathy. Muscle Nerve 1997; 20: 665–673.
25. Bednařík J, Lukáš Z, Vondráček P. Critical illness polyneuromyopathy: the electrophysiological components of a complex entity. Intensive Care Med 2003; 29: 1505–1514.
26. Levy MM, Fink MP, Marshall JC, et al. 2001 SCCM/ESICM/ACCP/ATS/SIS International Sepsis Definitions Conference. Crit Care Med 2003; 31: 1250–1256.
27. Bolton CF. Neuromuscular manifestations of critical illness. Muscle Nerve 2005; 32: 140–163.
28. Khan J, Burnham EL, Moss M. Acquired weakness in the ICU: critical illness myopathy and polyneuropathy. Minerva Anestesiol 2006; 72: 401–406.
29. Latronico N. Neuromuscular alterations in the critically ill patient: critical illness myopathy, critical illness polyneuropathy, or both? Intensive Care Med 2003; 29: 1411–1413.
30. Latronico N, Bertolini G, Guarneri B, et al. Simplified electrophysiological evaluation of peripheral nerves in critically ill patients: the Italian multi-centre CRIMYNE study. Crit Care 2007; 11: R11.
31. Carpenter S, Karpati G. Pathology of skeletal muscle. Oxford: Oxford University Press, 2001.
32. Lefaucheur JP, Nordine T, Rodriguez P, Brochard L. Origin of ICU acquired paresis determined by direct muscle stimulation. J Neurol Neurosurg Psychiatry 2006; 77: 500–506.
33. Khan J, Harrison TB, Rich MM, Moss M. Early development of critical illness myopathy and neuropathy in patients with severe sepsis. Neurology 2006; 67: 1421–5.
34. Showalter CJ, Engel AG. Acute quadriplegic myopathy: analysis of myosin isoforms and evidence for calpain-mediated proteolysis. Muscle Nerve 1997; 20: 316–322.
35. Massa R, Carpenter S, Holland P, Carpati G. Loss and renewal of thick myofilaments in glucocorticoid-treated rat soleus after denervation and reinnervation. Muscle Nerve 1992; 15: 1290–1298.
36. Mozaffar T, Haddad F, Zeng M, et al. Molecular and cellular defects of skeletal muscle in an animal model of acute quadriplegic myopathy. Muscle Nerve 2007; 35: 55–65.
37. Holland P. Glucocorticoid excess induces preferential depletion of myosin in denervated skeletal muscle fibers. Muscle Nerve 1987; 10: 428–438.
38. Deconinck N, Van Parijs V, Becker-Bleukx G, Van den Bergh P. Critical illness myopathy unrelated to corticosteroids or neuromuscular blocking agents. Neuromusc Disord 1998; 8: 186–192.
39. Tennilä A, Salmi T, Pettila V, et al. Early signs of critical illness polyneuropathy in ICU patients with systemic inflammatory response syndrome or sepsis. Intensive Care Med 2000; 26: 1360–1363.
40. Larsson L, Li X, Edström L, et al. Acute quadriplegia and loss of muscle myosin in patients treated with nondepolarizing neuromuscular blocking agents and corticosteroids: mechanisms at the cellular and molecular level. Crit Care Med 2000; 28: 34–45.
41. Coakley JH, Nagendran K, Honavar M, Hinds C. Preliminary observations on the neuromuscular abnormalities in patients with organ failure and sepsis. Intensive Care Med 1993; 19: 323–328.
42. Latronico N, Shehu I, Seghelini E. Neuromuscular sequelae of critical illness. Curr Opin Crit Care 2005; 11: 381–390.
43. Guarneri B, Bertolini G, Latronico N. Long-term outcome in patients with critical illness myopathy or neuropathy:

the Italian multicentre CRIMYNE study. J Neurol Neurosurg Psychiatry 2008;79: 838–41.
44. Latronico N, Guarneri B. Critical illness myopathy and neuropathy. Minerva Anestesiol 2008; 74: 319–23.
45. Ramsay DA, Zochodne DW, Robertson DM, Nag S, Ludwin SK. A syndrome of acute severe muscle necrosis in intensive care unit patients. J Neuropathol Exp Neurol 1993; 52: 387–398.